# Improved Design of a Three-degree of Freedom Hip Exoskeleton Based on Biomimetic Parallel Structure

by

Min Pan

A Thesis Submitted in Partial Fulfillment
of the requirements for the Degree of

Master of Applied Science

in

The Faculty of Engineering and Applied Science

Mechanical Engineering Program

University of Ontario Institute of Technology

July, 2011

# Abstract

The external skeletons, Exoskeletons, are not a new research area in this highly developed world. They are widely used in helping the wearer to enhance human strength, endurance, and speed while walking with them. Most exoskeletons are designed for the whole body and are powered due to their applications and high performance needs.

This thesis introduces a novel design of a three-degree of freedom parallel robotic structured hip exoskeleton, which is quite different from these existing exoskeletons. An exoskeleton unit for walking typically is designed as a serial mechanism which is used for the entire leg or entire body. This thesis presents a design as a partial manipulator which is only for the hip. This has better advantages when it comes to marketing the product, these include: light weight, easy to wear, and low cost. Furthermore, most exoskeletons are designed for lower body are serial manipulators, which have large workspace because of their own volume and occupied space. This design introduced in this thesis is a parallel mechanism, which is more stable, stronger and more accurate. These advantages benefit the wearers who choose this product.

This thesis focused on the analysis of the structure of this design, and verifies if the design has a reasonable and reliable structure. Therefore, a series of analysis has been done to support it. The mobility analysis and inverse kinematic solution are derived, and the Jacobian matrix was derived analytically. Performance of the CAD model has been checked by the finite element analysis in Ansys, which is based on applied force and moment. The comparison of the results from tests has been illustrated clearly for stability

and practicability of this design. At the end of this thesis, an optimization of the hip exoskeleton is provided, which offers better structure of this design.

# Acknowledgments

Working on this thesis took lots of time and effort, but the process has been both interesting, enjoyable and was a great learning experience. The reason for that is I have been working alongside many knowledgeable and intelligent colleagues. I would like to thank them for their great dedication and support for me during this period.

First and foremost, I would like to express my deepest gratitude to my supervisor, Dr. Dan Zhang, for his continuous support, encouragement and guidance throughout the research and my graduate study. I would also like to thank him for allowing me and giving me the opportunity to use and work in the excellent Robotics and Automation Laboratory. Dr. Zhang has broad knowledge, percipience and motivation on all his research projects, which encouraged me throughout my study. I would like to thank him for his valuable supervision, full support and review of the manuscript. This work would and could never be what it is like right now without his contribution.

In particular, I also offer thanks to Mr. Zhongzhe Chi, who has been played an important role in the way I approached my Master degree. His invaluable advises and guidance always get me out from bottlenecks. I would not have been able to solve the problems I have encountered without his assistance with his insights and experience. Also my sincerest thanks to all the members of the Robotics and Automation Laboratory at UOIT for their intelligent advises and kind encouragement. They are such a group of lovely people, who always share ideas and information with each other. They are always ready to lend a help hand to others regardless in academia or life. It has been a pleasure

and a privilege to study in such a warm environment though the weather in winter is really cold.

Last but not least, I would like to give my deepest thanks to my Mum, Dad and brother for always being there for me and keeping my ego in check. I would not be able to continue my graduate study without their financial and support. And finally, my thanks to the most special man in my life for his patience and understanding as well as his effort in pushing me.

# Table of Contents

Abstract ..... ii
Acknowledgments ..... iv
Table of Figures ..... viiiiii
Table of Tables ..... x
Chapter 1 Introduction ..... 1
1.1 Literature Review ..... 4
1.2 Subject of the Study ..... 8
1.3 Motivation ..... 9
1.4 The organization of the Thesis ..... 9
Chapter 2 Biomechanical Gait Analysis ..... 11
2.1 Regular Human Gait Cycle ..... 11
2.2 Kinematics and Kinetics of the Gait ..... 14
2.3 Muscle Action in Gait Cycle ..... 17
Chapter 3 General Design of the Hip Exoskeleton Unit ..... 19
3.1 The Purpose of the Hip Exoskeleton Unit ..... 19
3.1.1 Requirements on the Structure ..... 19
3.1.2 Requirements on Applicability ..... 20
3.1.3 Requirements on Economic Consideration ..... 21
3.2 Hip Exoskeleton Geometric Structure ..... 22
3.2.1 Position Analysis ..... 22
3.2.2 CAD Design ..... 24
3.3 Kinematics Analysis ..... 27
3.3.1 Mobility Analysis ..... 27
3.3.2 Inverse Kinematics Analysis ..... 33
3.3.3 Jacobian Matrix ..... 36
3.3.4 Stiffness Analysis ..... 37
3.4 Sensing and Controlling of the System ..... 41
3.4.1 Sensor Selection and Placement ..... 42
3.4.2 Control Motor Selection and Placement ..... 46

3.5 The Hip Exoskeleton Interface to the Wearers ....48
Chapter 4 System Optimization ....51
4.1 FEA Analysis ....51
4.1.1 Force ....52
4.1.2 Moment ....57
4.2 Workspace Evaluation ....61
4.3 Stiffness Optimization ....62
4.4 Achievable Improvement of Exoskeleton ....65
4.4.1 Development on Geometry ....65
4.4.2 Development on Comfort Level ....69
Chapter 5 Results and Discussion ....74
Chapter 6 Conclusions ....77
Chapter 7 Future Work ....79
7.1 Prototype ....79
7.2 Materials ....80
7.3 Sensor and Motor ....81
7.4 Further Test and Optimization ....81
Reference ....83
Appendix ....86
Appendix I: FEA Analysis of the Improved Structure ....86
Appendix I.I: Force Application ....86
Appendix I.II: Moment Application ....88
Appendix II: FEA Report of the Improved Structure ....91

# Table of Figures

Figure 1.1: The Basic Structure of a Serial Robotic Manipulator ..... 2
Figure 1.2: The Basic Structure of a Parallel Robotic Manipulator ..... 3
Figure 1.3: CNC Mechanism Tool..... 4
Figure 1.4: Cyberdyne Hal-5 ..... 5
Figure 1.5: Berkeley Lower Extremity Exoskeleton ..... 5
Figure 1.6: Spring Walker ..... 6
Figure 1.7: Murdered Professor's Walking Aid ..... 7
Figure 2.1: Principal Planes of the Human Body in a Standard Anatomic Position ..... 12
Figure 2.2: Eight Phases in a Gait Cycle ..... 12
Figure 2.3: A Normal Gait Cycle..... 13
Figure 2.4: Sagittal Plane Hip Motion ..... 15
Figure 2.5: Sagittal Plan Thigh Motion ..... 115
Figure 2.6: Moment and Power Profiles of Hip Motion..... 16
Figure 2.7: Muscle Action during Gait..... 17
Figure 3.1: CAD Model of the Designed Hip Exoskeleton ..... 25
Figure 3.2: Prismatic Joint ..... 28
Figure 3.3: Universal Joints ..... 28
Figure 3.4: Simplified Schematic Diagram of the Hip Exoskeleton Unit ..... 29
Figure 3.5: A Simplified Limb of the Manipulator Structure..... 30
Figure 3.6: Stiffness Results in Z direction of the Hip Exoskeleton ..... 39
Figure 3.7: Stiffness Results in Y direction of the Hip Exoskeleton..... 40
Figure 3.8: Stiffness Results in X direction of the Hip Exoskeleton..... 40
Figure 3.9: Theory of Sensing and Controlling ..... 42
Figure 3.10: Surface EMG Signal Processing and Data Processing Circuit..... 44
Figure 3.11: Placement of SEMG Sensor Electrodes ..... 445
Figure 3.12: The Location of Servo Motors ..... 46
Figure 3.13: Servo Motor Working Principle..... 47
Figure 3.14: The Structure of Limit Switch..... 48
Figure 3.15: CAD Model with two Leg Exoskeletons ..... 50
Figure 4.1: Finite Element Model of the Hip Exoskeleton..... 52

Figure 4.2: Total Deformation based on Applied Force ..... 52
Figure 4.3: Deformation in X, Y, Z-axis based on Applied Force ..... 54
Figure 4.4: Equivalent Stress based on Applied Force ..... 555
Figure 4.5: Equivalent Elastic Strain based on Applied Force ..... 56
Figure 4.6: Total Deformation based on Applied Moment..... 57
Figure 4.7: Deformation in X, Y, Z-axis based on Applied Moment ..... 59
Figure 4.8: Equivalent Stress based on Applied Moment..... 60
Figure 4.9: Equivalent Elastic Strain based on Applied Moment..... 60
Figure 4.10: Workspace Volume of the Hip Exoskeleton ..... 62
Figure 4.11: Workspace Volume Optimization Results ..... 64
Figure 4.12: Upgrading CAD Model of the Hip Exoskeleton ..... 66
Figure 4.13: Lower Leg Comparison between Two CAD Modelsl..... 67
Figure 4.14: Joints Comparison Between Two CAD Models ..... 68
Figure 4.15: Total Deformation of Updated Model based on Applied Force..... ..69
Figure 4.16: Lower Leg Belt with an Inner Gimbal at Static Position…….....70
Figure 4.17: Lower Leg Belt with an Inner Gimbal at Moving Position……..……71
Figure 4.18: Lower Leg Belt with a Spherical Gimbal at Static Position…….....71
Figure 4.19: Lower Leg Belt with a Spherical Gimbal at Moving Position……..72
Figure 5.1: Move Forward…….74
Figure 5.2: Move Backward ..... 74
Figure AIII.3: Move Right..... 75
Figure AIII.3: Move Right..... 75
Figure AI.1: Finite Element Model of the Updating Hip Exoskeleton..... 86
Figure AI.2: Total Deformation based on Applied Force..... 86
Figure AI.3: Deformation in X, Y, Z-axis based on Applied Force ..... 87
Figure AI.4: Equivalent Stress based on Applied Force..... 87
Figure AI.5: Equivalent Elastic Strain based on Applied Force..... 88
Figure AI.6: Total Deformation based on Applied Moment ..... 88
Figure AI.7: Deformation in X, Y, Z-axis based on Applied Moment..... 89
Figure AI.8: Equivalent Stress based on Applied Moment ..... 89
Figure AI.9: Equivalent Elastic Strain based on Applied Moment ..... 90

# Table of Tables

Table 3.1: Summary of Human Data for Design ..... 22
Table 3.2: Hip Normal Range of Motion ..... 23
Table 3.3: The Designed Hip ROM ..... 24
Table 3.4: Critical Dimensions of the Manipulator ..... 26
Table 4.1: Optimal Design Parameters for Maximizing Workspace Volume ..... 64

# Chapter 1

# Introduction

Currently, robots are not far away from people's life, such as a surgery arm, service robots, entertain robots, etc. According to the Webster's New World College Dictionary, "a robot is any anthropomorphic mechanical being built to do routine manual work for human beings". However, the Robotics Institute of America gives a more general definition – "a robot is a re-programmable multi-functional manipulator designed to move material, pars, tools, or specialized devices, through variable programmed motions for the performance of a variety of task" [1] To simplify it, a robot is a mechanism that is able to perform tasks on its own or with control [1]. In the past few years, the demand for high performance robots for daily human activities increased rapidly due to the advancement of robotics technology.

Robots are classified into different categories based on various criteria. There are some common criteria used to classify the robots: the size of the robots – micro robots and macro robots; the drive technology – electric, hydraulic, and pneumatic; the workspace geometry; the degrees of freedom; the motion characteristics; and the most comprehensive one, kinematic structure – serial robots, parallel robots, and hybrid robots.

A serial structured robot is also called an open-loop manipulator which is consisted by a number of links connected with either a prismatic or a revolute joint in an

open kinematic chain [2] as shown in Figure 1.1 [3]. The most significant advantage of a serial robot is the large workspace, so it is able to take up a sizable work area easily. Serial manipulator is one of the most common industrial robots due to its large volume occupation. That is because it can be used to carry relatively heavy load or do heavy duty tasks. Therefore, serial robots are the most basic ones selected for heavy load designs or projects.

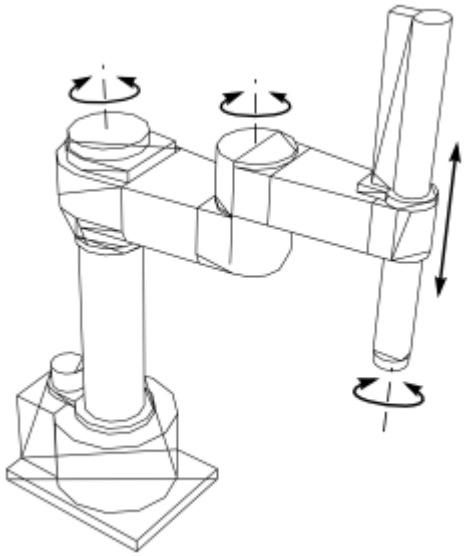

**Figure 1.1: The Basic Structure of a Serial Robotic Manipulator [3]**

Different from a serial robot, a parallel robot has two platforms which are connected by at least two kinematic chains, and the motion is achieved by the end-effector platform [2] as shown in Figure 1.2 [5]. Parallel robots are usually selected to satisfy the need for high accuracy tasks because they have higher operational accuracy, broader range of load capacity, better task flexibility, better reliability and shorter cycle time than that of serial robots [4]. On the other hand, parallel robots have much more complex operation than that of serial ones, and they have limitation on workspace.

Overall, the selection of the robotic structure is based on the requirements of the applications.

**Figure 1.2: The Basic Structure of a Parallel Robotic Manipulator [5]**

In the past few years, more and more parallel mechanisms are chosen because of their high dynamic performance and high stiffness. As a result, the development of the parallel kinematic mechanisms is attracting more and more researchers and industry companies. At the same time, more parallel robot structures are utilized in real applications, such as milling machines, and surface grinders. The 5-axis reconfigurable parallel robotic machine in the Robotics and Automation Laboratory of UOIT is a typical parallel structure based machine tool (Figure 1.3).


**Figure 1.3: CNC Machine Tool**

Because of the attributes of high stiffness, better accuracy, parallel kinematic mechanisms are widely used in biomechanics, such as exoskeleton. There are three principal areas that biomechanics are generally divided into: performance, injury, and rehabilitation [6]. However, this criterion is not strict – some biomechanics have the future that fits all three areas. Based on verity of requirements, different kinematic structures are picked to build different kinds of exoskeletons.

## 1.1 Literature Review

The idea of using exoskeletons to help people with the daily life dates back to 1890 when an apparatus was used for facilitating working, running, and jumping [7]. So far, there are a verity of exoskeletons have been developed for different purposes -- to support or protect the inner skeleton, carry heavy load, and help mankind in the daily life.

Some designs have been fully developed and started to launch on the market, such as Cyberdyne Hal-5 (Figure 1.4) [8], Berkeley Bleek Exoskeleton (Figure 1.5) [9]. Some of them are still in the testing or research stage, such as Spring Walker (Figure 1.6) [7], and Murdered Professor Walking Aid (Figure 1.7) [11], etc. Due to the large demand, the exoskeleton is going to play a much more important role later.

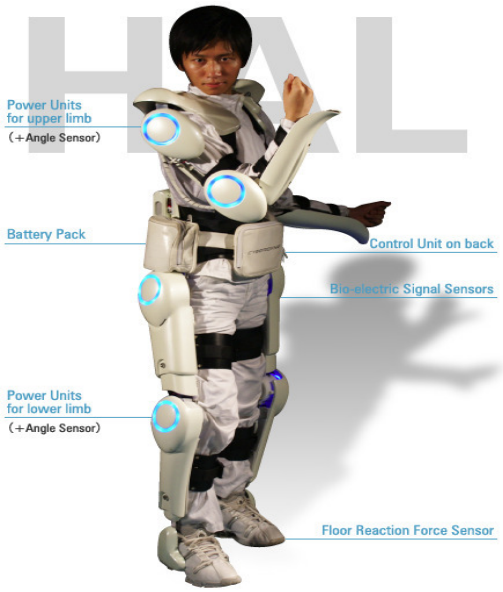


**Figure 1.4: Cyberdyne Hal-5 [8]**

**Figure 1.5: Berkeley Lower Extremity Exoskeleton [9]**

Cyberdyne Hal-5 is a “cyborg-type robot” that is designed for expanding and improving the physical capability of the person who wears it [8]. This robot can be separated into two parts: upper body parts and lower body parts, so people can wear half of it for certain activities without carrying extra load. Cyberdyne Hal-5 can perform most of the daily activities, such as standing, walking, climbing up and down stairs, holding and lifting, so it can be applied in various fields. Also, it can be used for both indoor and outdoor activities due to its hybrid control system [8]. So far, it is the most successful exoskeleton for human routine tasks.

Berkeley lower extremity exoskeleton is mainly designed for the people who have to carry significant loads on their backs with minimal effort over any type of terrain along unstructured outdoor paths. This robot has seven degree of freedom per leg, and four of them are powered by liner hydraulic actuator that can provide a large power [9] [10]. The principle behind this exoskeleton is that “the linear hydraulic actuators add power to the hip, knee, and ankle joints, and then an internal combustion engine provides the necessary electric and mechanical power for the exoskeleton” [7]. As a result, the wearer is able to carry a significantly heavy load.

**Figure 1.6: Spring Walker [7]**

**Figure 1.7: Murdered Professor's Walking Aid [11]**

The "Spring Walker" was defined as a spring assisted lower body exoskeleton, which was developed in 1991 [7]. It has "the capabilities of running and leaping of all animals, and it allows the wearer to run up to 35mph and leap up to 5 feet into the air" [11].Therefore, it can be concluded as a complex, human powered, kinematic exoskeleton, which is consisted of a kinematic linkage whose joints incorporated springs [7]. As it can be seen, the human feet do not touch the ground because the legs of the "Spring Walker" are in series to the human.

The Murdered Professor's Walking Aid was designed in order to recover from a disease called Sarcophenia, which causes the lost of skeletal muscle [11]. The power is added on to the lower leg and feet, and assists the leg moving forward and backward. This exoskeleton should be classified into to the rehabilitation biomechanics category. After it is been completed, it should be able to help a lot of patients.

## 1.2 Subject of the Study

As mentioned above, robots are able to work by themselves after engineers or scientists programmed them, but the fact is that the robots need to be supervised, edited and improved to satisfy the growth requirements from time to time. It is the same as exoskeleton. As time goes by, further and more specific requirements come into sight.

If taking exoskeleton as an example, it is easy to explain. There are some developed mechanisms which can help people move around, such as a scooter. However, it is not that convenient when people are in a small space, such as in a room, so a wearable mechanism is required. As a result, Cyberdyne Hal-5 could be a solution. Nevertheless, people want to have something especial for their hip if they only have hip problems rather than have their entire body or entire leg covered by mechanism. In order to meet the requirement, a partial mechanism is a better solution. However, it has to be able to have the same ability as the wearer request, for instance, assisting to do the routine movements – walking.

The hip exoskeleton unit introduced in this thesis is designed and analyzed for the people who need special assistant with the hip movements. Comparing with a whole body mechanism, a partial manipulator unit is more convenient and much lighter. As a result, this product should take the people who have had hip surgeries, the elderly who cannot move their legs properly as a target market. Almost all existing exoskeleton assistant mechanisms are designed as a serial structure or a hybrid one, but the above mentioned target market have request of safety rather than speed. Therefore, a parallel structure manipulator is more suitable due to the advantage of accuracy.

## 1.3 Motivation

In summary, the thesis presents an improved architecture to a fully actuated three-degree of freedom parallel structure hip exoskeleton unit. Specifically, the parallel structure of this biomechanics was analyzed, and it has proved that the design of the manipulator is ready to go to the next step - prototype. Also, sensors and motors have been introduced, and this provides a guideline to the future research. More or less, the partial manipulator idea will lead people to consider developing lighter and easier robots to satisfy more practical requirements. Therefore, these analyses will guide the future research effort.

## 1.4 The organization of the Thesis

This thesis postulates the following questions and attempts to prove the solutions by several methods.

- **Hypothesis I**: It is reasonable to design a parallel structure three-degree of freedom hip exoskeleton unit that helps wearers to move their legs properly;
- **Hypothesis II**: The designed structure is reasonable, reliable, convenient, and state-of-the-art.

This thesis consists of seven chapters and the road map of this thesis process as follows:

Chapter 2 introduces the background of some terms associated with human walking and human gait cycle data at the hip. Also, it gives a brief idea of the muscle motion which affects the sensors detection.

Chapter 3 presents the CAD model of the hip exoskeleton unit. Kinematic analysis consisted by mobility analysis, inverse kinematics analysis, Jacobian matrix analysis and stiffness analysis is fully discussed, which give the detailed answer to the thesis questions. At the end of this chapter, control and actuation that includes sensors and motors are introduced in general. This chapter is the major part of the solution of the thesis postulate.

Chapter 4 focuses on the optimization of the designed system. First, a FEA analysis with a computer program called ANSYS is brought in to assist proving the structure of the model. Then, the optimization and potential improvement of the unit are given. This chapter is also one of the major contents to the thesis postulate.

Chapter 5 deals with the results and discussion based on the data and comparison obtained in the previous chapters.

Chapter 6 brings together the most important information discussed and lead to the final conclusion of this thesis.

Chapter 7 provides suggestions and a guideline for the next steps and future work that could improve the design to a higher level.

# Chapter 2

# Biomechanical Gait Analysis

This chapter presents the background of the biomechanics– particular human walking biomechanics and introduced the muscle motion during a regular gait cycle. The energetic of walking during a walking cycle is described. This information provides the requirements for the hip exoskeleton unit. From this detail information, the specifications of the actuation and control of the proposed exoskeleton are introduced.

## 2.1 Regular Human Gait Cycle

In order to better understand the relation of human body's joints, a Cartesian coordinate system can be used to display relation of a human body (Figure 2.1), and the three defined planes are useful in biomechanics analysis. As described below: the X-Y plane is called the transverse plane (or horizontal plane) that divides the body into upper and lower parts; the X-Z plane is called sagittal plane (or median plane) that divides the body left to right; the Y-Z plane is called coronal plane (or frontal plane) that divides the body front to rear [6]. By using this three defined planes, the gait cycle can be analyzed, since walking of human being is a three dimensional motion. In the following discussion, the sagittal plane is the only one taking into the analysis because there is has a much larger motion comparing with the other two planes [12].

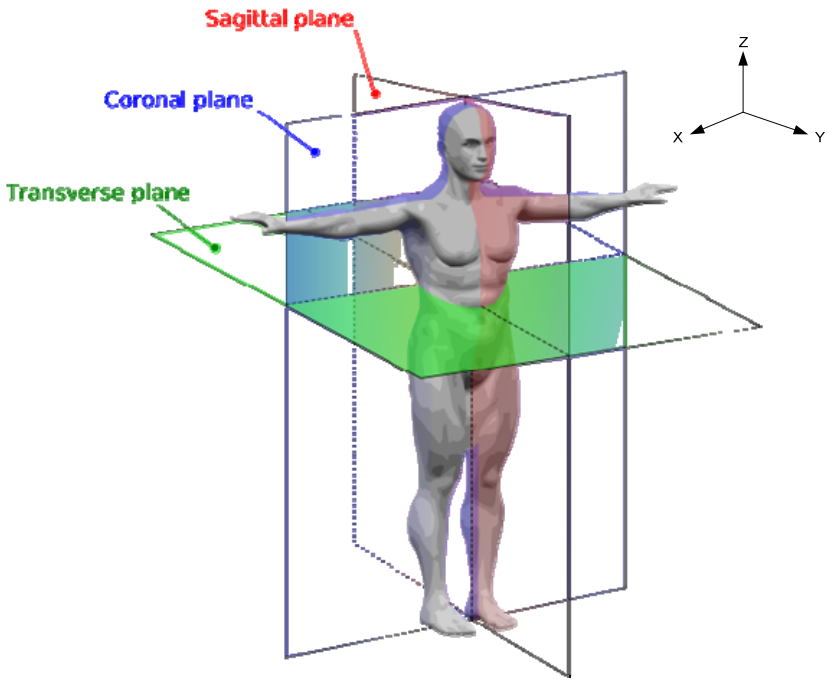


**Figure 2.1: Principal Planes of the Human Body in a Standard Anatomic Position [6]**

According to Dr. Jacquelin Perry [2], gait analysis is consisting of Normal and Pathological Function. There are eight walking phases included in a gait cycle, which can be grouped into two periods: stance and swing [12]. Figure 2.2 shows the outline of eight walking phases in a gait cycle, which also provides a detailed simulation of the individual joint motion in the limb diagram.

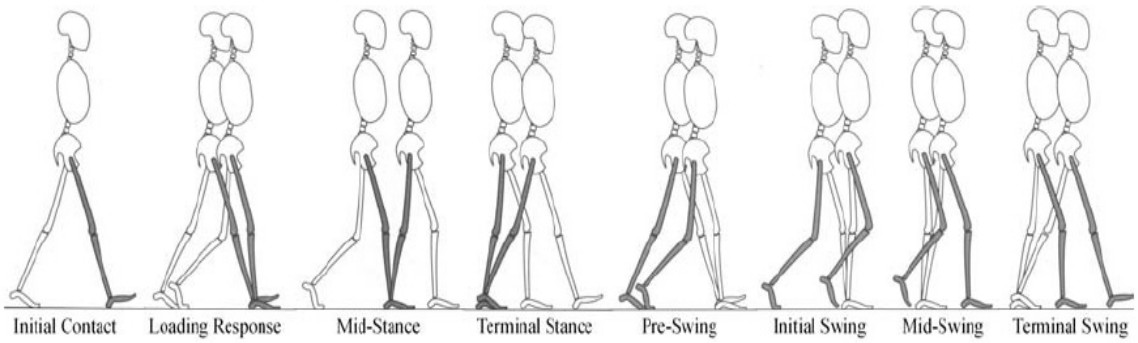


**Figure 2.2: Eight Phases in a Gait Cycle [12]**

Figure 2.3 is made based on the analysis mentioned above and the research has been done for the gait cycle, which shows the relationship between the walking periods and phases, which is also considered as the divisions of the gait cycle. If a full normal gait cycle is set as 100%, each of the phases has a certain part of it, but not equal to each other as shown in the following figure. There are two tasks that should be in the stance period: one is called weight acceptance, and the other is called single limb support; then the swing limb advancement is completed in the swing period to complete the entire gait cycle [12]. In a simple explanation, first, the body is giving an order to move forward. Then, the body is decelerated and stabilized by the muscles at the leg which includes hip, knee and ankle. At the end of the stance period, a pre-swing step is achieved, that is where the ankle is powered by the weight transferred from the hip and knee in order to move the body forward. One thing needs to be mentioned here that the pre-swing phase is considered as the last step of the stance period as well as the first step of the swing period. As Figure 2.3 shown, each step has a different time range.

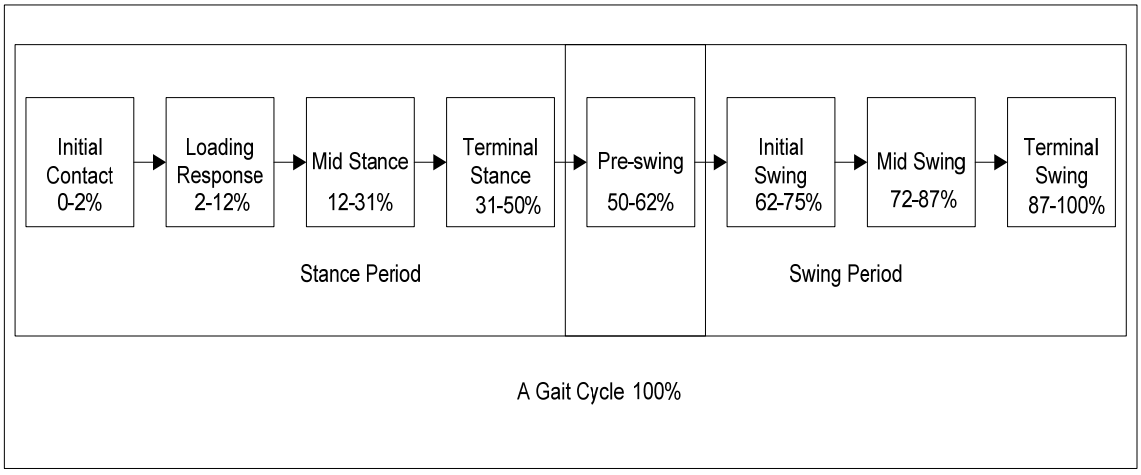


**Figure 2.3: A Normal Gait Cycle**

The principle behind the gait cycle could help to extract the requirements of the design that will be discussed in the next chapter. However, due to the purpose of this thesis, only the hip kinematics and kinetics are going to be fully studied in this chapter.

## 2.2 Kinematics and Kinetics of the Gait

As defined, biomechanics are the applications of mechanical principles to biological or living systems, which include humans, animals, organs, and cells [6]. Most commonly, biomechanics are considered as the mechanics which are applied on human body. In order to develop the most adaptable and suitable mechanism, the kinematics and kinetics of the motion need to be completely understood.

As mentioned above, the major motion of the hip during a gait cycle on the sagittal plan. At the same time, the hip motion follows an approximate sinusoidal pattern as shown in Figures 2.4 [6] [12] [13] (this figure is built based on the data obtained from the reference, the same as Figures 2.5 – 2.6). This figure also gives the range of the hip motion, which is in the range of -20 to 40 degree. Here the positive motion means flexion while the negative motion means extension. From the Figures 2.3 and 2.4, the peak hip motion is in the Loading Response Phase and the Mid Swing Phase, which is reasonable because the two legs have the largest distance between them at these two positions. The low point is between the Terminal Stance and the Pre-swing phases, and that was the same as expected.

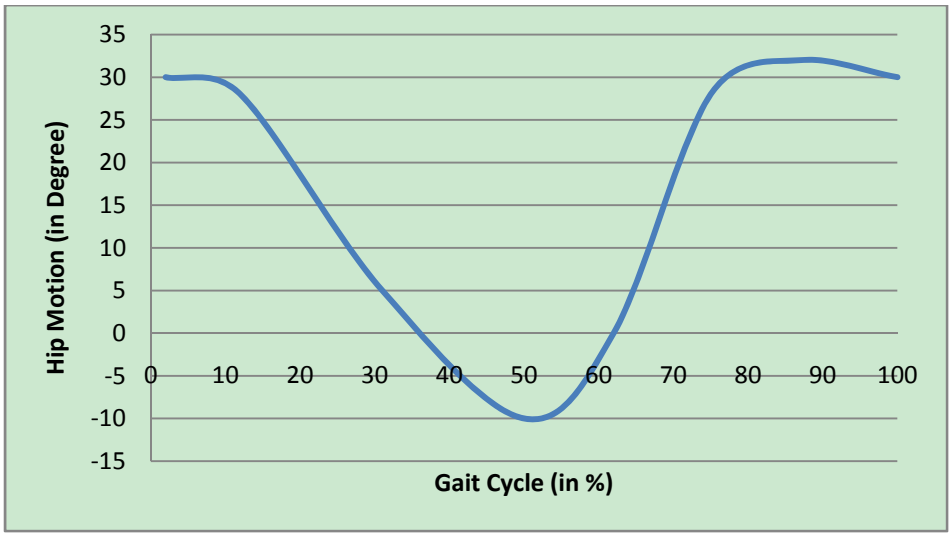


Figure 2.4: Sagittal Plane Hip Motion

Because the hip exoskeleton end-effector is on the thigh, and the thigh motion is taken into consideration when the manipulator is designed. The thigh motion is similar to the hip motion, which also follows an approximate sinusoidal pattern. Comparing the Figures 2.4 and 2.5 [6] [12] [13], the major difference between these two motions is the motion range. The thigh motion range is between -25 to 30 degree. The reason for that is the position difference [12]. In other words, the hip exoskeleton should be fine if it satisfies the hip motion requests.

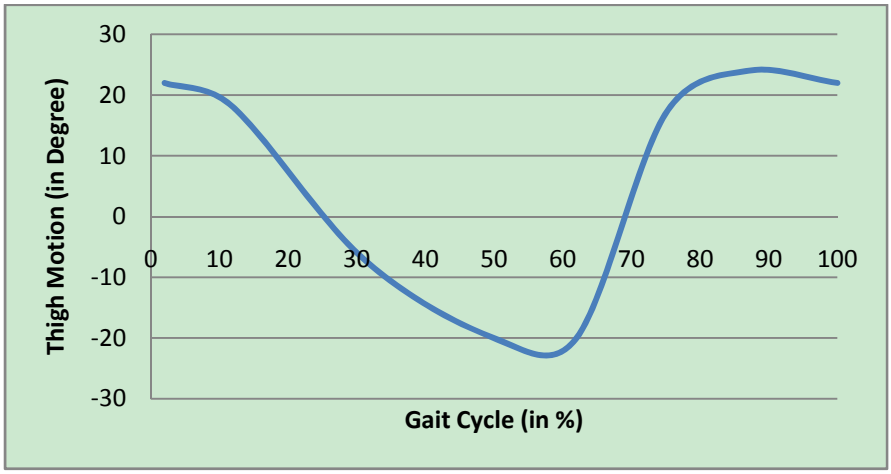


Figure 2.5: Sagittal Plan Thigh Motion

The hip moment and power profiles of the gait cycle can be shown in Figure 2.6 [6] [12] [13]. The hip moment and power can be considered as the combination of the work from all different muscles. In this case, there are three elements counted: extensor, flexor, and thigh. The extensor moment and power are still set as positive, and the flexor moment and power are set as negative. The range of the moment is between -130N.m and 130 N.m, and the range of the power needed for the hip motion is in a range of -100N.m to 150 W. For the same reason, if the moment and the power profile can supply the hip motion, it is big enough to supply the thigh motion. The peak negative power needed is in the phase of Terminal Stance, and the peak positive power needed is in the Pre-swing phase that is called "pull-off" [13].

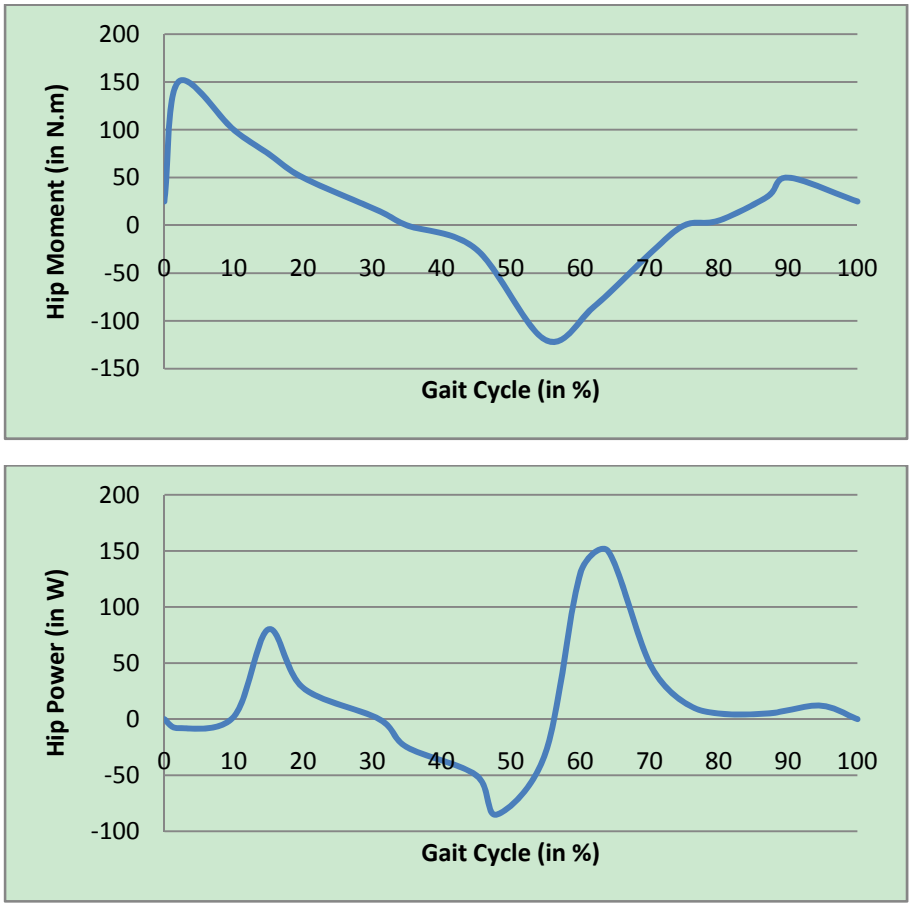


**Figure 2.6: Moment and Power Profiles of Hip Motion**

The hip exoskeleton unit should be able to accommodate the hip's basic motion of which is flexion/extension, abduction/adduction, and medial/lateral rotation (3-DOF motion). Also, it should be able to supply the power needed for the hip and thigh motion as the profiles show. As expected, the study of the kinematics and kinetics of hip helps to generate the general ideas of the design of the control and actuation parts of the hip exoskeleton. More specific requirements of the kinematics and kinetics of hip will be discussed in the following chapters.

## 2.3 Muscle Action in Gait Cycle

In a gait cycle, the action of the muscles which controls the major action of the hip is studied in order to apply the principles. The major activities of theses muscles that are considered as flexor/extensor and abductor/abductor are shown in Figure 2.7 [12].

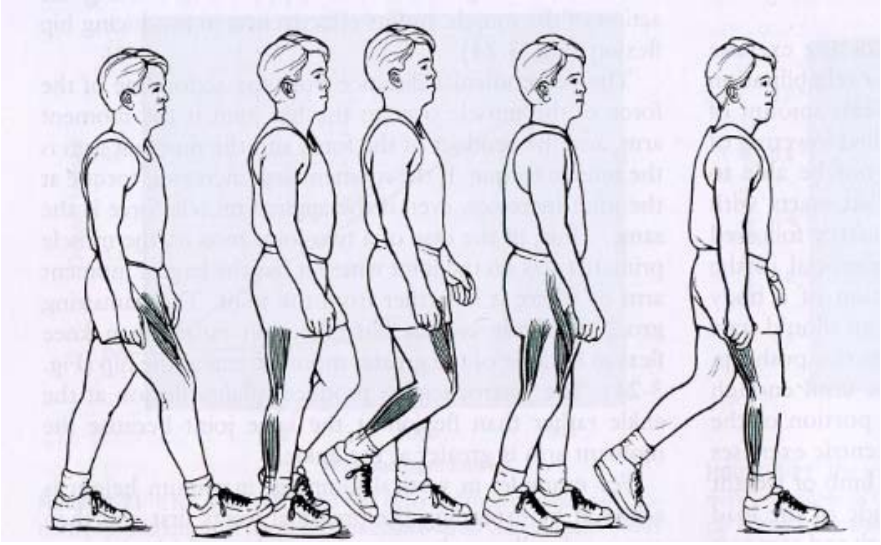

(a) (b) (c) (d) (e)

**Figure 2.7: Muscle Action during Gait [12]**

In this figure, only the thigh muscles are named because they are the ones that act on the exoskeleton. At each step, only few of them actually work. In Figure 2.7, (a): Sartorius and Rectus femoris; (b): Biceps femoris; (c) Rectus femoris and adductor longus; (d): Rectus femoris, Biceps femoris, and Sartorius; (e): Biceps femoris and Adductor fagnus [10].

During a normal gait cycle, there are five primary muscles act for flexion/extension and abduction/adduction which are called Recues femoris, Biceps femoris, Sartorius, Adductor longus, and Adductor magnus [14]. As discussed above, there are two periods in a gait cycle: stance and swing. In the stance period, these muscles are extensors and adductors. On the other hand, these muscles become flexors during the swing period. As a consequence, a fact is that a walking action can be actuated possibly if the muscle action can be detected and passed to an actuator.

In general, the kinematics and kinetics of the hip offers the desire on the motor part of the designed hip exoskeleton, the principle of the muscle activity in gait provides the requirements on the sensor due to the type of sensor is selected for the mechanism.

# Chapter 3

# General Design of the Hip Exoskeleton Unit

## 3.1 The Purpose of the Hip Exoskeleton Unit

The primary purpose for developing this manipulator is to provide the wearers the assistant they need during normal gait motion. Therefore, certain conditions have to be met at the same time in designing and building this unit. The basic requirements on the robotic manipulator -- hip exoskeleton -- are high operational accuracy, adaptability, dexterity, and reliability, which can be grouped in the following three categories.

### 3.1.1 Requirements on the Structure

Based on the current study, most of the existing exoskeleton robots are serial structure due to its large workspace and easy to control, and most of these manipulators do not require a high accurate movement. For example, there is no difference for the people who wear BLEEX when the exoskeleton helps them move a little bit further or higher. Another significant character of these existing exoskeletons is the large occupation.

For this design, the precision of the manipulator is one of the critical criteria. The reason is that it may not be a major issue to have a low accurate movement exoskeleton

for a healthy person, but it proves to be a big challenge for the wearers who are injured or need to rehabilitate from a hip surgery. These people do not need a fast movement or carrying heavy loads but a more precise support. In order to keep them safe and comfortable, a parallel structure based design for hip exoskeleton is necessary.

To accommodate a normal hip motion during walking, the hip exoskeleton has to be able to perform motion of flexion/extension, abduction/adduction, and medial/lateral rotation (3-DOF motion). A PUU, (prismatic joint - universal joint - universal joint), structure of the links is proposed to fulfill the desired work.

A reasonable and reliable structure is the most important part of this manipulator. To verify the structure, a series of analysis has been completed after the hip exoskeleton model is built in SolidWorks.

### 3.1.2 Requirements on Applicability

Different wearers need different sizes of hip exoskeletons, so that the manipulators can provide a good fit and suit them best. However, it is tedious, expensive and implausible to have each and every hip exoskeleton custom made. To come up with general design specifications that would be suitable for most people is a bug challenge in the designing process. This is discussed later in greater detail.

Also, the sizes of the wearers are very diversified – different heights and different weights. A regular hip exoskeleton has to be strong enough for most of people. Hence, there is a specific requirement on the rigidity of the system, and it is one of the most important criteria to verify the structure of this design.

The manipulator is used to assist a regular daily activity – walking, so this design does not need to have any feature to assist other activities, such as running, sitting, and jumping. Nevertheless, the wearers have to sit sometime while they are wearing the hip exoskeleton. In that situation, the exoskeleton must be easy to take off or put on.

### 3.1.3 Requirements on Economic Consideration

There is wear or tear during the usage, and some parts may break before other parts do. In most cases, it is not worth buying a new suit and should just replace the broken part if the important parts of the hip exoskeleton are still in good conditions, so there are requirements on repair and replacement for certain parts of the manipulator.

In short, the designed hip exoskeleton has to be designed to satisfy all the following requirements:

1. A parallel robotic structure is necessary;
2. The assistance robot moves forward, backward, and sideway;
3. High accuracy – safety issue;
4. Enough stiffness – strong enough;
5. Light weight – easier to carry;
6. Adjustable – fit most people;
7. Easy to wear/take off - convenient;
8. Easy to assemble – comfort level;
9. Modular design for repair convenience – economic concern.

## 3.2 Hip Exoskeleton Geometric Structure

To build the CAD model, a typical wearer needs to be selected because the human data is going to be refereed. In view of that a fundamental structure of the hip exoskeleton should be able to sustain most wearers (reliable for big size people), the selected wear is a thirty years old male who provides the following body data for the design without taking tolerance into consideration. This data are reasonably close to that of the MIT test participant who was of the same age [7].

**Table 3.1: Summary of Human Data for Design [7]**

| Elements | Unit | Dimensions |
|---|---|---|
| Age | year | 30 |
| Sex | male | - |
| Height | cm | 178 |
| Weight | Kg | 85 |
| Waist size | cm | 130 |
| Top part of the thigh size | cm | 58 |
| Low part of the thigh size | cm | 50 |
| Leg length | cm | 100 |
| Walking speed | m/s | 0.65±0.15 |

### 3.2.1 Position Analysis

The movement of the hip for a regular walking motion is considered as a three-degree of freedom (3DOF) motion in three motion planes (x-y plane, y-z plane, and x-z plane). These three planes can be called as transverse plan, coronal plane, and sagittal plane.

The hip range of motion (ROM) of a normal gait cycle in healthy individuals reported in the literature provides the following data according to the obtained data from the relevant materials [6] [14].

**Table 3.2: Hip Normal Range of Motion [6] [14]**

| **Reference/ Unit** | **Flexion** | **Extension** | **Abduction** | **Adduction** | **Medial Rotation** | **Lateral Rotation** |
|---|---|---|---|---|---|---|
| | **cm** | **cm** | **degree** | **degree** | **degree** | **degree** |
| Roass and Andersson | 12 ± 2.3 | 9 ± 3.2 | 39 ± 7.2 | 31 ± 7.3 | 33 ± 8.2 | 34 ± 6.8 |
| Roach and Miles | 12.1 ± 1.3 | 12 ± 5 | 42 ± 11 | - | 32 ± 8 | 32 ± 9 |
| Departments of the Army | 12 | 10 | 45 | 30 | 45 | 45 |
| Gerhardt and Rippstein | 12.5 | 15 | 45 | 15 | 45 | 45 |
| Average | 12.15 | 11.5 | 42.75 | 25.33 | 38.75 | 39 |

The above data are referred from healthy individual; the people who need to wear the manipulator cannot have a larger ROM than it. If the manipulator can achieve the above ROM, it is more than good enough for a regular wearer. Also, the exoskeleton ROM is different from the inner-skeleton. Thus, the designed exoskeleton has to meet the following possible position ranges in Table 3.3 in order to help people to achieve the possible average daily activities.

Table 3.3: The Designed Hip ROM [6] [12] [14]

| Movement Plane | Motion | Maximum Displacement | Designed Displacement |
|---|---|---|---|
| Sagittal Plane | Forward | 60 degree | 70 degree |
| | Backward | 30 degree | 35 degree |
| Coronal Plane | Up/Down | 10 cm | 15 cm |
| Transverse Plane | Outside | 45 degree | 50 degree |
| | Inside | 20 degree | 25 degree |

After a model is built, a series of comprehensive analysis will be tested to quantify and validate this designed structure, such as mobility analysis and inverse kinematic analysis.

Furthermore, this design has to take the considerations on motor control, sensors and actuator, and manufacturing material.

### 3.2.2 CAD Design

The primary CAD model of the 3-DOF P-U-U parallel structure hip exoskeleton has been built with SolidWorks (see Figure 3.1) based on the previous research and analysis has been done.

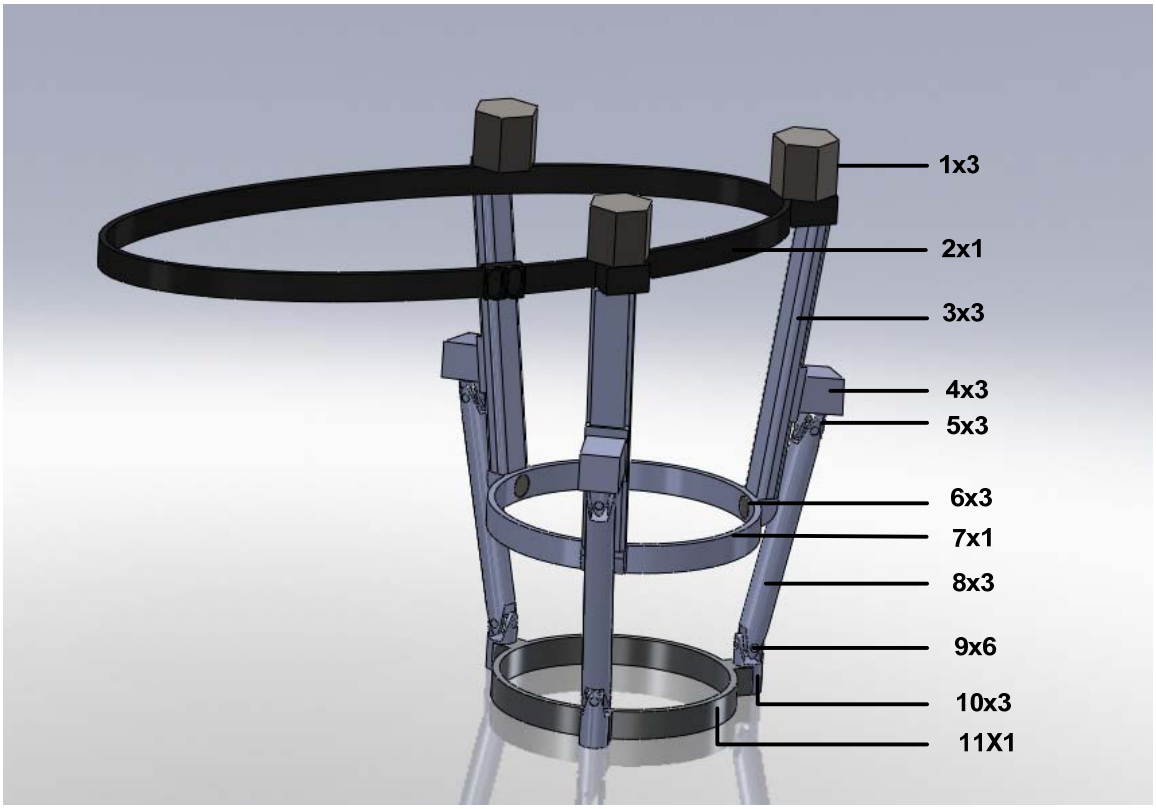


**Figure 3.1: CAD Model of the Designed Hip Exoskeleton: (1) Motor (2)Waist belt (3) Upper leg (4) Leg joints (5)Upper leg joint (6)Sensor connecting point (7) Upper leg belt (8) Lower leg (9)screw (10) Lower leg joint (11) Lower leg belt**

This model is built by taking a regular size person as a dimension reference in Table 1. As the figure shows, the top part is the waist belt that will be fixed on patient's waist, and the size of the belt can be adjusted based on the size of waist of the operator. As a result, the full amount weight of the structure will be carried on the patient's waist. This could be a problem for the patients who may not be able to carry such a heavy structure.

The second belt and the top thigh belt are tied on the top part of thigh, which can be adjusted the size as the waist belt. The purpose of this belt is to fix the path of the bottom poles. The bottom thigh belt is tied on the bottom of the thigh, and it senses the

motion of the leg and actuates the motion to the poles in order to generate the movement of the manipulator. As a result, three motors and five sensors are needed though there are six poles due to the power needed. Also, there is no need for cable to pass the signals due to the position of sensors. The entire system can be considered as a non-cable-driven parallel mechanism.

Based on dimensions of an average size person, the most important dimensions of the structure (Table 3) are modeled by calculating the displacement and motion output of the work platform or the motion of the legs. These dimensions are from the CAD model that introduced above, and will be used for further analysis.

**Table 3.4: Critical Dimensions of the Manipulator**

| Part Names | Dimensions | Units |
|---|---|---|
| Inner waist | 1300 | mm |
| Outer waist | 1420 | mm |
| Thickness of waist | 5 | mm |
| Length of lower leg (l) | 200 | mm |
| Thickness of the upper leg | 20x30 | mm |
| Length of upper leg | 180 | mm |
| Diameter of the lower leg | 20 | mm |
| Inner of the upper thigh length (R) | 565.48 | mm |
| Inner of the lower thigh length (r) | 502.65 | mm |
| Diameter of the belt joint | 20 | mm |
| Height of the belt joint | 40 | mm |
| Angle between the upper leg and the leg belt (θ) | 70 | degree |
| Angle between each leg | 120 | degree |

The weight of the hip exoskeleton is not determined due to the variety of the materials used for each part.

## 3.3 Kinematics Analysis

The structure of the entire system is verified by completing the following kinematics analysis.

### 3.3.1 Mobility Analysis

The degrees of freedom (DOF) of a mechanism are the number of independent parameters or inputs needed to specify the configuration of the mechanism completely. The DOF of a mechanism or mobility determination can be examined by using the Chebychev-Grübler-Kutzbach's Formula [15]:

$$M = d(n - g - 1) + \sum_{i=1}^{g} f_i \tag{1}$$

Where:

$M$ : Degrees of freedom of a mechanism,

$d$ : DOF of the space in which a mechanism is intended to function ($d = 3$ for planar motion, and $d = 6$ for spatial motion),

$n$ : Number of links in a mechanism, including the fixed link,

$g$ : Number of joints in a mechanism, assuming that all joints are binary,

$f_i$ : Degrees of relative motion permitted by joints $i$.

This parallel hip exoskeleton can be simplified as a 3 P-U-U (prismatic, universal, and universal) joints manipulator. The three motion poles actuated by the prismatic joints which are connected to the motor (Figure 3.2), and pass the signal to the end effector-platform by the two universal joints (Figure 3.3). A prismatic joint has one degree of

freedom and imposes five constraints between the paired elements, and a universal joint has 2 degree of freedom [2]. As a result, each limb of the manipulator has:

$$f_i = 1+2+2=5 \; DOFs \qquad (2)$$

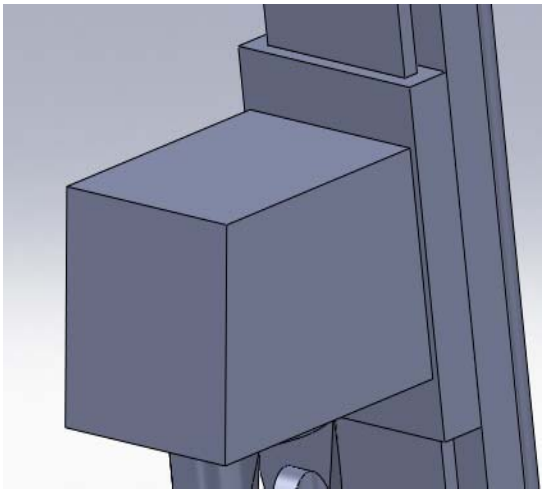

**Figure 3.2: Prismatic Joint**

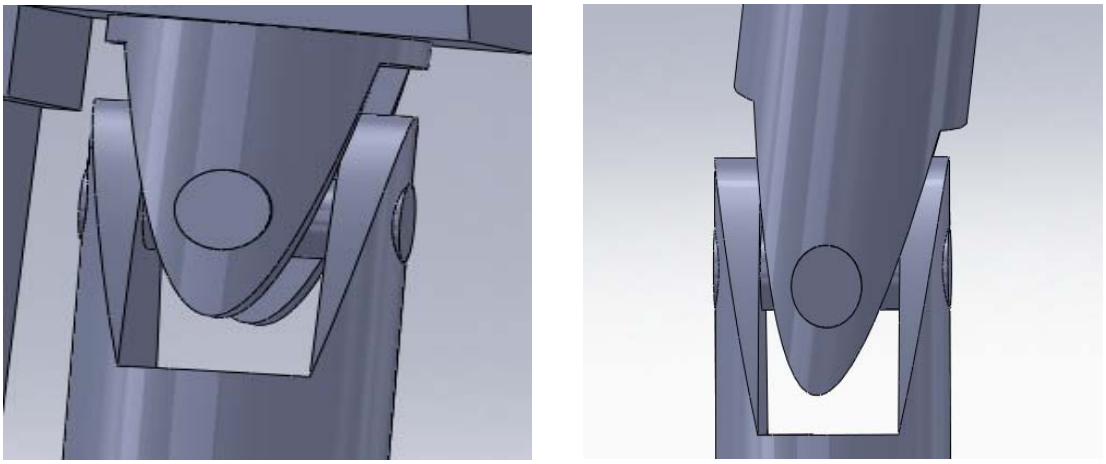

**Figure 3.3: Universal Joints**

The simplified hip exoskeleton can be shown as a schematic diagram in Figure 3.4. By analyzing this schematic diagram, we can get the DOF of the hip exoskeleton is three by applying the Chebychev-Grübler-Kutzbach's formula,

With d =6; n = 8; g = 9; $f_i$ = 5,

$$M = 6 \times (8 - 9 - 1) + 3 \times (1 + 2 + 2) = 3 \qquad (3)$$

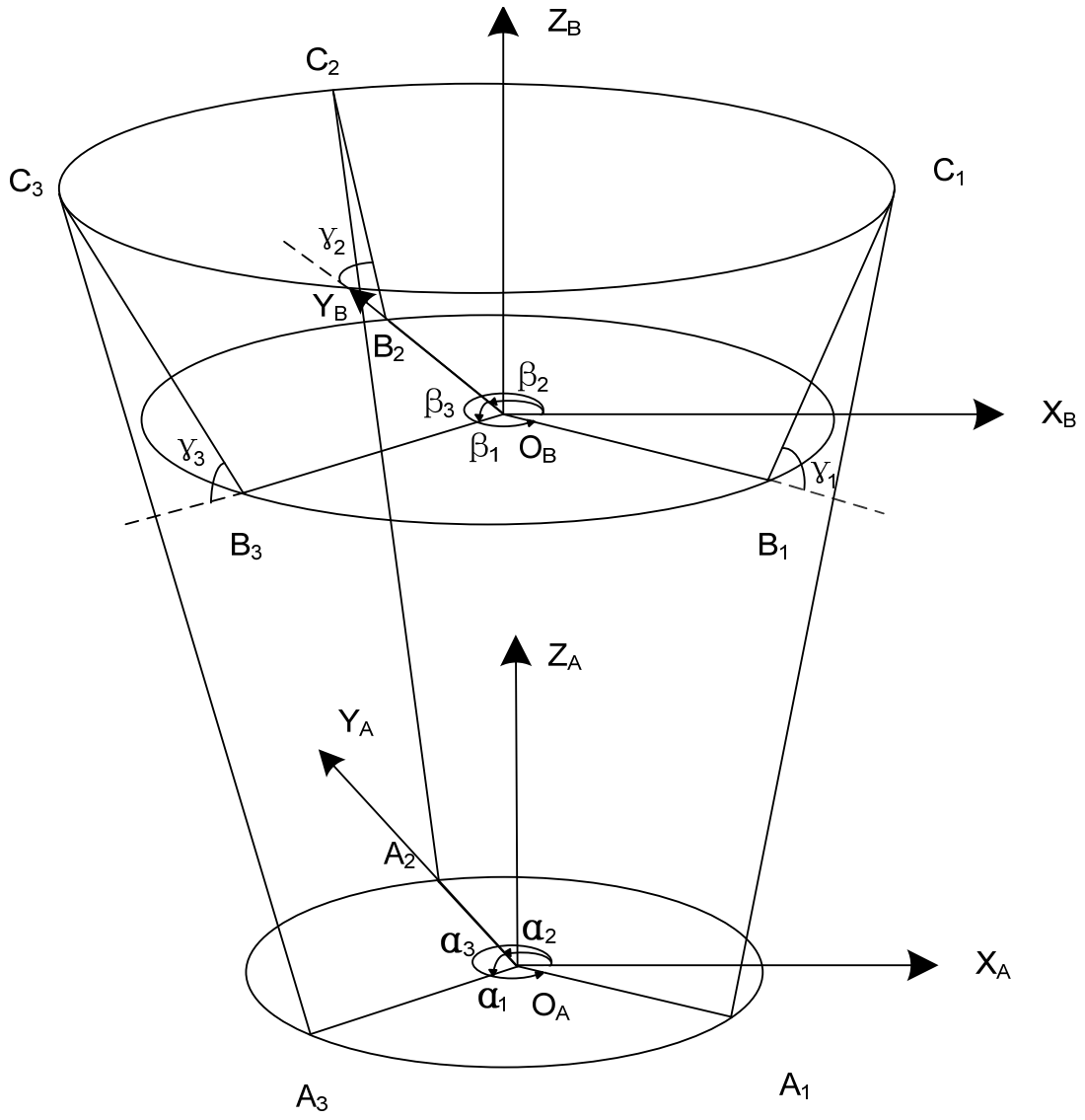


**Figure 3.4: Simplified Schematic Diagram of the Hip Exoskeleton Unit**

From Figure 3.4, we can see that this manipulator has two platforms, the base platform, $B_1B_2B_3$, and the end-effector moving platform, $A_1A_2A_3$. The coordinate axis of the inertial frame is labelled as $O_B$-$X_BY_BZ_B$ at the center of the base platform, and $Y_B$-axis is aligned with the point $B_2$. The moving frame denoted the coordinate axis as $O_A$-$X_AY_AZ_A$, and $Y_A$-axis is coincident with the point $A_2$. The motions of the end-effect platform on the bottom are caused by the actuators which are posited on the top base

platform. The prismatic joints realize the path for the moving legs with the top universal joints. The end-effector platform moves by taking the reaction from the bottom universal joints which connected to the bottom legs of the manipulator [16].

As discussed above, the 3 DOFs represents the translations which are along X axis, Y axis and Z axis since the motions are constrained by the six universal joints (three on the top, three on the bottom). In order to analyse the structure of the manipulator, a limb of the entire system is analyzed. The following figure shows a limb view of the parallel structure hip exoskeleton.

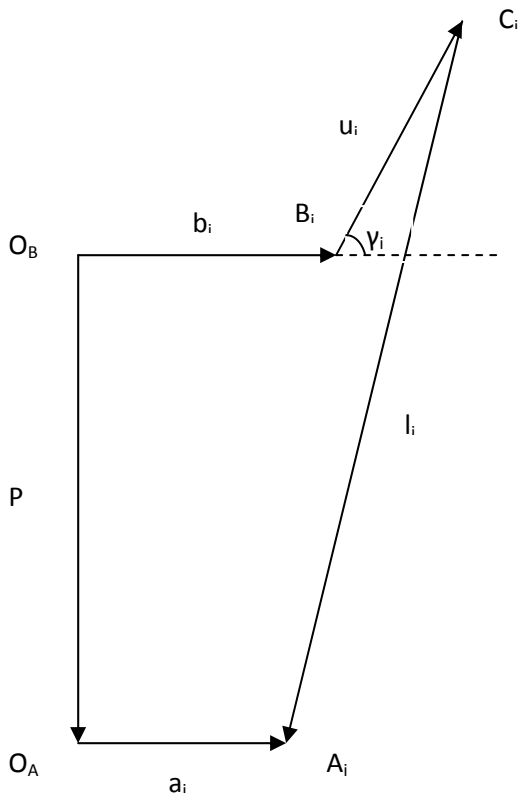


**Figure 3.5: A Simplified Limb of the Manipulator Structure**

As shown in Figure 3.5, the reference coordinate system $O_B$-$X_BY_BZ_B$ at the center of the Base-plate is established, $Y_B$-axis will pass through the point $B_2$. $O_A$-$X_AY_AZ_A$ at

the center of the middle-plate and $Y_A$-axis will pass through the point $A_2$. Also, we can get the following statement from Figure 3.5.

1. $\mathbf{p}_A^B = \begin{bmatrix} p_X & p_Y & p_Z \end{bmatrix}^T$ is the vector from $O_B$, the origin of the base frame, to $O_A$, the origin of the moving platform,
2. $u_i = \begin{bmatrix} u_{ix} & u_{iy} & u_{iz} \end{bmatrix}^T$ is the vector from $B_i$ to the first universal joint $C_i$. Note that $\|u_i\| = u_i$ is the length of the $i^{th}$ actuator,
3. $\mathbf{l}_i = \begin{bmatrix} l_{ix} & l_{iy} & l_{iz} \end{bmatrix}^T$ is the vector from $C_i$ to $A_i$ of the $i^{th}$ leg. It should be noted that $\|\mathbf{l}_i\|$ is constant for each leg,
4. $\alpha_i$ and $\beta_i$ define the $A_i$ and $B_i$ location (measured from x) within the horizontal plane,
5. $\gamma_i$ defines the angle between $C_i$ and the horizontal platform,
6. $i$ defines the number of legs, $i$ = 1, 2, 3 in this paper.

Dr. Lung-Wen Tsai indicates that a parallel manipulator is classified as symmetrical if it satisfies the three conditions which are [2]:

- The number of limbs is equal to the number of degrees of freedom of the moving platform;
- The type and number of joints in all the limbs are arranged in an identical pattern;
- The number and location of actuated joints in all the limbs are the same.

In this thesis, the designed hip exoskeleton has 3DOF structure, and it has three limbs. Hence, this parallel manipulator is a symmetrical one.

Parallel mechanisms are grouped into three categories in general: planar, spherical, and spatial mechanisms. The connectivity of a limb, $C_k$, is a bright criterion to enumerate and classify parallel manipulators by applying the Connectivity Equation [2].

$$\sum_{k=1}^{m} C_k = (\lambda + 1)M - \lambda \tag{4}$$

With a condition of that the connectivity of a limb should not be greater than the motion parameter and less than the DOF of the moving platform, which is [2]:

$$M \le C_k \le \lambda \tag{5}$$

Where:

M: is the numbers of degrees of freedom;

λ: is the degree of freedom of the space in which a mechanism is intended to function;

$C_k$: is the system connectivity.

m: is the number of limb

In this thesis, the manipulation has 3 DOF and three limbs, so λ =3, M=3. Substituting λ and M into Eq. (4) and (5), we get

$$C_1 + C_2 + C_3 = 4M - 3 = 9 \tag{6}$$

And

$$3 \le C_k \le 3 \tag{7}$$

Therefore, the connectivity of each limb should be equal to 3, which means that each limb should have 3-DOF in its joints. This manipulator is a planar parallel manipulator because all the moving links in the mechanism perform planar motion [1]. Overall, the P-U-U structure of the hip exoskeleton is feasible based on the above calculation.

### 3.3.2 Inverse Kinematics Analysis

The purpose of the inverse kinematic analysis is to initialize the movement of the actuator from a given position of the mobile platform [17]. As shown in Figure 3.4, the actuator path of prismatic joints is located on the base platform and the moving platform (end effector) is parallel to the base, and Z-axis is perpendicular to the base and moving platforms.

The position vectors of points $A_i$ and $B_i$ with respect to platforms A and B can be written as

$$^{|A}a_i = \left[a_i \cos\alpha_i, a_i \sin\alpha_i, 0\right]^T \tag{8}$$

$$^{|B}b_i = \left[b_i \cos\beta_i, b_i \sin\beta_i, 0\right]^T \tag{9}$$

So the actuator vector $\mathbf{u}_i$ on the base platform and the end-effector position vector $\mathbf{p}$ can be expressed as

$$u_i = \left[u_i \cos\gamma_i \cos\beta_i, u_i \cos\gamma_i \sin\beta_i, u_i \sin\gamma_i\right]^T \tag{10}$$

$$p = \left[\, p_x, p_y, p_z \,\right]^T \tag{11}$$

The inverse kinematics analysis is to determine the displacement of the actuated variables for a known position and orientation of the end-effector. The joint motions can be derived from this vector loop as shown in Eq. (12).

$$l_i = a_i + p_i - b_i - u_i = \begin{bmatrix} a_i \cos\alpha_i + p_x - b_i \cos\beta_i - u_i \cos\gamma_i \cos\beta_i \\ a_i \sin\alpha_i + p_y - b_i \sin\beta_i - u_i \cos\gamma_i \sin\beta_i \\ p_z - u_i \sin\alpha_i \end{bmatrix} \tag{12}$$

Which yields:

$$\begin{aligned} l_i^2 &= [a_i + p - b_i - u_i]^T [a_i + p - b_i - u_i] \\ &= (a_i \cos\alpha_i + p_x - b_i \cos\beta_i - u_i \cos\gamma_i \cos\beta_i)^2 + \\ &\quad (a_i \sin\alpha_i + p_y - b_i \sin\beta_i - u_i \cos\gamma_i \sin\beta_i)^2 + (p_z - u_i \sin\alpha_i)^2 \end{aligned} \tag{13}$$

The above equation can be written as a function of $u_i$ by considering $u_i$ is the only unknown. The reason is that the length $l_i$ will not change during the operation; $\gamma_i$ will not change during the operation as well; $a_i, b_i, \alpha_i, \beta_i$ can be measured; and $p$ is given. To solve $u_i$, Eq. (13) can be written in the form of Eq. (14).

$$\begin{aligned} &u_i^2 (\cos\gamma_i^2 \cos\beta_i^2 + \cos\gamma_i^2 \sin\beta_i^2 + \sin\gamma_i^2) - \\ &2u_i \left\{ \cos\gamma_i \left[ \cos\beta_i (a_i \cos\alpha_i + p_x - b_i \cos\beta_i) + \sin\beta_i (a_i \sin\alpha_i + p_y - b_i \sin\beta_i) \right] + (p_z \sin\gamma_i) \right\} \\ &+ (a_i \cos\alpha_i + p_x - b_i \cos\beta_i)^2 + (a_i \sin\alpha_i + p_y - b_i \sin\beta_i)^2 + p_z^2 - l_i^2 = 0 \end{aligned} \tag{14}$$

Because $(\cos\gamma_i^2 \cos\beta_i^2 + \cos\gamma_i^2 \sin\beta_i^2 + \sin\gamma_i^2) = 1$, the above equation can be rewritten as:

$$u_i^2 - 2u_i\left\{\cos\gamma_i\begin{bmatrix}\cos\beta_i(a_i\cos\alpha_i + p_x - b_i\cos\beta_i)\\ +\sin\beta_i(a_i\sin\alpha_i + p_y - b_i\sin\beta_i)\end{bmatrix} + (p_z\sin\gamma_i)\right\}$$
$$+(a_i\cos\alpha_i + p_x - b_i\cos\beta_i)^2 + (a_i\sin\alpha_i + p_y - b_i\sin\beta_i)^2 + p_z^2 - l_i^2 = 0$$

(15)

This is a quadratic function equation of $\mathbf{u_i}$. By quadratic rule, there are two solutions for a quadratic equation as the following equation shown with relevant A, B and C.

$$\mathbf{u}_i = \frac{-B \pm \sqrt{B^2 - 4AC}}{2A} \tag{16}$$

However, the solution in this thesis means the motion of the vector between $B_iC_i$, which has to be the position number since it means the actuator is located above the translated leg and enhance the stiffness of the structure [18]. This will be proved in the later section. At this point, there is only one negative solution in this case as shown below regarding to the direction set up for the system. Also, Since A = 1 in this case, the solution of $\mathbf{u_i}$ can be defined as

$$\mathbf{u}_i = \frac{-B - \sqrt{B^2 - 4C}}{2} \tag{17}$$

Where:

$$\begin{cases} B = -2\left\{\cos\gamma_i\left[\cos\beta_i(a_i\cos\alpha_i + p_x - b_i\cos\beta_i) + \sin\beta_i(a_i\sin\alpha_i + p_y - b_i\sin\beta_i)\right] + (p_z\sin\gamma_i)\right\} \\ C = (a_i\cos\alpha_i + p_x - b_i\cos\beta_i)^2 + (a_i\sin\alpha_i + p_y - b_i\sin\beta_i)^2 + p_z^2 - l_i^2 \end{cases}$$

(18)

Since there is one solution for one leg, there are totally three solutions for the given mobile platform position. After each $u_i$ is solved, the translation of the entire manipulator is analyzed. A stiffness analysis can be developed from these results.

### 3.3.3 Jacobian Matrix

Jacobian matrix is defined as the matrix of all first order partial derivatives of a vector valued function and the motions of this design can be defined by independent parameters [1]. The Jacobian matrix **J** of this 3-DOF mechanism relates the linear velocity of the moving platform can be defined by the vector of input joint rates $\dot{\mathbf{x}}$ and the vector of the required actuator motion $\dot{\mathbf{u}}$.

$$\dot{\mathbf{u}} = J\dot{\mathbf{x}} \tag{19}$$

With

$$\begin{cases} \dot{\mathbf{u}} = \left[u_1, u_2, u_3\right]^T \\ \dot{\mathbf{x}} = \left[v_x, v_y, v_z\right]^T \end{cases} \tag{20}$$

In this design, the manipulator has a parallel kinematic structure with intersecting rails. According to Tsai [1], differentiating Eq. (15) with respect to time yields,

$$\dot{\mathbf{x}} = \bar{\omega}_i \times \mathbf{l}l_i + \dot{u}\ \mathbf{u}_i \tag{21}$$

Where $\bar{\omega}_i$ is the angular velocity of the link $A_iC_i$.

Dot-multiplying $I_i$ on both sides of Eq. (14) yields

$$\mathbf{l}_i^T \dot{\mathbf{x}} = \mathbf{l}_i^T \mathbf{u}_i \dot{u} \tag{22}$$

Since i=1, 2, 3, Eq. (19) has to be written three times for the Jacobian matrix form, which gives the final actuator's Jacobian matrix.

$$\dot{\mathbf{u}} = J\dot{\mathbf{x}} \tag{23}$$

With

$$\mathbf{J} = \begin{cases} \mathbf{l}_1^T / \left(\mathbf{l}_1^T \mathbf{u}_1\right) \\ \mathbf{l}_2^T / \left(\mathbf{l}_2^T \mathbf{u}_2\right) \\ \mathbf{l}_3^T / \left(\mathbf{l}_3^T \mathbf{u}_3\right) \end{cases} \tag{24}$$

### 3.3.4 Stiffness Analysis

There are many elements which affect the stiffness of a mechanism. For a parallel mechanism, these elements are stiffness of the joints, the structure and materials of the legs and platforms, the geometry of the structure, and the end-effector position and orientation [3].

In this case, only the wrench applied on the moving platform will be considered. This wrench can be any force or moment that causes deformations of the moving platform, which can be described by Eq. (25).

$$\mathbf{w} = \mathbf{K}\delta\mathbf{p} \tag{25}$$

Where:

**K**: is the generalized stiffness matrix;

$\mathbf{w}$ : is the wrench vector meaning the force or the torque that acts on the moving platform; and it is can be represented as $\boldsymbol{w} = \begin{bmatrix} F_x & F_y & F_z & \tau_x & \tau_y & \tau_z \end{bmatrix}^T$;

$\delta p$ : is the vector of the linear and angular deformation of the moving platform; and it can be represented as $\delta \mathbf{p} = \begin{bmatrix} \dot{x} & \dot{y} & \dot{z} & \dot{\theta}_x & \dot{\theta}_y & \dot{\theta}_z \end{bmatrix}^T$.

The wrench vector that is caused by the force and moment applied on the actuators can also be described by the transpose of the Jacobian matrix J, which has been explained by Merlet [12] as the following equations:

$$\mathbf{w} = \mathbf{J}^T \mathbf{f} \tag{26}$$

$$\delta \mathbf{q} = \mathbf{J} \delta \mathbf{p} \tag{27}$$

Where yields:

$\mathbf{f}$ : is the vector represents the force or moment of the actuator;

$\delta \mathbf{q}$ : is the deformation of the actuator.

The force/torque and displacement applied on the actuator can be specified as Eq. (28) by Hookes' law.

$$\mathbf{f} = \mathbf{K}_J \delta \mathbf{q} \tag{28}$$

Where: $\mathbf{K}_J$ is the actuator stiffness matrix in a diagonal form that is $\mathbf{K}_J = \begin{bmatrix} k_1 & k_2 & k_3 \end{bmatrix}$, and $k_1, k_2$ and $k_3$ represent the joint stiffness of each actuator. Combined Eqs. (28) and (27) with Eq. (26), the wrench vector becomes:

$$\mathbf{w} = \mathbf{K} \delta \mathbf{p} \tag{29}$$

With the stiffness matrix **K** that can be rewritten as:

$$\mathbf{K} = \mathbf{J}^T \mathbf{K}_J \mathbf{J} \tag{30}$$

The results of the stiffness of the hip exoskeleton are shown as in Figures 3.6 to 3.8.

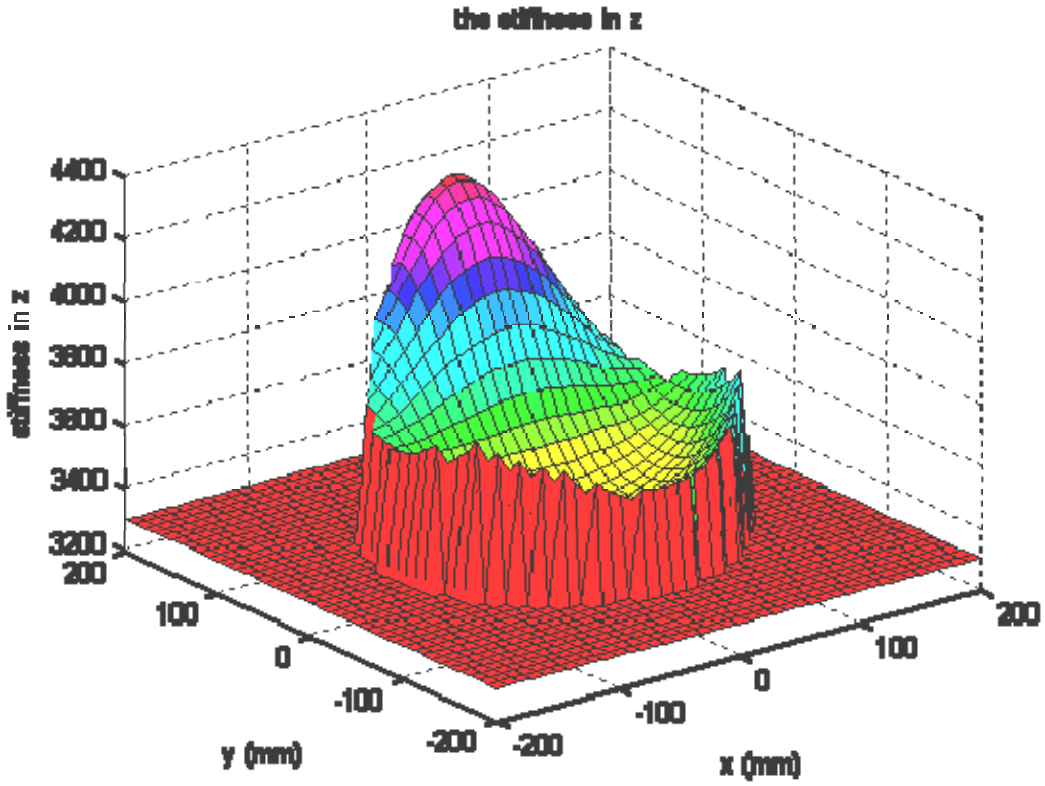


**Figure 3.6: Stiffness Results in Z direction of the Hip Exoskeleton**

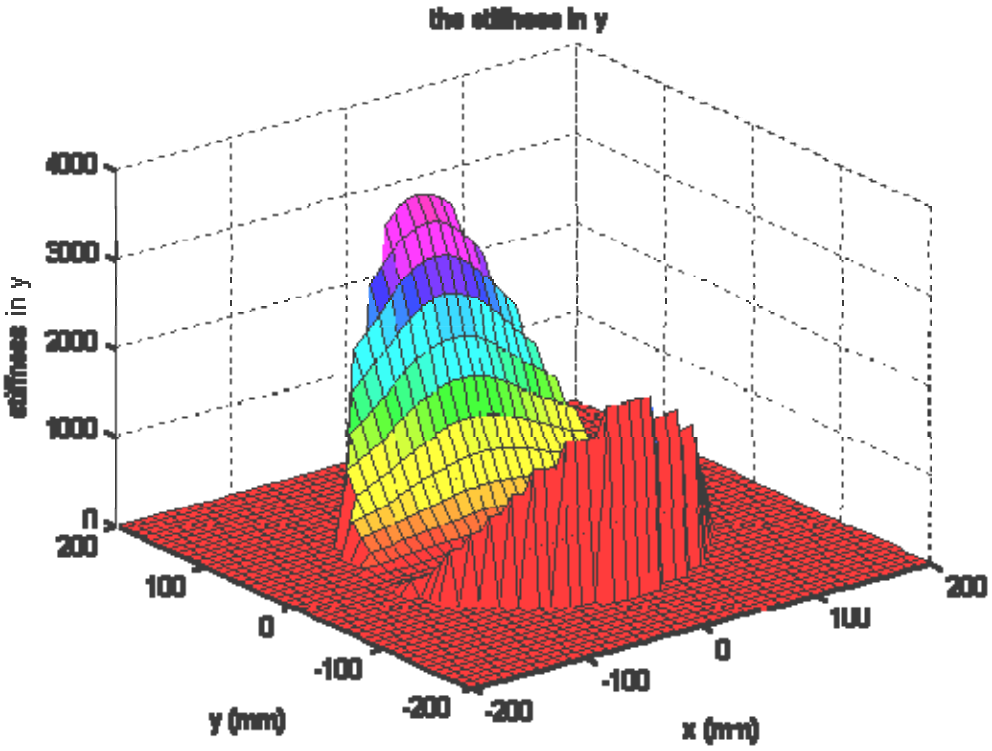


**Figure 3.7: Stiffness Results in Y direction of the Hip Exoskeleton**

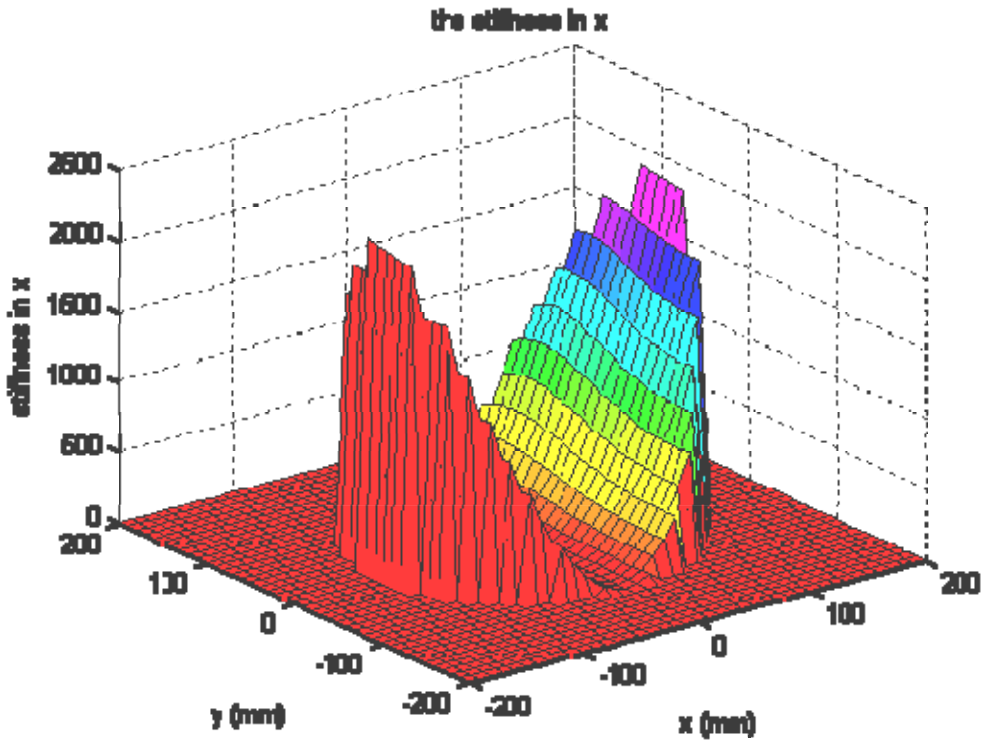


**Figure 3.8: Stiffness Results in X direction of the Hip Exoskeleton**

First, the above results have certified the symmetrical parallel structure that was introduced in Section 3.3.2. That is because each diagram shows that stiffness is symmetrical referring in all x, y, and z-axes. Second, all three figures show that the results are controlled in a reasonable range, which means the stiffness of the hip exoskeleton structure is fully tested. Therefore, the design of the manipulator has a reliable structure of the stiffness analysis.

## 3.4 Sensing and Controlling of the System

Beside an ideal mechanical structure, the sensing and controlling parts of a manipulator design are also critical. Irrational design or selection of the electrical part of a mechanism can cause circuit malfunctions, and thus lead to the failure of the entire system. Therefore, the selection of a powerful sensing and controlling unit is very important.

The theory of sensing and controlling of the three-degree of freedom parallel structured hip exoskeleton can be simplified in Figure 3.9.

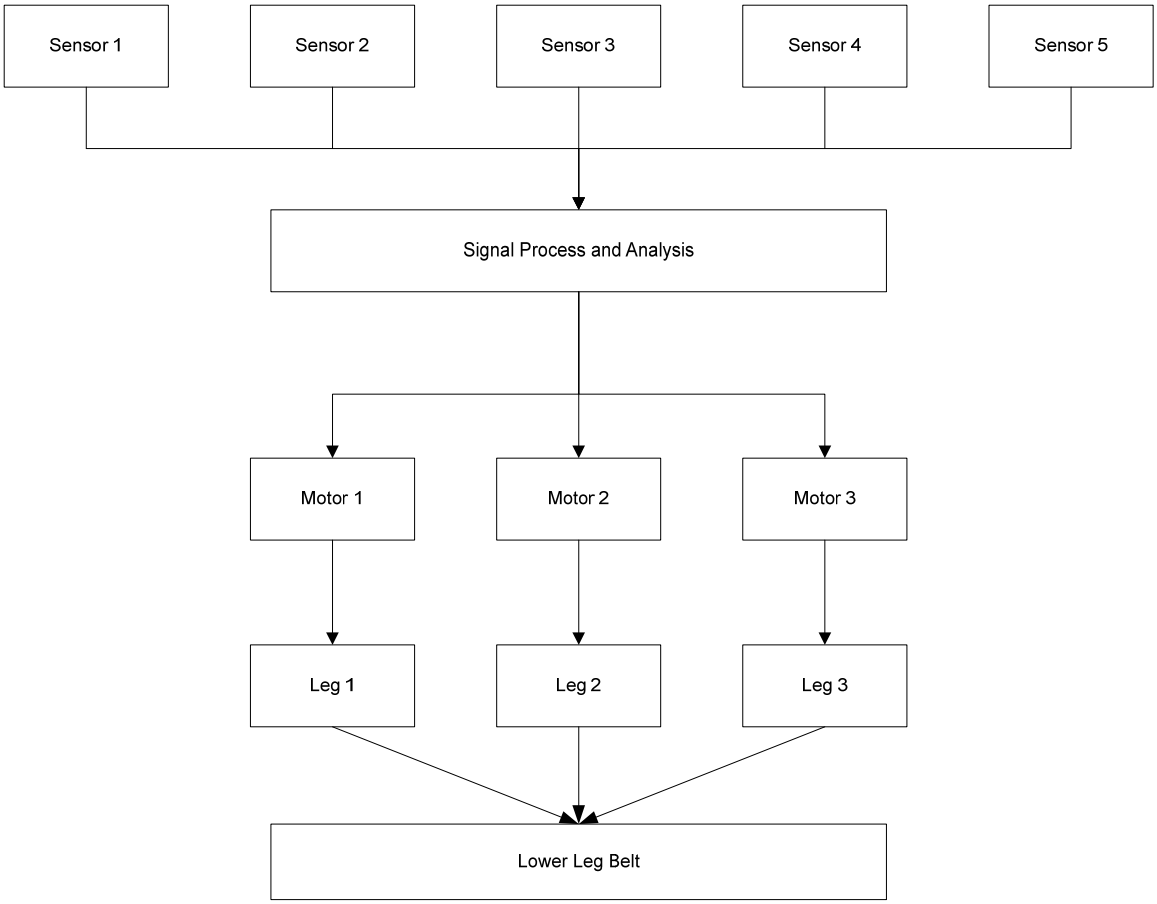


**Figure 3.9: Theory of Sensing and Controlling**

The selected sensors are in the positions where they can detect the certain signals. Then, these signals are transferred to a single chip, which are used for sampling and analyzing. After that, the processed signals are sent to the motors which control the actuator of the mechanical. At the end, the end-effector, the lower leg belt achieves the final movement.

## 3.4.1 Sensor Selection and Placement

There are several different types of sensors that can be installed in this system, such as pressure sensor [19], position sensor [20], and etc. A decision on the selection of

sensor needs to be made in further research step. However, circuit malfunction can easily take place if simple or inaccurate sensors are installed to detect an over complex signal. As a result, the complexity of the motion signal is one of the factors to consider while selecting sensors for a manipulator.

In this case, human movement is a motion, and the signals come from this motion is also complex. Though the hip movement is only a part of the entire human movement, it is still considered as a complex motion. Therefore, advanced and reliable sensors should be chosen for this hip exoskeleton unit in order to avoid circuit malfunction that for ensure the action of the unit.

As one of the most crucial measurement tool approaches for muscle activity, the research of the surface electromyography (SEMG) has been developed significantly in the past ten years [21]. Surface electromyography signals represent the electrical activity of a specific muscle during contractions. As a consequence, SEMG can be used in practical mechanisms for a variety of purposes with possible and suitable assistance of modern signal processing method, such as the applications in the nerve-muscle-skeleton modeling, artificial limb control, and hip exoskeleton system [21].

In the design of this hip exoskeleton, the multichannel surface electromyography sensor is utilized to acquire the SEMG signals that are from the wearers' thigh muscles. The entire signal and data processing circuit is in Figure 3.10. Ag-Agcl detecting electrodes are stuck to the five primary muscles of thigh, so that the signals collected form SEMG sensors is firstly processed by signal process circuit. After that, the processed SEMG signal is sent to the data processing module to be analyzed. Then, the

analyzed SEMG signal is transferred into the standard digital pulse signal, which is used as the command to control the movement of motors in further process.

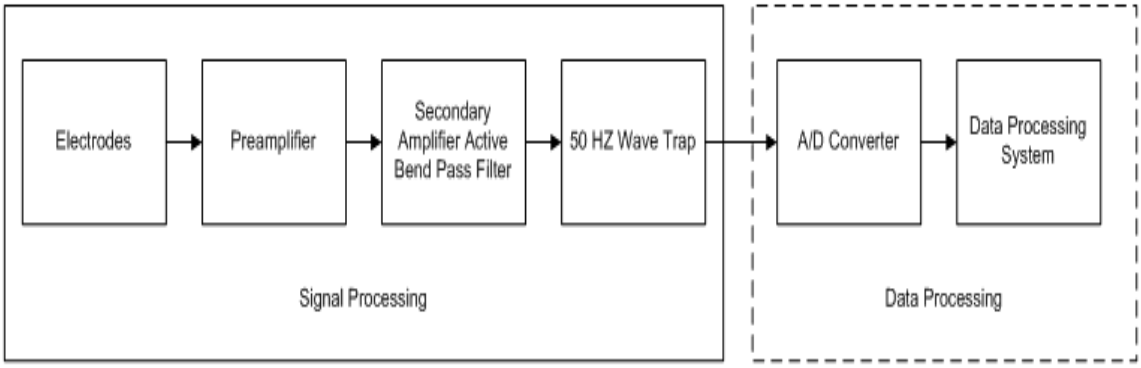


**Figure 3.10: Surface EMG Signal Processing and Data Processing Circuit**

According to the earlier chapters, the five primary muscles (Recues femoris, Biceps femoris, Sartorius, Adductor longus, and Adductor magnus) control the hip motion during a normal gait cycle. In other words, Recues femoris and Biceps femoris control the flexion/extension movement of the thigh; Adductor longus and adductor magnus control the abduction/adduction movement of the thigh; and Sartorius controls the medial/lateral rotation movement of the thigh. In this designed unit, the SEMG signals are collected and analyzed by five Ag-AgCl electrodes which are stuck on the surface of the five muscles in order to detect the human thigh motion during a gait cycle.

Due to the properties of the SEMG signals – weak and sensitive, some preparative and additional work needs to be done. For example, in order to avoid interruption on the sensor electrodes signal collection, fine hairs need to be removed and skin needed to be cleansed before sick the electrodes on the proper position of the thigh.

The choice of locations to place the SEMG sensor electrodes are very important because of the need for forbidding the circuit malfunctions. Regarding to the function of the five primary muscles and the properties of the SEMG sensors, the electrodes can be located as the following figures [12].

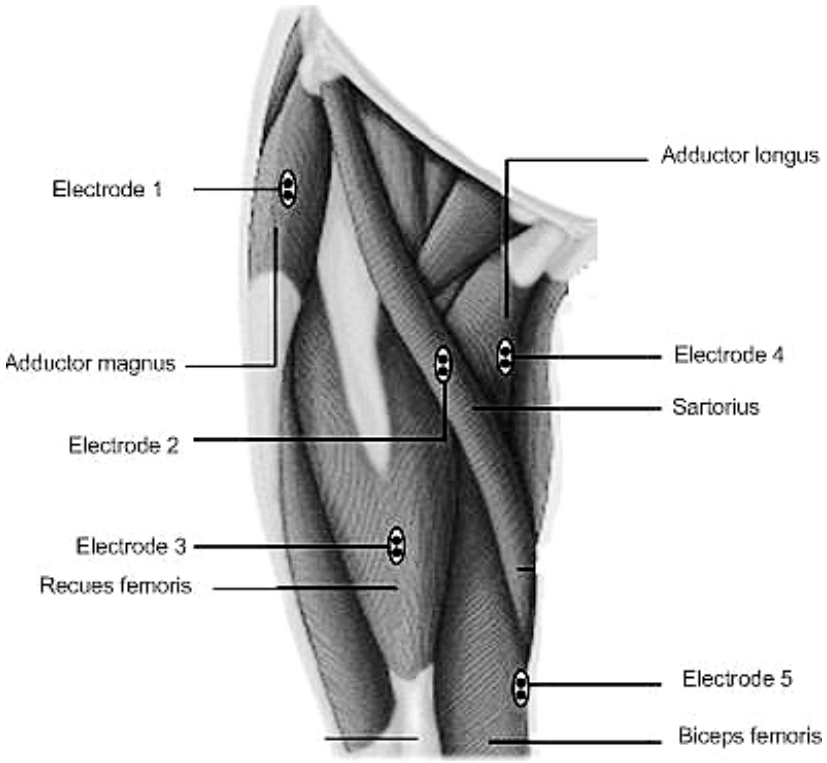


**Figure 3.11: Placement of SEMG Sensor Electrodes [12]**

Five electrodes are separately placed on the surface of the thigh skin. In addition, they should be closed to the part of the muscles where there are the maximum activates. Also, these five electrodes are almost evenly disturbed due to the position of muscles, which is a benefit to this design because the influence between electrode signals is minimized [21]. As a result, these five electrodes are connected to the upper leg belt which is on the first working platform of hip exoskeleton with the best performance.

### 3.4.2 Control Motor Selection and Placement

The selection of the motor could be another major issue in this thesis. First, the size of the motor affects the dexterity of the hip exoskeleton. Second, motors have a significant weight which could be the major contribution on the whole mechanism.

The hip exoskeleton is helping the people who cannot walk properly, so the hip exoskeleton does not need a large power assistant that could be harmful to them. For this reason, the safety factor of the system is another issue in the design process which is directly related to the motor. Control is another area needed to be considered with the motors. The efficiency of the motor is also a key point within the design. DC Motor is considered as the first choice in the current research stage.

Within this thesis, the motors are considered as an actuator to attain the lower leg belt movement to assistant moving wearers' legs. These motors are located on the waist belt support points as shown in Figure 3.12.

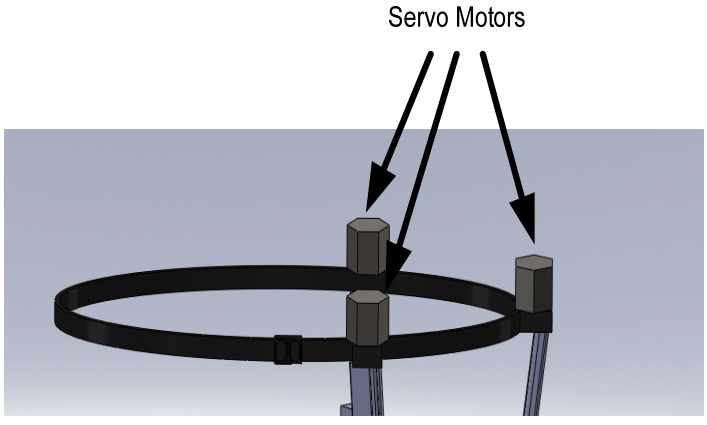


**Figure 3.12: The Location of Servo Motors**

Servo motor is first recommendation that can be utilized in the designed unit. The reason is that servo motor is one of the most common and accurate motors. There are several advantages by choosing this type of motors. First, Servo motors are well known because its accuracy in controlling the speed of motion and the position of movement [22]. By using this type of motor, the tolerance of this system can be minimized and the precision of the movement can be ensured. Second, the servo motor has a kind of relatively small device called servo that has an output shaft. This shaft has a fairly fast signal processing time [23]. In that case, the motor is able to receive the signal and make the response in a short time. A simplified servo motor working principle related to the hip exoskeleton is shown in following figure.

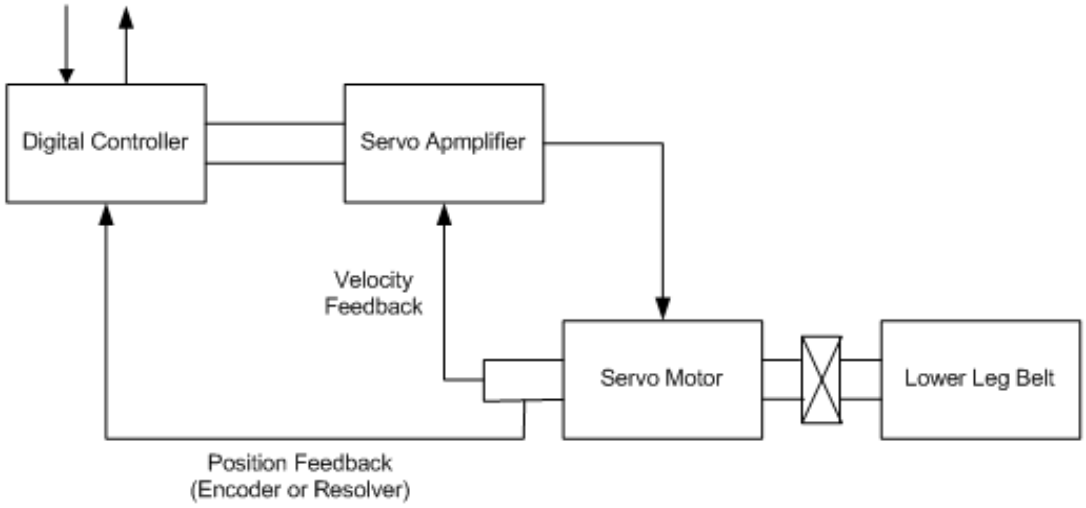


**Figure 3.13: Servo Motor Working Principle**

To optimize the motor motion, limit switches are adopted. Limit switches are used to control the reaction from the motors. A basic structure of a limit switch is shown in Figure 3.14. The theory of the limit switch is that the roller of the limit switch hits the

lance and cuts out the power of the servo motor to limit the reaction of the upper legs of the exoskeleton when they have reached the expected position [24].

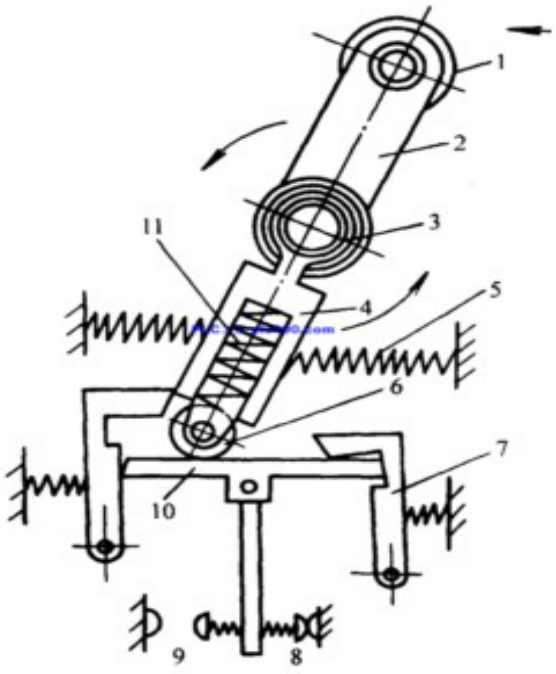


**Figure 3.14 [25]: The Structure of Limit Switch: (1): Roller; (2): Upper rocker arm; (3, 5, 11): Spring; (4); Stock; (6): Pulley; (7): Clamp; (8, 9) Touch Spot; (10): Transverse plate (25)**

## 3.5 The Hip Exoskeleton Interface to the Wearers

In order to take care of the wearers' conformability, the design of the manipulator needs to be as adaptable as possible. There are several design issues of this mechanism that have been taken into consideration.

First, the targeted wearers had either been injured or are weak, so they cannot carry heavy loads. The hip exoskeleton is used to assist their walking during regular daily life; it is more likely to be a hindrance rather than being helpful if the weight of the mechanism is too heavy. In this design, a simple parallel kinematics structure is chosen,

which has a much lower moving mass compare to that of serial structure. Second, this design does not require a large amount of building materials. As a result, this unit can be considered as a lightweight structure when comparing with other present ones.

The waist belt of the hip exoskeleton unit is planned to fix on the waist, and the two leg belts are fixed on the thigh. Wearers have different sizes of waist and thighs, and it is impossible to make the product custom made. Therefore, adjustable waist belt and upper leg belt is a potential solution for this problem. In the CAD model above, the waist belt has been made in an adjustable form and all the analysis are based on the adjustable design. In the future prototype, both belts should be built in an adjustable form.

Due to the structure of this exoskeleton, the wearers are not able to sit while wearing this unit. To solve this problem, this structure has designed to assembly easily. If the upper legs are screwed on the waist belts supporting points, the wearers can take the upper legs out when they need to sit down, and put them back after they stand up. On the other hand, people are able to replace the wear out parts without difficulty with this feature.

More than that, there is only one leg exoskeleton (the leg part of the hip exoskeleton unit) attached on the waist belt. If there is a need, two of them can be attached on the waist belts as shown in the following Figure.

**Figure 3.15: CAD Model with two Leg Exoskeletons**

# Chapter 4

# System Optimization

The availability and adaptability have been provided by the above analysis, but there is still something to investigate to optimize the designed unit to achieve a better result on performance. For instance, further analysis can be done to examine the kinematic behaviours of the manipulator. In this thesis, the stiffness of the unit is one of the critical conditions for the success of the designed structure. Therefore, the stiffness optimization of the hip exoskeleton is superior supplementary analysis for verifying and improving the design. Other improvements, such as reduction of the material used in certain parts (Figure 4.11), can be considered as system optimization as well.

## 4.1 FEA Analysis

In order to further verify the performance and kinematic behaviours of the design, finite element analysis (FEA) is conducted to perform the examination. ANSYS Workbench is used to perform the tests of the deformation, stress and strain when a force and a moment were applied on this structure. The finite element model is established as shown in Figure 4.1. The three joins (P-U-U) of the unit are taking into consideration during the analysis. The type of the unit is SOLID 187 which is provided by ANSYS Workbench. The element is defined by 10 nodes having three degrees of freedom at each node: translations in the nodal X, Y and Z directions. The material of the elastic body is

Structural Steel, and its elastic modulus E = 2.e+011 [Pa], Poisson's ratio μ = 0.3, the density of ρ = 7850 kg $m^{-3}$.

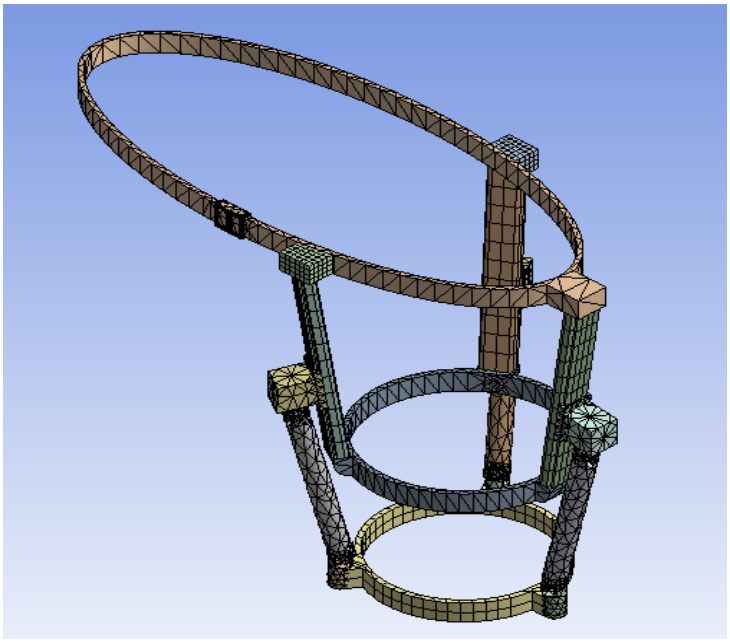

Figure 4.1: Finite Element Model of the Hip Exoskeleton

### 4.1.1 Force

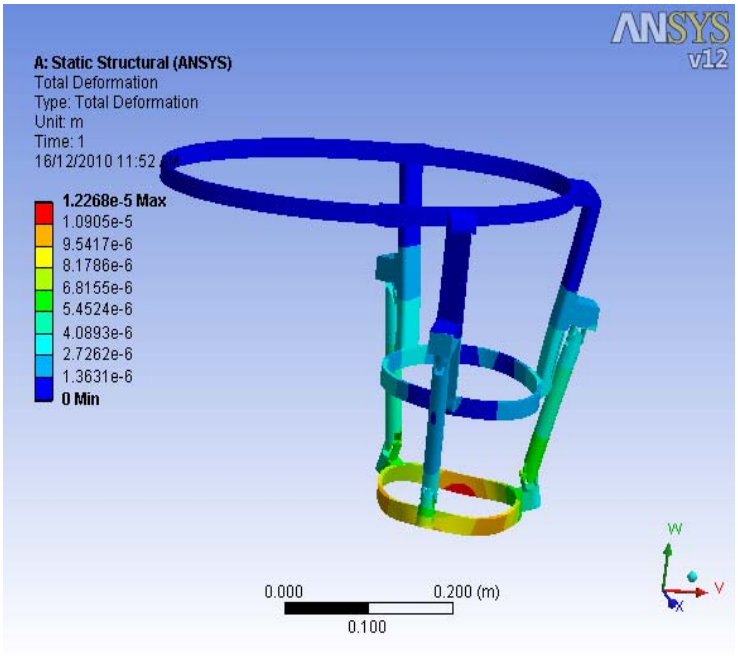


Figure 4.2: Total Deformation based on Applied Force

The objective of the deformation analysis is to detect the change of the structure when applying a force on the structure. The total deformation shown in Figure 4.2 has been enlarged 1800 times of its actual deformation when a reasonable size of force is applied on this structure. The force is 200N which is in the direct to the bottom of the structure. From the figure, we can observe that the first deforming part is the lower leg belt because it is where the force is applied on. Also, the waist belt and the upper legs did not show any deformation even after the result had been enlarged to 1800 times, which means the structure of this design is reasonable and reliable.

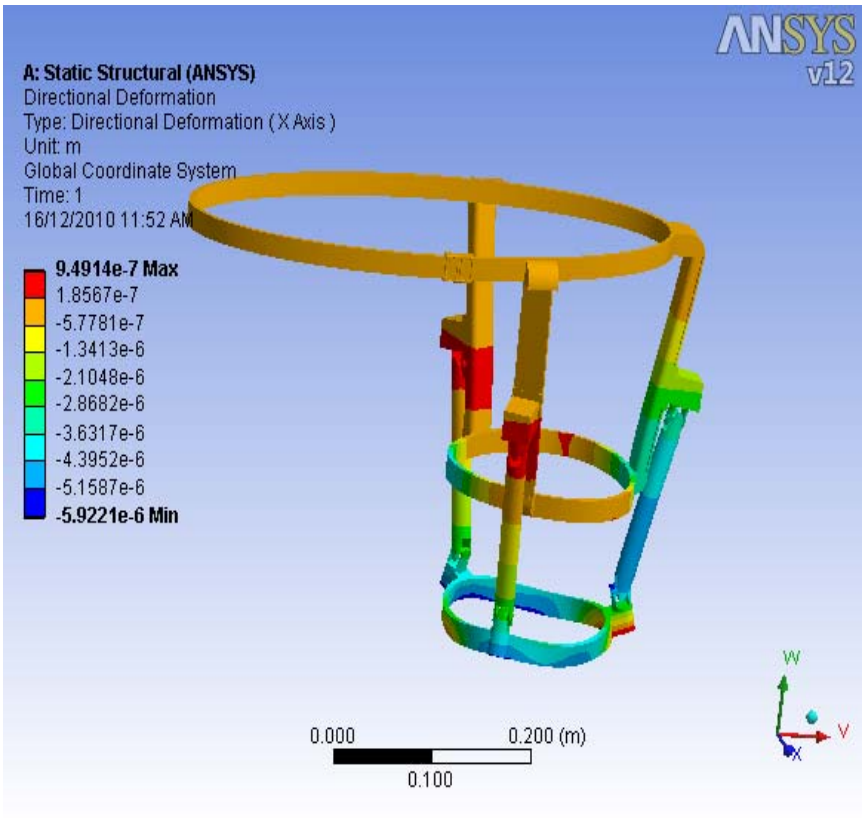


(a)

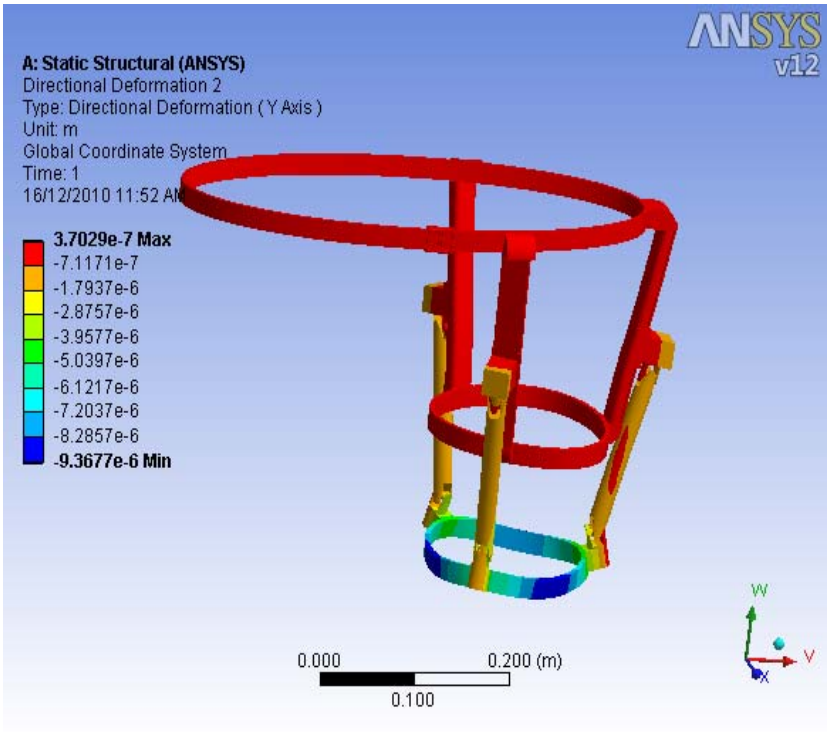


(b)

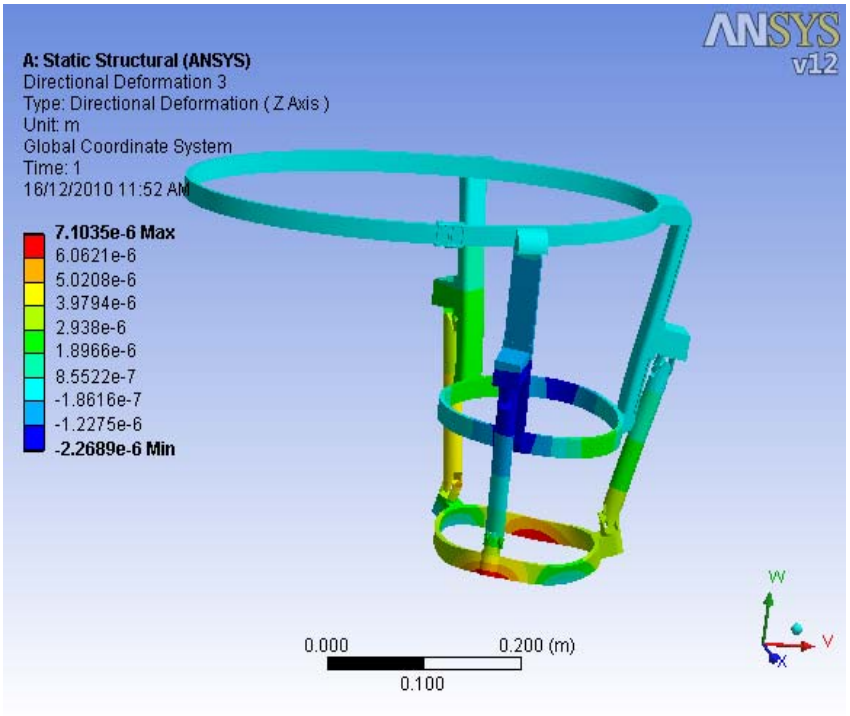


(c)

**Figure 4.3: Deformation in X, Y, Z-axis based on Applied Force: (a) X-axis; (b) Y-axis; (c) Z-axis**

Figure 4.3 shows the components of the total deformation in X, Y, and Z-axes, and these three deformation components totally different from each other. Since the force is applied perpendicular to the plane of the lower leg belt, the deformation direction in Z-axis is the largest among the three directions, and the deformation direction in Y-axis is the smallest. However, all these deformations have been expanded to 1800 times of its actual size, so these deformations will not damage the structure of the manipulator though there were some maximum values appeared in the above figures.

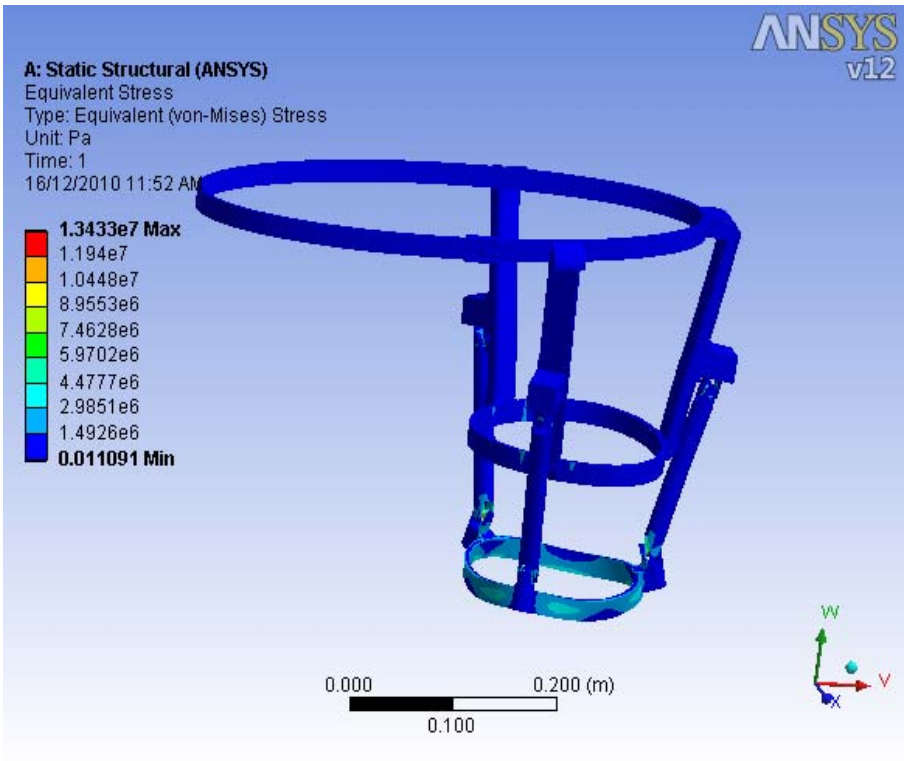


**Figure 4.4: Equivalent Stress based on Applied Force**

An equivalent stress test (von-Mises) also has been done for this structure. From the Figure above, the maximum stress in this structure is about $3x10^6$ Pa, which is on the lower leg belt and the lower universal joints. However, this result has been enlarged 1800

times. Also, most parts of this structure are under the minimum stress. Therefore, the equivalent stress analysis is evidenced that the structure of the design is satisfied.

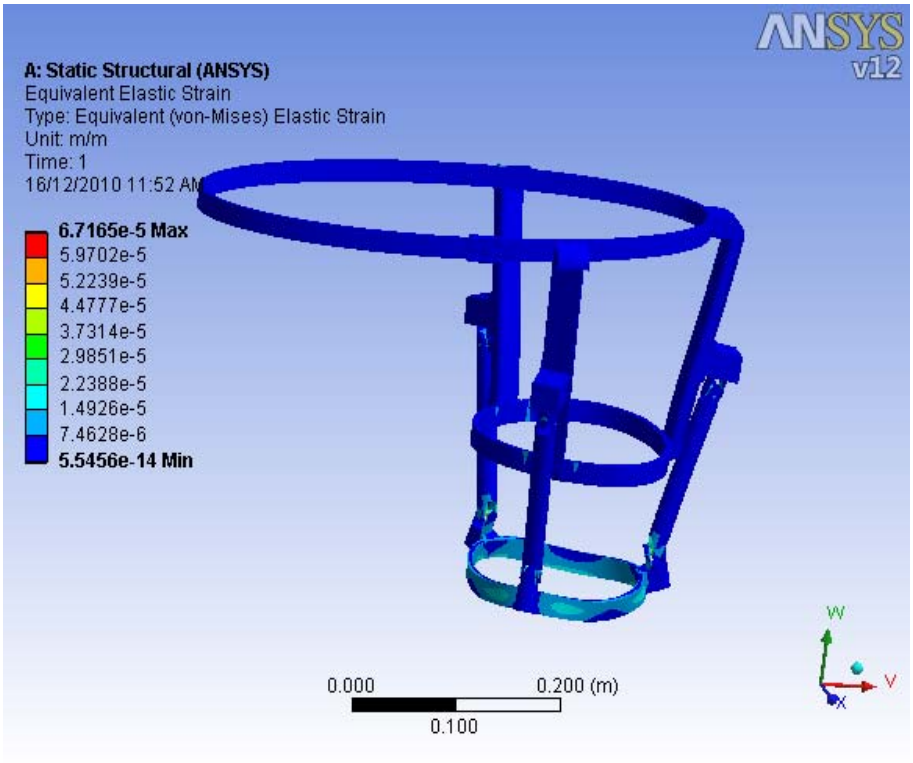


**Figure 4.5: Equivalent Elastic Strain based on Applied Force**

The result of the equivalent elastic strain test is very similar to the result of the equivalent stress test. The maximum strain is on the lower leg belt and the lower universal joints, and most parts of this structure are under the minimum stain, so the applied force will not destroy the structure of this design. Therefore, this test is also an evidence to prove that this design is commonsensical.

### 4.1.2 Moment

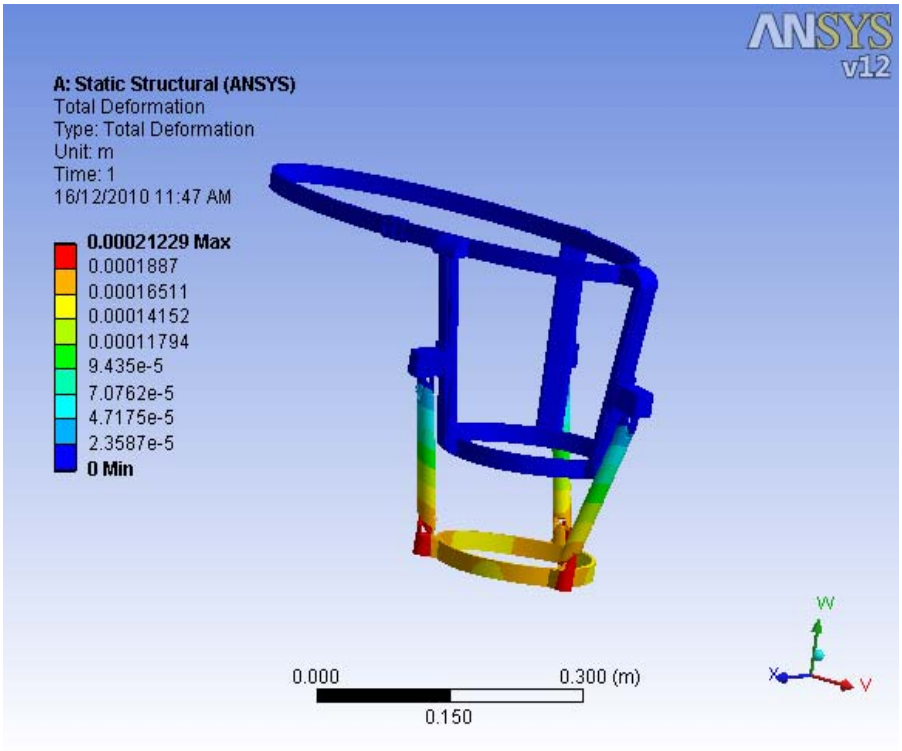


**Figure 4.6: Total Deformation based on Applied Moment**

The structure of the designed structure has been tested after applying a certain force, and has been proved that the design was reasonable and stable. To verify the above result, a moment is applied on this structure to test the deformation, equivalent stress, and equivalent elastic strain. The same as the force test, all results has been increased to 1800 times larger than its original ones.

The moment in this case is still applied on the lower leg belt, and perpendicular to the plane of the lower leg belt. The same as the force test, the maximum deformation is on the bottom part of the robot. Some unexpected rotations appeared in the total deformation Figure, the reason is the transaction had been enlarged to 1800 times as well.

It is well known that parallel manipulators have relatively small workspaces compared with the serial counterparts.

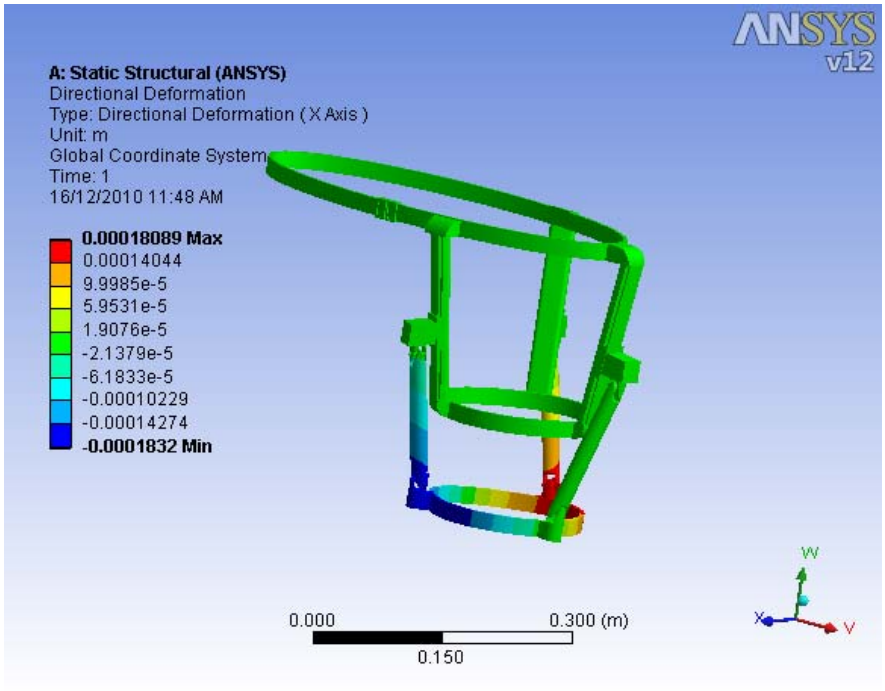


(a)

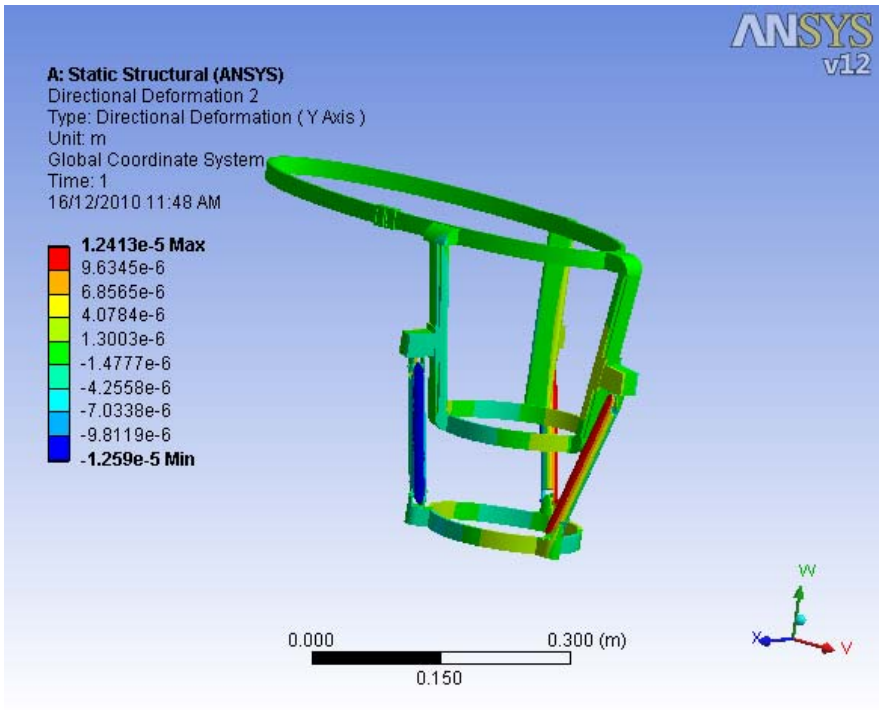


(b)

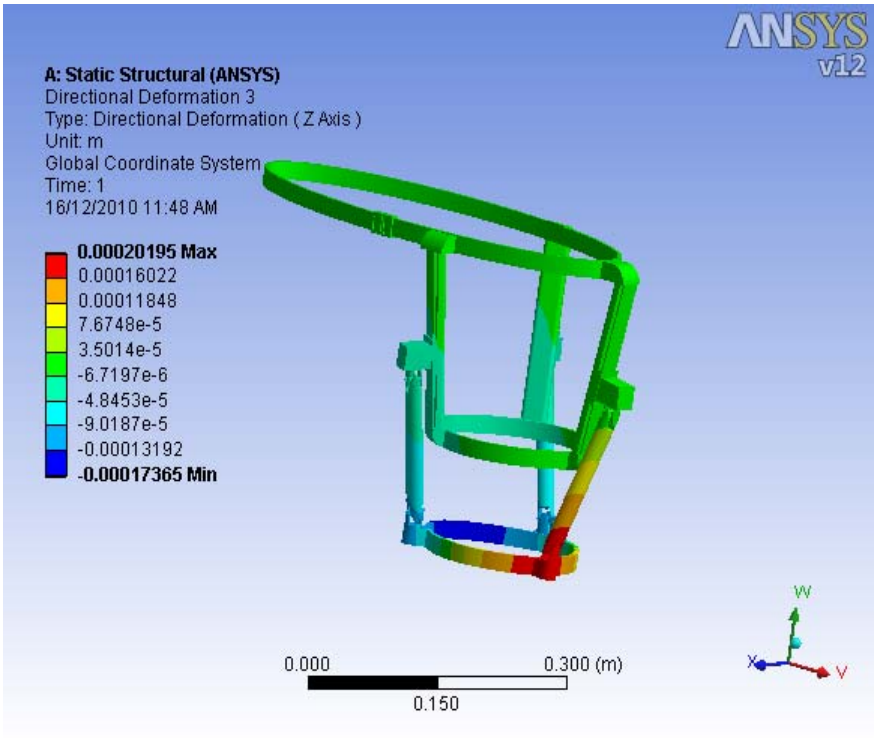


(c)

**Figure 4.7: Deformation in X, Y, Z-axis based on Applied Moment: : (a) X-axis; (b) Y-axis; (c) Z-axis**

Figure 4.7 shows the directional deformations in X, Y, Z-axes when applying a moment on the lower leg belt of the structure, which matched the Figure 4.3. Most parts of the structure are under a relatively small deformation even the results had been enlarged. The same as Figure 11 shown, the maximum deformation was in Z-axis and it is 0.00020195m, and the smallest deformation was in X-axis that is 0.000012413m. These deformations are really small in the tests, and they should be even smaller when they are in 1:1 scale.

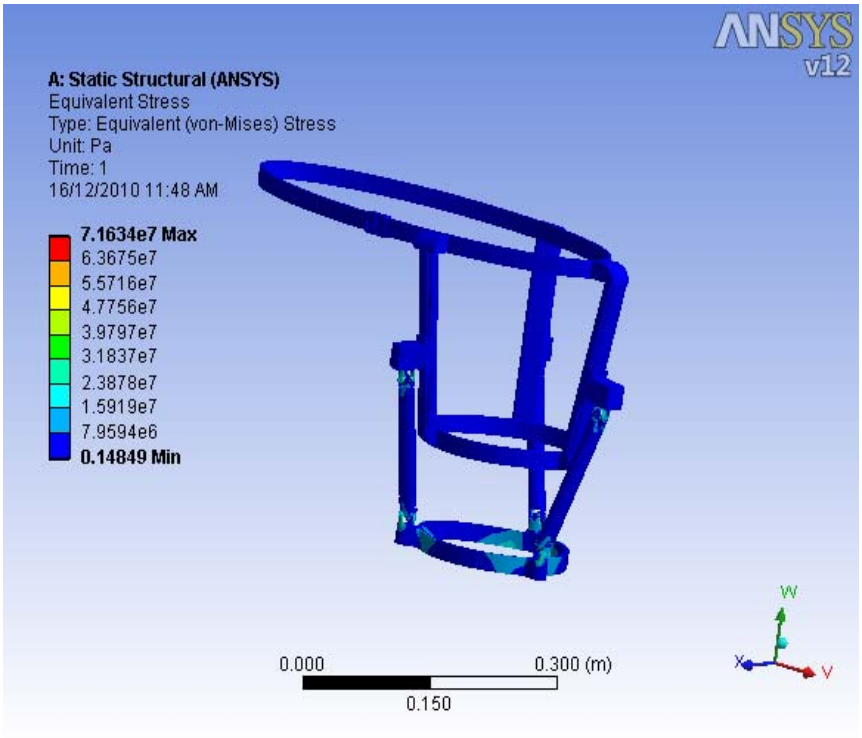


**Figure 4.8: Equivalent Stress based on Applied Moment**

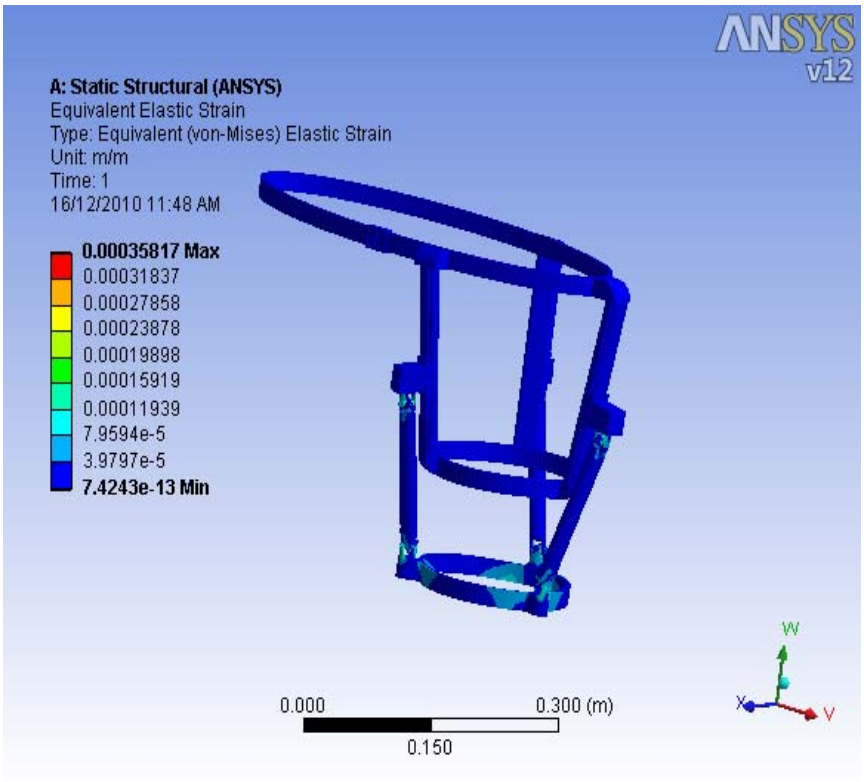


**Figure 4.9: Equivalent Elastic Strain based on Applied Moment**

Compared Figures 4.8 and 4.9 with Figures 4.4 and 4.5 for the equivalent stress and equivalent elastic strain, they are almost identical except the rotation ones. As discussed above, the rotation can be negligible in a real test. The maximum stress in this structure is about $7x10^7$ Pa, which is on the lower leg belt and the lower universal joints. This value is about 20 times larger than the applied force. Compare with the applied force figure with the applied moment figure, we can obtain that the deformation directions are the same, but the degrees of deformation are different. The reason is the magnitude of the applied force and the moment were the same, but the magnitude is not the same when they are converted to the either force or moment.

## 4.2 Stiffness Evaluation

The workspace of a parallel manipulator can be defined as a reachable region of the origin of a coordinate system attached to the center of the moving plate [17]. The workspace of the hip exoskeleton can be generated numerically by MATLAB based on the following algorithm:

1. Set volume = 0;
2. Call workspace algorithm;
3. Set the steps of $\theta$ and $\varphi$ as $\theta_0$ and $\varphi_0$;
4. Calculate on unit volume by volume = $\rho$ x $\rho\sin\theta$ x $\rho\sin\varphi$ + volume;
5. End of the loop.

As a result, the workspace volume is generated as shown in Figure 4.10.

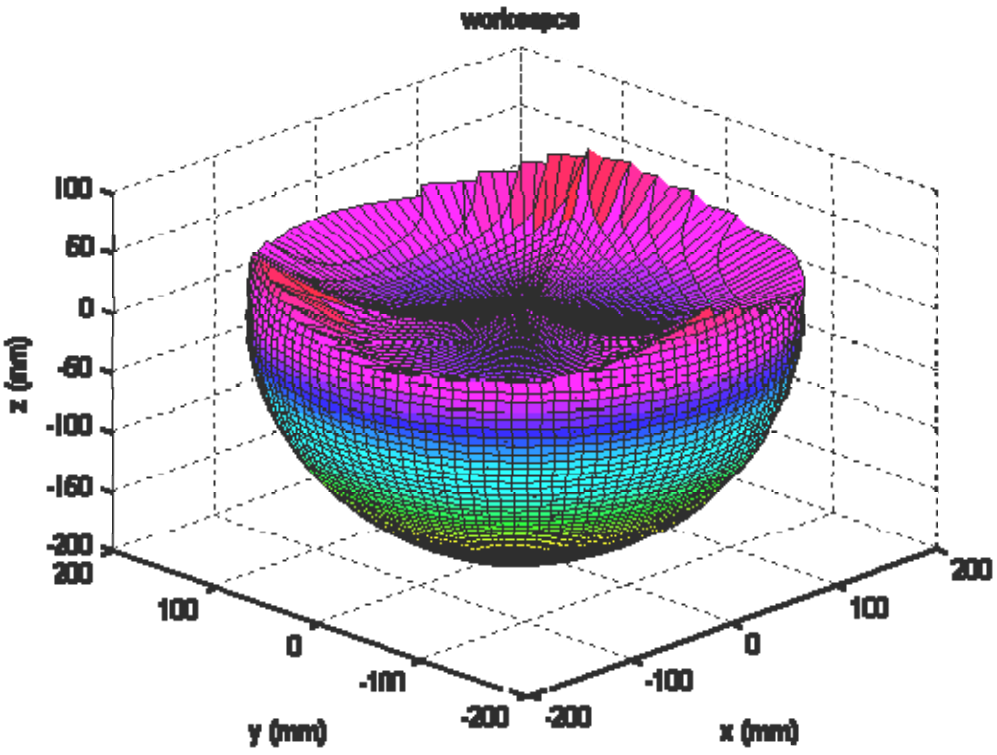


Figure 4.10: Workspace Volume of the Hip Exoskeleton

## 4.3 Stiffness Optimization

In this thesis, the objective of the stiffness optimization is to obtain the best geometrical parameters and behaviour parameters which guide to a better structure of the mechanism.

In the following optimization process, the Genetic Algorithms (GAs) are used to conduct the optimal design of the system in terms of better system workspace. GAs is well known to solve both liner and nonlinear problems by presenting a population of possible solutions or individuals, and these solutions/individuals are evaluated with respect to the degree of fitness that indicates how well the solutions/individuals will fit

the optimization problems [3]. GAs has the following advantage of robustness and good convergence properties [4]:

- GAs do not require any knowledge or gradient information about optimization problems;
- Discontinuities presents on the optimization problems have little effect on overall operation;
- Be able to solve large scale problems;
- Applicable for variety of problems.

For the designed hip exoskeleton structure, there are four optimization parameters chosen for the optimization: the radius of the lower leg belt (R), the radius of the upper leg belt (r), the lower leg length (l), and the angle between the lower leg and the fixed platform (θ). These parameters are chosen because they are the variables that have the largest influence of the structure, and these variables maybe have to be adjusted for different set of the hip exoskeleton units. The relationship between the stiffness and these parameters can be described by the following equation:

$$K_{stiffness} = f(R, r, l, \theta) \tag{31}$$

With the parameters potential range which is taken 10% offset from the original design:

$$\begin{cases} 72mm < R < 88mm \\ 81mm < r < 99mm \\ 180mm < l < 220mm \\ 63^o < \theta < 77^o \end{cases} \tag{32}$$

The objective function is convergent to the maximum point after 88 generations as shown in Figure 4.10, and the best choices of the parameters results that are listed in Table 4.1.

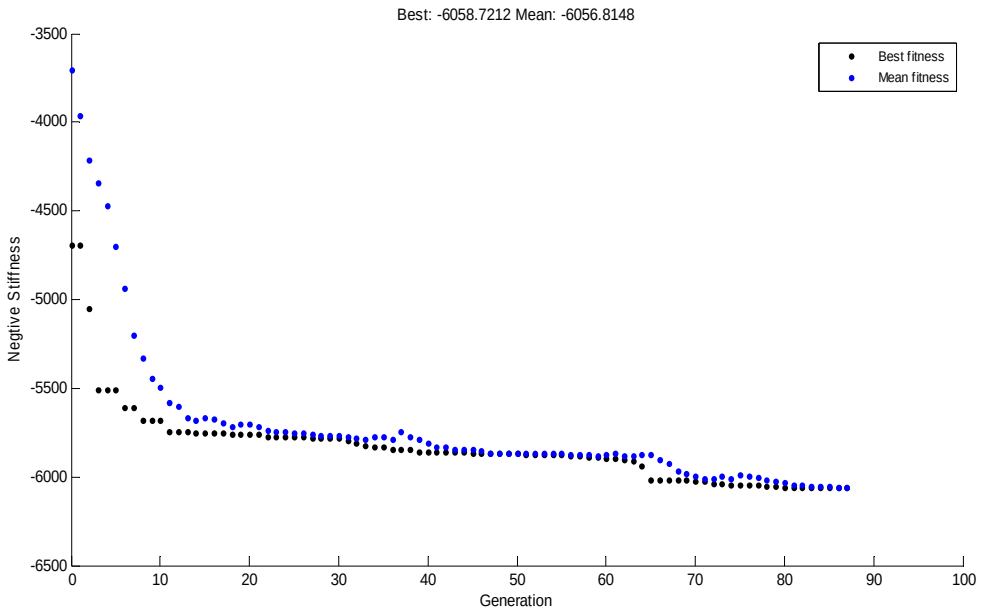


**Figure 4.11: Stiffness Optimization Results**

**Table 4.1: Optimal Design Parameters for Maximizing Stiffness**

| Optimal Values | Unit | 1st Choice | 2nd Choice | 3rd Choice |
|---|---|---|---|---|
| R | mm | 88 | 87.991 | 87.999 |
| r | mm | 81.004 | 81.114 | 81.012 |
| l | mm | 219.998 | 219.134 | 214.063 |
| θ | degree | 63.002 | 63.011 | 63.002 |
| $K_{stiffness}$ | N/mm | 6664.857 | 6432.889 | 6058.721 |

As seen from the above table, the optimal values are almost on the boundary condition. The reason is that the results of numerical calculation of the optimization have linear relationship. The best result will appear on one end of the range. With the optimized values of the parameters obtained above, the unit stiffness can be improved. As a result, the structure of the hip exoskeleton can be improved, and a better performance based on stiffness can be achieved.

## 4.4 Achievable Improvement of Exoskeleton

### 4.4.1 Development on Geometry

Other than test the unit and modify parameters of the design, there are some other improvements that can be applied on the structure, such as the development of the geometry of the structure (Figure 4.11).

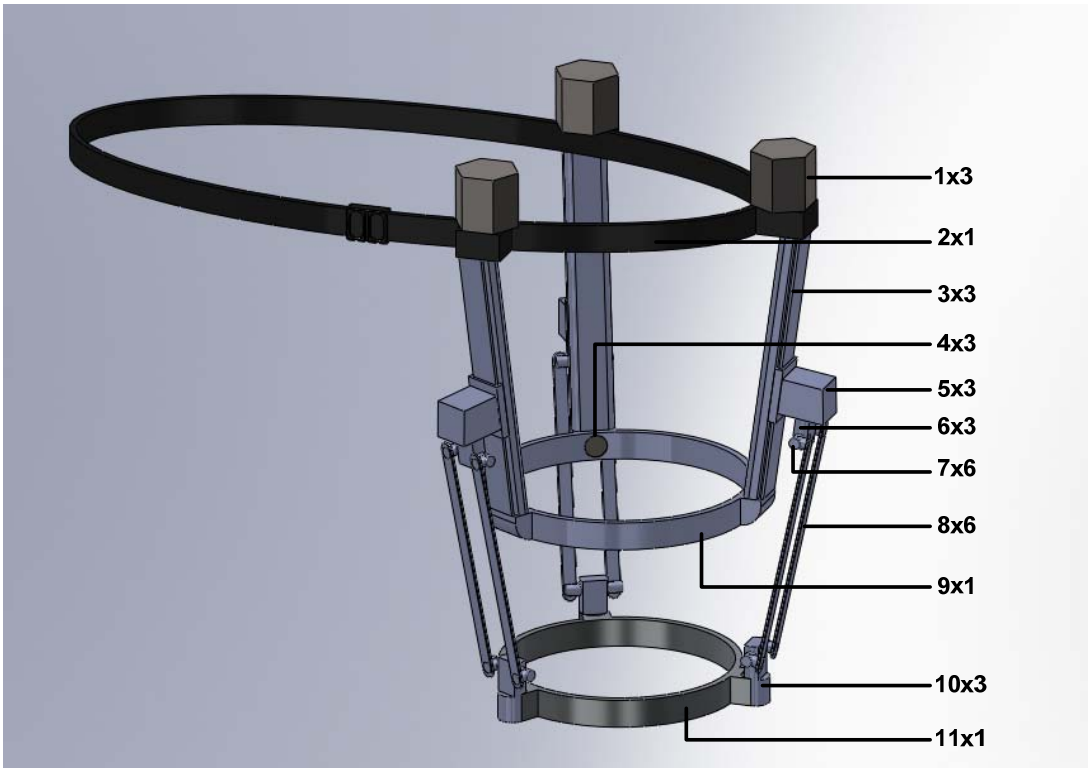


**Figure 4.12: Upgrading CAD Model of the Hip Exoskeleton: (1) Motor (2)Waist Belt (3) Upper leg (4)Sensor connecting point (5) Leg joint (6)Upper leg joint (7)Screw (8) Lower leg(9) Upper leg belt (10) Lower leg joint (11) Lower leg belt**

As shown in the Figure 4.11, one of the most obvious changes is the shape of the lower legs. A clearer comparison of the lower legs has been made in Figure 4.12. The first design has solid lower legs, but they are flat sticks in the second design. There are two considerations to make this change. First, the sticks are much lighter than the solids legs, so it is easier for the wearer. Second, the stick design could save material in the manufacturing process, which could reduce the total cost of fabricating the structure. As long as the stiffness is not reduced, the thinner the leg, the better the design is. An FEA analysis of the updated design is presented in the following section to prove that the improvement of the leg has no negative effect on the stiffness of the structure (Figure 4.13 and Appendix I).

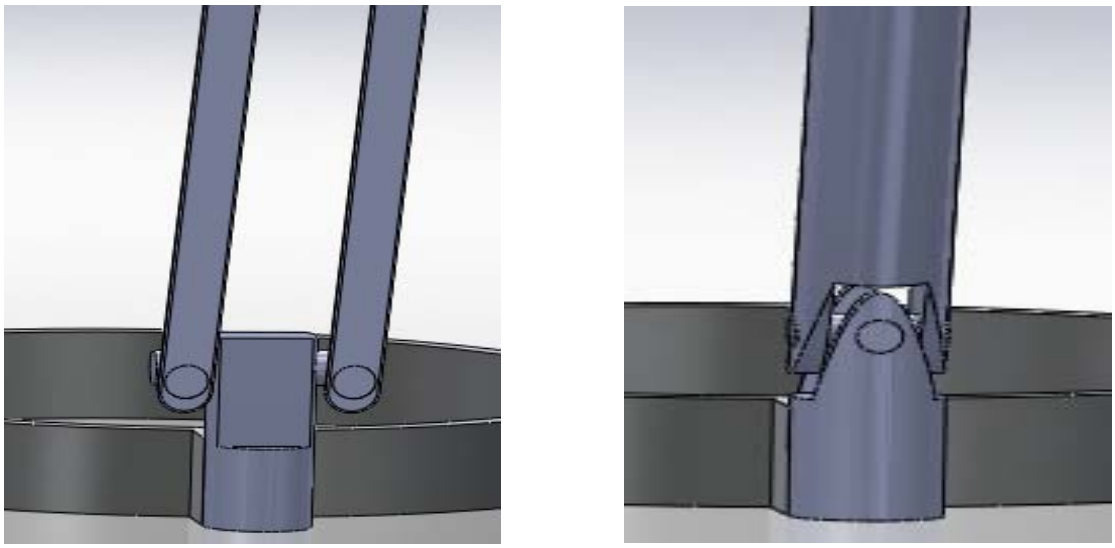

(A) (B)

**Figure 4.13: Lower Leg Comparison between Two CAD Models: (A) Updated (B) Original**

Another improvement of the model is the joints. In the original design, the three joints for the legs are in PUU structure, and the three joints make the 3 DOF of the structure. In the updated design, the prismatic joint stays the same, but the universal joints are replaced by two revolute joints (Figure 4.13). According to Dr. Lung-Wen Tsai [2], "the universal joint is essentially a combination of two intersecting revolute joints", so the updated model still has 3DOF [1]. On the other hand, the new joint is much stronger than the original ones (Figure 4.14 & Appendix I). Thus, the improvement of the joints only has a positive influence of the performance of the mechanism.

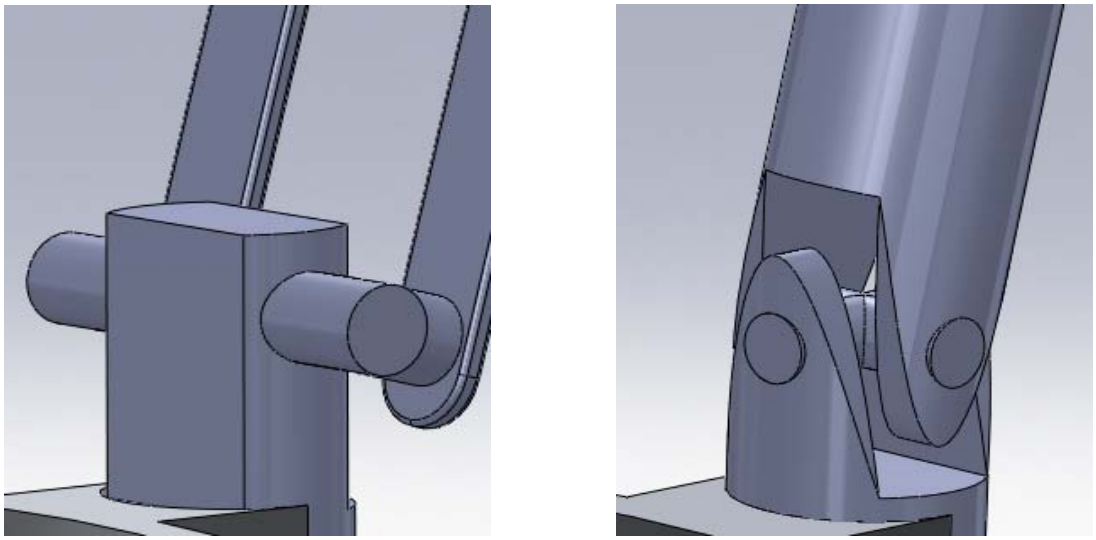

(A) (B)

**Figure 4.14: Joints Comparison Between Two CAD Models: (A) Updated (B) Original**

In order to prove that the changing of the structure actuators does not affect its performance, a revised FEA has been generated. The results are not exactly the same as the previous ones, but it is similar if one compares Figure 4.2 with Figure 4.14. The maximum deformation is still on the lower leg belt, which means the changing of joints will not change the stiffness of the entire unit. Consequently, both changes on the new model are considered as improvements of the structure.

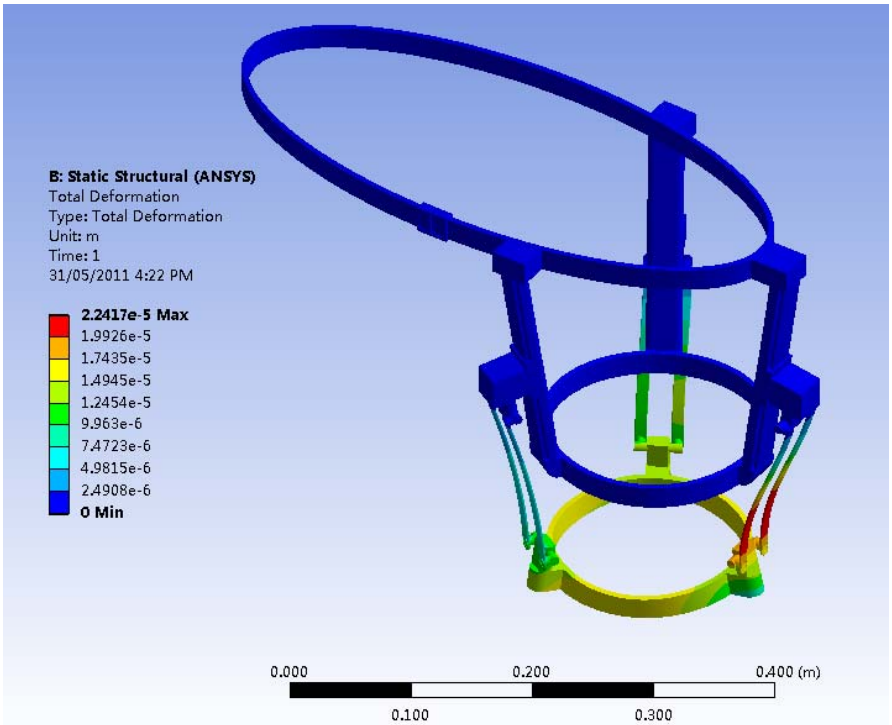


**Figure 4.15: Total Deformation of Updated Model based on Applied Force**

More detailed FEA results of the updated CAD model are in Appendix I and the detailed FEA report is attached in Appendix II. Also, in order to show the hip exoskeleton motion unaffected, detailed motion diagrams for the updated CAD model are provided in the following figures.

## 4.4.2 Development on Comfort Level

As mentioned above, the hip exoskeleton can perform translation mentions shown in Appendix III. It is not very comfortable to if the movement of the upper leg is large because there will be angle between the lower platform and the leg. One solution that can improve the comfort level of the structure is that to install an inner leg gimbal inside of the lower leg belt as shown in Figure 4.15.

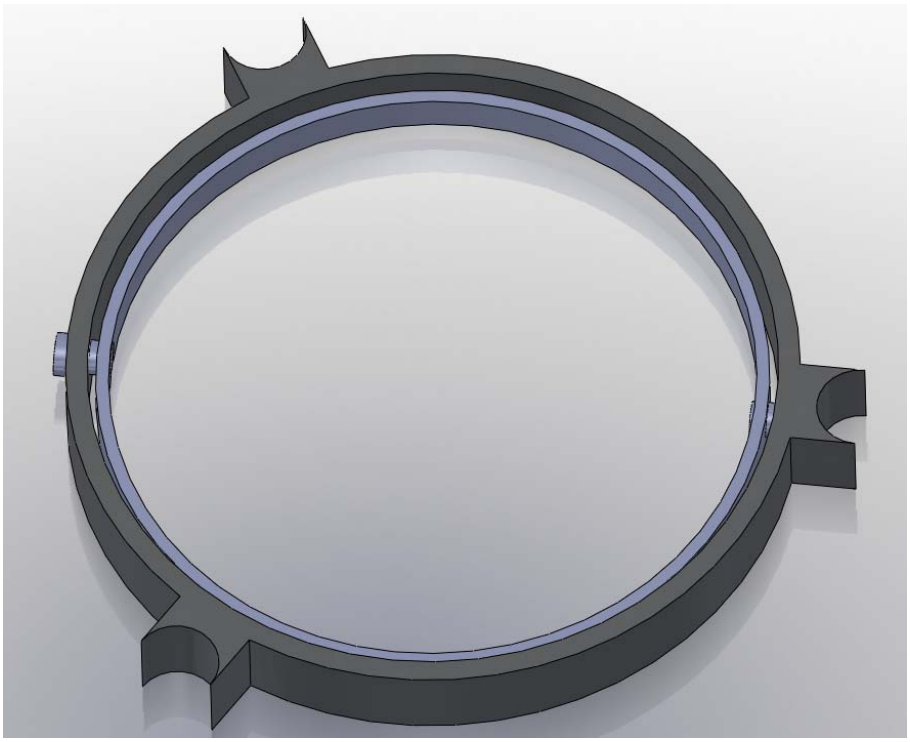

**Figure 4.16: Lower Leg Belt with an Inner Gimbal at Static Position**

Gimbals are considered as “a pivoted support that allows the rotation of an object about a single axis” [26]. In this design, the inner gimbal can be tied on the lower part of the thigh instead of the lower leg belt. At a static position, the lower leg belt and the inner gimbal are parallel to each other (see Figure 4.15). When there is a movement, the lower leg belt still performs the translation, but the inner gimbal rotates with the movement of the leg as shown in Figure 4.16.

Since this inner gimbal is installed inside of the lower leg belt, it does not change the structure of the hip exoskeleton. Therefore, the previous analysis is still available after the inner gimbal is installed. The only result is that it increases the comfort level of the entire design.

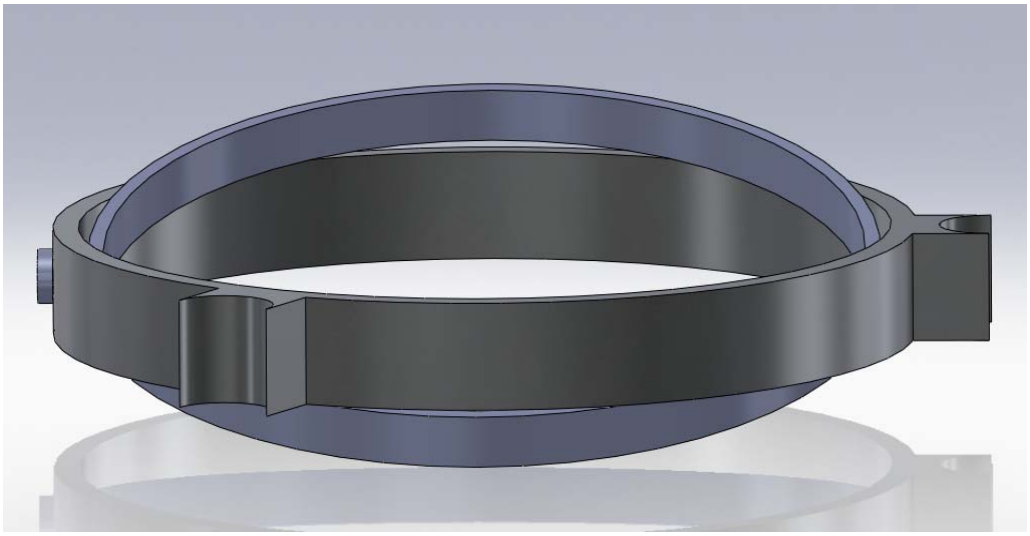

**Figure 4.17: Lower Leg Belt with an Inner Gimbal at Moving Position**

Due to the small movement on the side ways (moving left and right), the inner gimbal is good enough for this design. However, a spherical gimbal (or called ball joint swivel bearing) can be a better choice for the hip exoskeleton. Inside of the lower leg belt, there is a ball shell joint as shown in Figure 4.17.

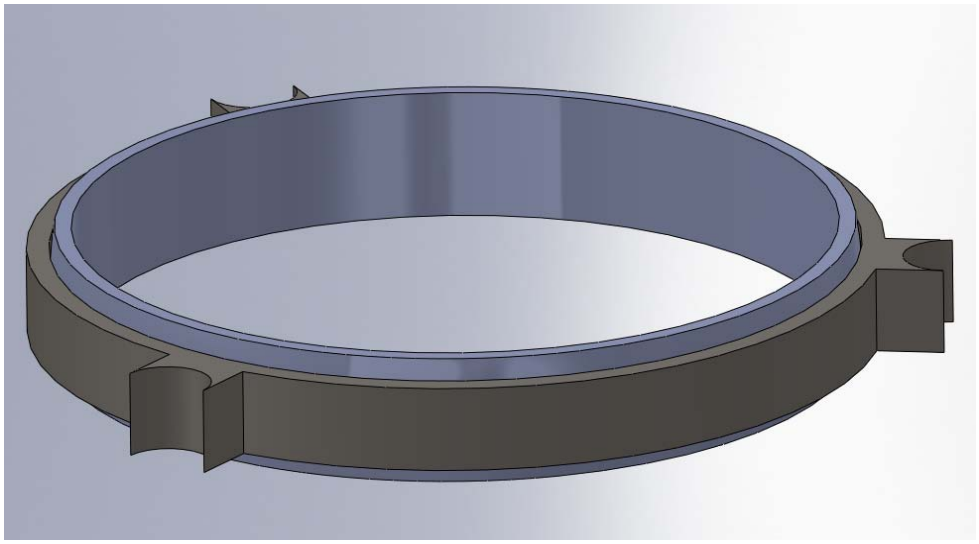

**Figure 4.18: Lower Leg Belt with a Spherical Gimbal at Static Position**

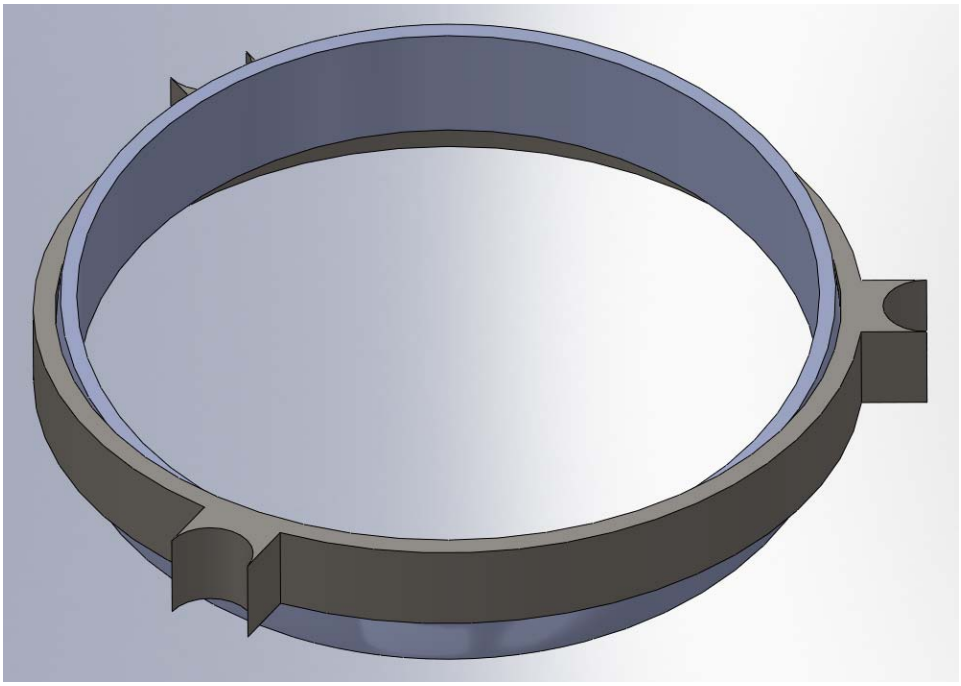

(a)

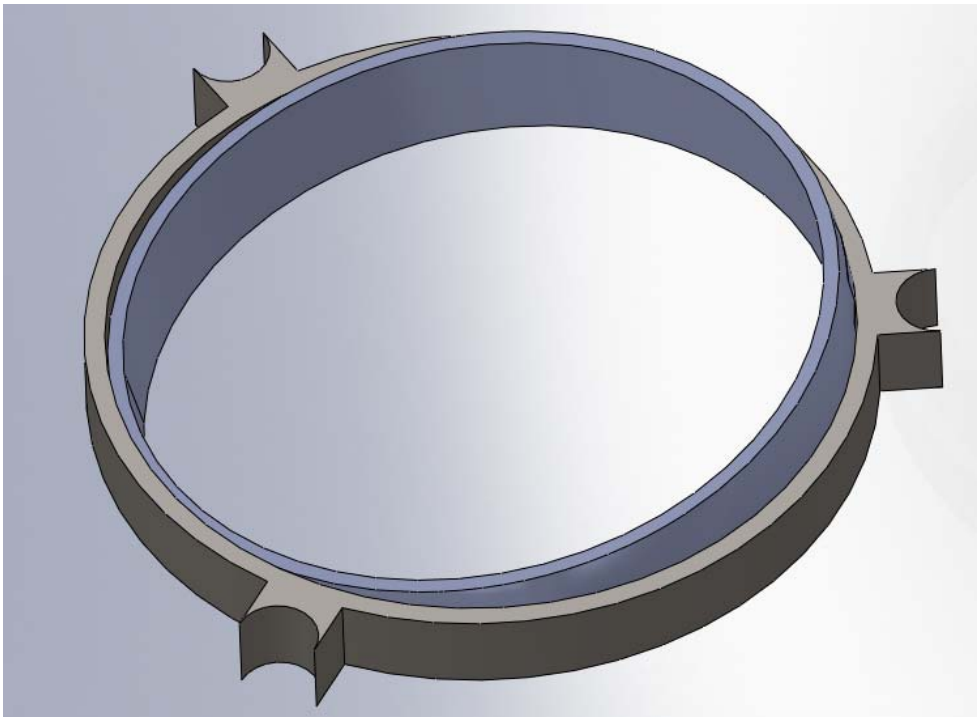

(b)

**Figure 4.19: Lower Leg Belt with a Spherical Gimbal at Moving Position: (a) Forward; (b) Sideways**

The advantage of a spherical gimbal is that it can rotate in all directions. Therefore, it avoids the limitation of the inner gimbal (compare Figure 4.18 with Figure 4.16). Another advantage of the spherical gimbal is that there is no screw needed in this unit, so it is more comfortable for the wearers.

The same as the inner gimbal, the spherical gimbal does not change the structure of the hip exoskeleton. As a result, the previous analysis is still available.

# Chapter 5

# Results and Discussion

With the theoretical results of the analysis, the CAD model is able to perform as required as shown in the following figures (Figure 5.1-5.4).

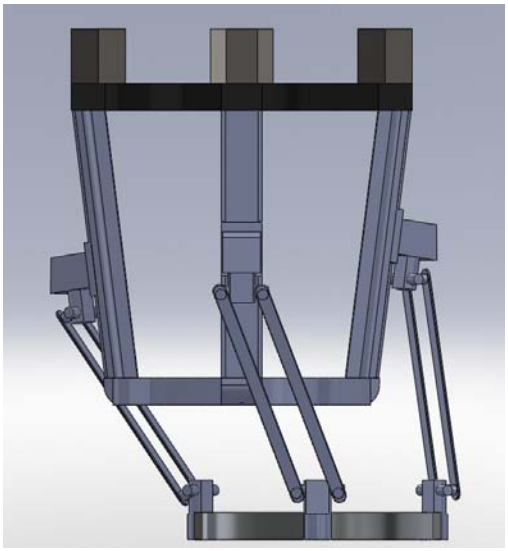

**Figure 5.1: Move Forward**

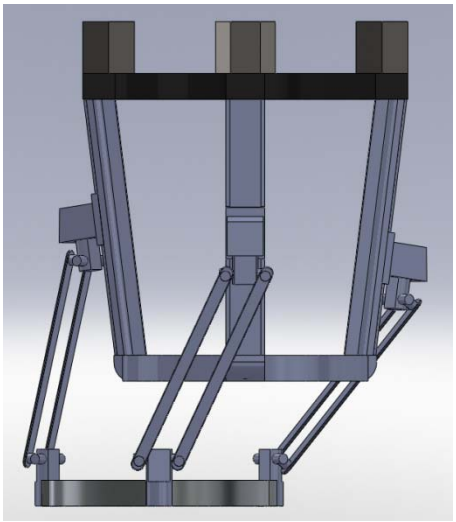

**Figure 5.2: Move Backward**

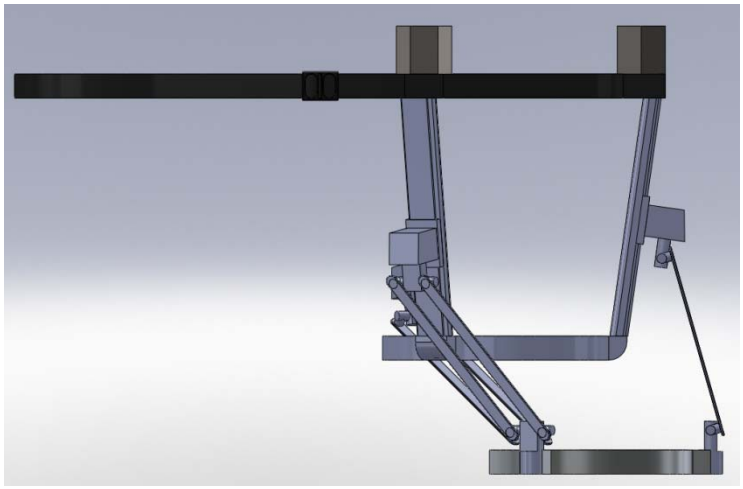

Figure 5.3: Move Right

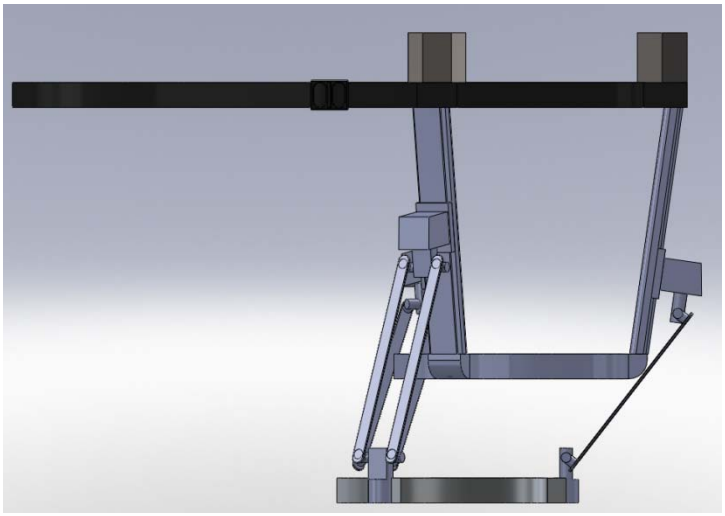

Figure 5.4: Move Left

Based on the previous analysis and the performance, the CAD model shows the viability of the parallel structure of the hip exoskeleton unit, which introduced the idea of partial manipulator. This mechanism is simple, lightweight, and has no extra components, and it should contain all the advantages that a parallel mechanism has.

The mobility analysis made in section 3.3.1 shows that this unit is able to perform the three-degree of freedom that a normal hip motion needs. The inverse kinematics

analysis presents the basic motion needed from the system by calculating the displacement of the actuated variables. By using this result of Jacobian Matrix, the first order partial derivatives of a vector valued function and the motions of this unit are defined by independent parameters. Until this point, the parallel configuration has been completely evaluated and been authenticated that this system is adaptable.

The FEA analysis verified the performance and stiffness of the system by providing very similar results with these ones calculated in MatLab. Though the stiffness of the system is not the only condition for making the structure, it offers a further improvement on the kinematic properties and structure of the design. Consequently, the optimization of the stiffness has proved that the structure of the designed mechanism is in a reliable range.

These above results show that this thesis has fully answered the hypothesis proposed in Chapter 1. It is reasonable to design a three-degree of freedom parallel structure hip exoskeleton unit that helps wearers to move their legs properly, and the parallel structure designed for this manipulator is novel reliable, convenient, and state-of-the-art.

Acceding to these results obtained, there are still some improvements which can be applied on this unit, such as a shoulder harness. With a shoulder harness, the weight of the hip exoskeleton is carried by the shoulders instead of the waist. As a result, the wears feel much more comfortable.

# Chapter 6

# Conclusions

In this thesis, the design of a three-degree of freedom parallel structure hip exoskeleton unit has been described in detail. While designing this structure, a list of requirements on structure, applicability, and economic consideration extracted from the normal human hip motion analysis is kept included. This hip exoskeleton is a novel one: first, the hip exoskeleton is fully built with a parallel structure, so that the advantages of a parallel structure are also owned, such as higher accuracy and stiffness, lower moving mass, and reduced installation requirements [4]. Also, comparing with the existing units, it is much smaller, which means it is much lighter and convenient to the. Last but not least, the P-U-U configuration of the exoskeleton unit meets all the needs of a hip motion.

A series of analysis of the structure has been completed in this thesis. - In order to achieve the basic hip activity, the exoskeleton unit has to accommodate the hip's three-degree of freedom motions which are flexion/extension, abduction/adduction, and medial/lateral rotation. The mobility analysis in the previous section has been proved that the P-U-U configuration meets this condition. The calculated inverse kinematic analysis and the Jacobian matrix analysis proved and supports that the parallel structure is reliable and accurate. The stiffness analysis proved that the structure of the manipulator is valid and reasonable. FEA analysis of the unit is another strong support of this design. Optimization that is used to analyze the requirements on stiffness, the mechanical

interferences and the geometric properties have been provided as well. Other than verify the structure of the hip exoskeleton, an additional work on sensing and control has been discussed in this thesis, which makes the future work of the entire project much easier.

Overall, this research has achieved the objectives of the thesis, and it is reasonable to design a three-degree of freedom parallel structure hip exoskeleton unit that helps wearers moving their legs properly. At the same time, the designed structure is reliable, convenient, and state-of-the-art. In addition to augmenting the complexity of mechanism, the advancement of this hip exoskeleton unit can contribute to the science of partial manipulator and lead to a better understanding of "locomotory biomechanics" [13] in an economical view in the future.

# Chapter 7

# Future Work

The structure has been tested and it has been approved that this design is reasonable and attainable, which means it is ready to go further. Therefore, the following fields can be considered as future work for the hip exoskeleton: building a prototype, chose the materials and perform further optimization on the structure of the prototype.

## 7.1 Prototype

Currently, the hip exoskeleton has been built in SolidWorks as a CAD model. Though the manipulator has satisfied all the visual mode requirements, a prototype will help to solve all the potential problems. Also, a prototype has much more contributions to a product than a CAD model does.

First of all, prototype is a real model of the manipulator, so it provides a visual model. Based on the visual model, some adjustments can be easily made, such as the size of the waist belt. These small adjustments will not affect the performance of the hip exoskeleton, but it will improve the applicability. It is hard to make these kind adjustments on a computer model than a prototype due to the intangibility of the CAD model.

Second, the hip exoskeleton model is moving perfectly in the program as shown in the previous chapters; however, we cannot assume that the wearers will feel perfectly

comfortable until they wear the actual hip exoskeleton on them. After the wearers have the manipulator on, they can find out how they feel and where need to be improved. Comparing with a computer model, it is easier to optimize the entire design on a prototype because it is easier to be adjusted.

Third, there are no errors or tolerances in a CAD model since every detention is ideal, but it is different in a prototype. Errors and tolerances are unavoidable in the real world, so a prototype is much closer to the reality than a computer model. As a result, a prototype provides much accurate data than a computer model for the future.

Last, a prototype can open people's mind better. After wearing a prototype, the designer will be able to understand it better and have more ideas on improving.

## 7.2 Materials

As mentioned above, this hip exoskeleton manipulator is build for the people who have difficulty in moving their hips. As a consequence, most of those people are not able to carry heavy load, such as a heavy hip exoskeleton. Therefore, the lighter the manipulator is, the more the wearers prefer, so the selection of the material of the hip exoskeleton can be another major subject in this case.

In order to keep the properties of this design, a strong, light, and tough material should be chosen. However, some light and suitable materials can be extremely expensive as manufacturing materials, such as, titanium, the material to build space station [25]. This design is targeted to average revenue family; there is no point to make this product expensive as most will not be able to afford it if is. As a result, how to

balance the design properties and material cost should be another consideration keep in mind when selecting the materials.

As suggestion, aluminum alloy is a first-rate choice since it is a tough, strong, and lightweight material [26]. Comparing with titanium, it is much cheaper. By choosing this material, the properties of this design can be fully kept. Certainly, there are some other materials to choose by doing further research, but this step should be able to complete in the prototype stage in order to save both money and time.

## 7.3 Sensor and Motor

The major task for this thesis is to build a parallel structure hip exoskeleton and authenticate the structure by multiple methods, which has been completed within the paper. This thesis also provides brief suggestions about the sensors and motors that should be chosen for this novel design. The criteria for sensors and motors have been specified in the previous chapter, and further researches need to be working on to select specific model to build the manipulator prototype in the future.

## 7.4 Further Test and Optimization

After building the prototype, some adjustments and improvements can be made on the actual manipulator. Most of potential changes should not affect the structure of this design to keep the basic performance, but few of them should be able to improve the quality of the hip exoskeleton unit. In order to get more accurate data for the future production, some tests and analysis on both the computer model and prototype have to be re-done after all the modifications.

Not all of the parts of this manipulator will have the same length of usage duration, which means some parts will break before other parts. In order to minimum the cost, the wearers will prefer to change the broken parts rather than purchase a new unit. Also, some wearers may not need to go to outside either due to their health conditions or the weather conditions. Nevertheless, they do not want to take the unit off because they still need to walk around. In these cases, the manipulator has to be easily assembled and disassembled as mentioned in the previous chapter. In order to best satisfy this need, the optimization of the assemblage should be achieved in the future as well.

Accessional items can be added on this unit in consideration of supplementary requirements from customers. Some of the wearers may not be able to put the unit on because their waists cannot carry the heavy load though the manipulator is fairly light. In that case, a pair of suspenders will be the best solution, which means the entire weight of the unit is on the shoulders rather than on the waist. This kind of optimization can always improve the range of the use of the manipulator.

Overall, there is still some room for improvement for the hip exoskeleton unit in order to lead an ideal position in the market after it has been produced.

# Reference

[1] Tsai, Lung-Wen. *Robot Analysis.* New York : John Wiley & Sons. Inc, 1999. 0-471-32593-7.

[2] Pratt, Jerry E. *The RoboKnee: An Exoskeleton for Enhancing Strength and Endurance During Walking.* New Orleans : IEEE, July 2004, Vol. 3. pp.1050-4729.

[3] Pan, Min; Chi, Zhongzhe and Zhang, Dan. *Novel Design of a Three DOFs MEMS-based Precision Manipulator.* Beijing : IEEE International Conference on Mechatronics and Automation, 2011. 120931.

[4] Zhang, Dan. *Parallel Robotic Machine Tools.* New York : Springer Science+Business Media, 2009. 978-1-4419-1116-2.

[5] Robots for All. [Online] September 26, 2007. [Cited: October 16, 2010.] http://www.google.ca/imgres?imgurl=http://1.bp.blogspot.com/_YvJKpyH_eDg/RuQuGX9dZGI/AAAAAAAAACI/wdMfAjCSN84/s400/adept.png&imgrefurl=http://openrobotics.blogspot.com/.

[6] Huston, Ronald L. *Principles of Biomechanics.* Boca Raton : Taylor & Francis Group, 2009. 13: 978-0-8493-3494-8.

[7] Valiente, Andrew. *Design of a Quasi-Passive Parallel Leg Exoskeleton to Augment Load Carrying for Walking.* Cambridge : LeTourneau University, 2003. 040122.

[8] Cyberdyne. *Robot Suit Hal.* [Online] Cyberdyne, Inc, Auguest 2010. [Cited: Noverber 2, 2010.] http://www.cyberdyne.jp/english/robotsuithal/index.html.

[9] Kazerooni, Racine and Huang, Steger. *On the Control of the Berkeley Lower Extremity Exoskeleton (BLEEX).* Barcelona : IEEE, April 2005. International Conference on Robotics and Automation. pp. 18-22.

[10] Hamill, Joshph and Knutzen, Kathleen M. *Biomechanical: Basis of Human Movement.* Baltimore : Lippincott Williams & Wikins, 2009. 987-0-7817-9128-1.

[11] Masood, M.A. Techhilla. *Covers Apple, Microsoft, Google & the Web.* [Online] August 9, 2010. [Cited: May 25, 2011.] http://www.techxilla.com/2010/08/09/worlds-top-10-exoskeletons/.

[12] Perry, Jacqelin and Burnfield, Judith M. *Gait Analysis: Normal and Pathological Function.* New Jersey : SLACK Incorporated, 2010. 978-1-55642-766-4.

[13] Walsh, James. *Biomimetic Design of an Under-Actuated Leg Exoskeleton For Load-Carrying Augmentation.* Cabbrege : Massachusetts Institute of Technology, 2006. 040122.

[14] Oatis, Carol A. *Kinesiology: the Mechanics & Pathomechanics of Human Movement.* Baltimore : Lippincott Williams & Wilkins, 2007. 978-0-7817-7422-2.

[15] Tsai, Lung-Wen and Sameer, Joshi. *Kinematic analysis of 3-DOF position mechanisms for use in hybrid kinematic machine.* Journal of Mechanical Design, June 2002, Journal of Mechanical Design, Vol. 124, pp. 245-253.

[16] Masory, Oren and Wang, Jian. W*orkspace evauation of stewart platforms.* 1995, Advanced Robotics, Vol 9, No.4, pp. 443-461.

[17] Xu, Qingsong and Li, Yangmin. *Kinematic analysis and design of a new 3-DOF translational parallel manipulator.* Jounral of Intellgent and Robotic Systems, July 2006, Journal of Mechanical Design, Vol.128, pp. 729-737.

[18] Li, Yangmin and Xu, Qingsong. *A new approach to the architecture optimization of a general 3-PUU translational parallel manipulator.* July 2006, Journal of Intelligent and Robotic Systems, Vol.46, pp.59-72.

[19] Meyer, Jan; Lukowicz, Paul and Troster, Gerhard. *Textile Pressure Sensor for Muscle Activity and Motion Dection.* Montreux : Wearable Computers (ISWC), October, 2006, Vol.6. pp.1114-6972.

[20] Hermens, Hermie J.; Freriks, Bart and *et al*. *Development of Recommendations for SEMG Sensors and Senor Placement Procedures.* Journal of Electromyography and Kinesiology, 2000, Vol. 2. pp.361-374.

[21] Gao, Zhen and Zhang, Dan. *Surface Electromyographic Sensor for Huamn Motion Estimation Based on Arm Wrestling Robot.* Sensors & Transducers Journal, June, 2010, Vol. 117, pp.50-61.

[22] Norton, Rober L. *Machine Design: An Integrated Approach.* Upper Saddle River : Pearson Education, Inc., 2006. 0-13-148190-8.

[23] Standard Technologies of the Seattel Robotics Society. *What is a Servos.* [Online] Seattle Robotics Society, July 2009. [Cited: May 26, 2011.] http://www.seattlerobotics.org/guide/servos.html.

[24] China Motor Information. *DZJ.* [Online] Nibe Xing Huang Automobile Service Ltd., May 09, 2011. [Cited: May 27, 2011.] http://www.jdzj.com/jdzjnews/2113970.html.

[25] Callister, William D. Jr. *Materials Science and Engineering: An Introduction.* New York : John Wiley & Sons, Inc., 2007. 0-471-73696-1.

[26] Bedrossian, Nazareth S.; Paradiso, Joseph and *et al*. *Steering law design for redundant single-gimbal control moment gyroscopes*. Journal of Guidance, Control and Synamics, 1990, Vol. 13, pp.0731-5090.

# Appendix

## Appendix I: Improved Structure FEA Analysis

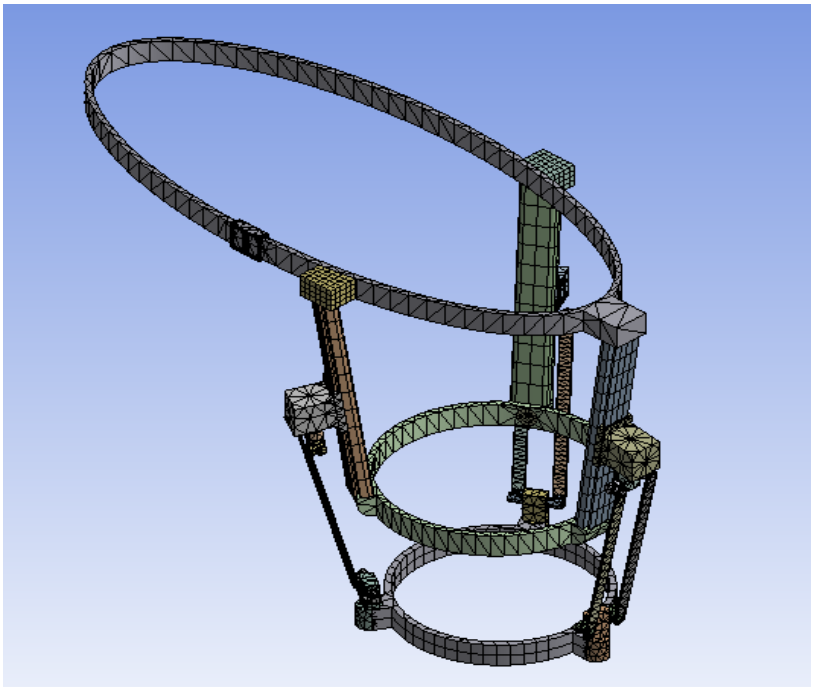

Figure AI.1: Finite Element Model of the Updating Hip Exoskeleton

## Appendix I.I: Force Application

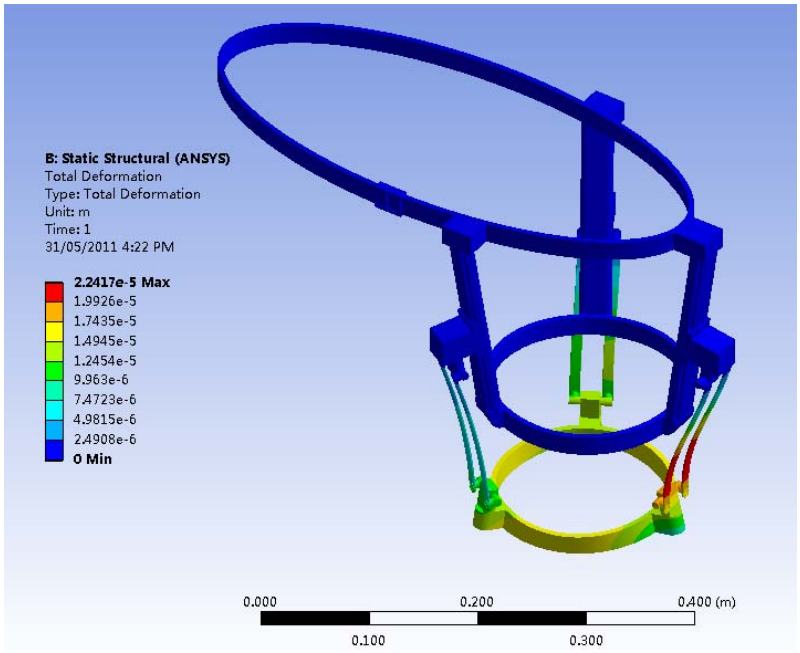


Figure AI.2: Total Deformation based on Applied Force

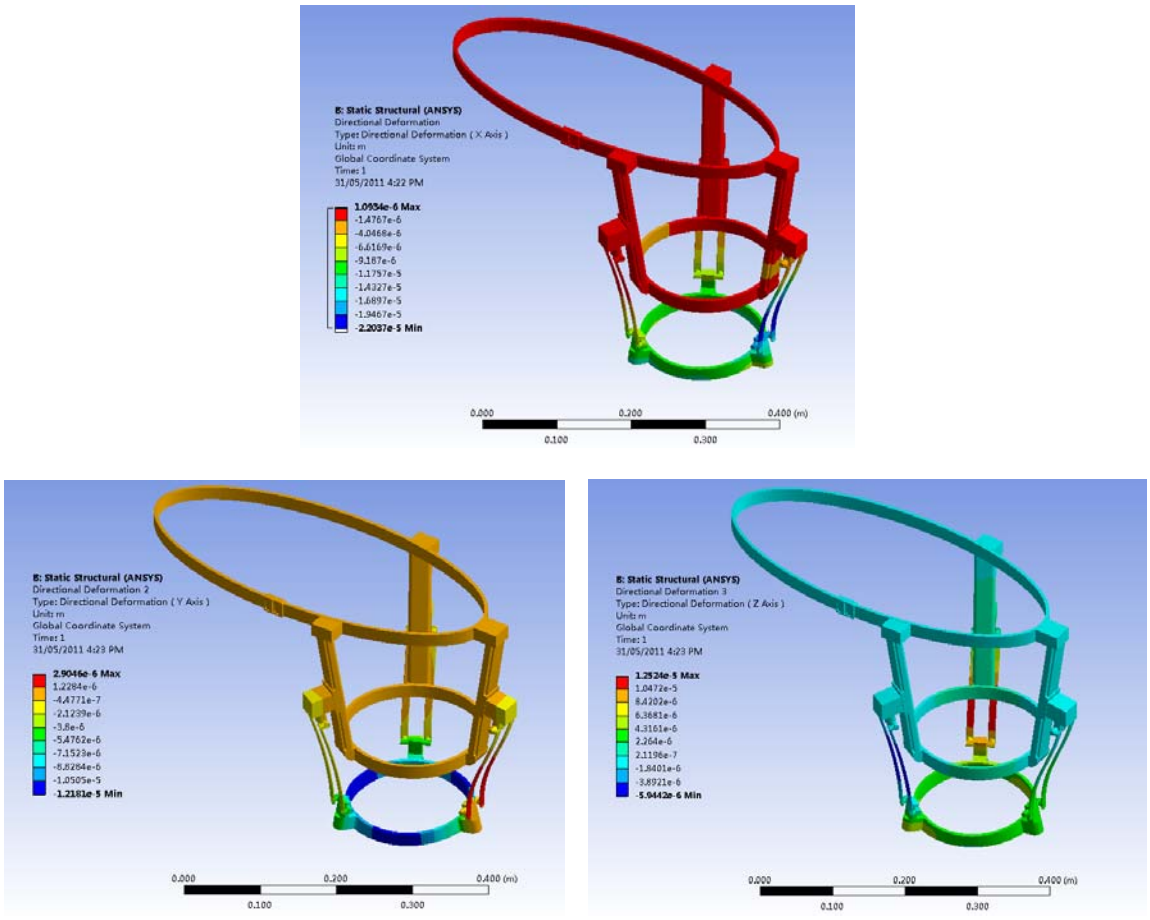


**Figure AI.3: Deformation in X, Y, Z-axis based on Applied Force**

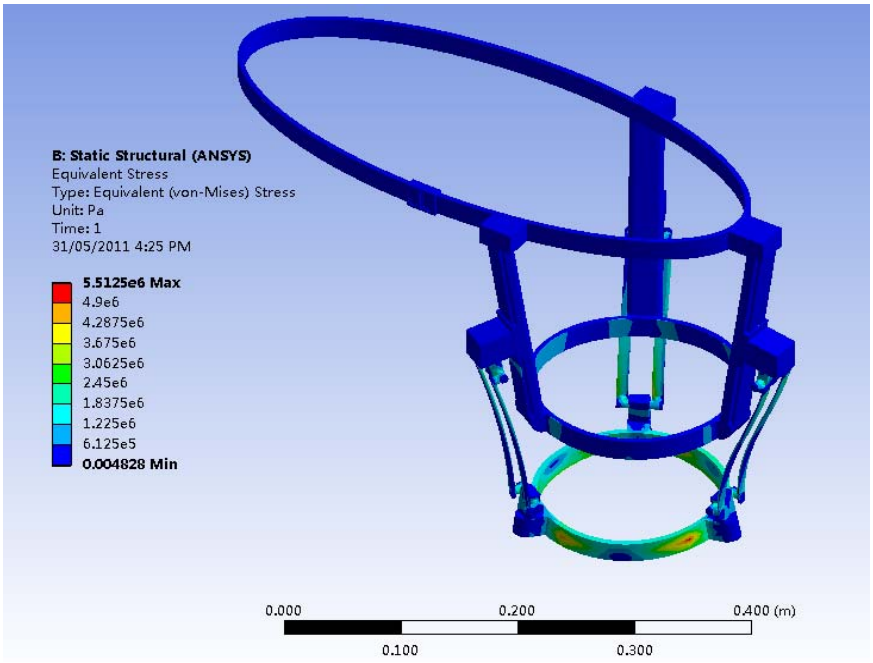


**Figure AI.4: Equivalent Stress based on Applied Force**

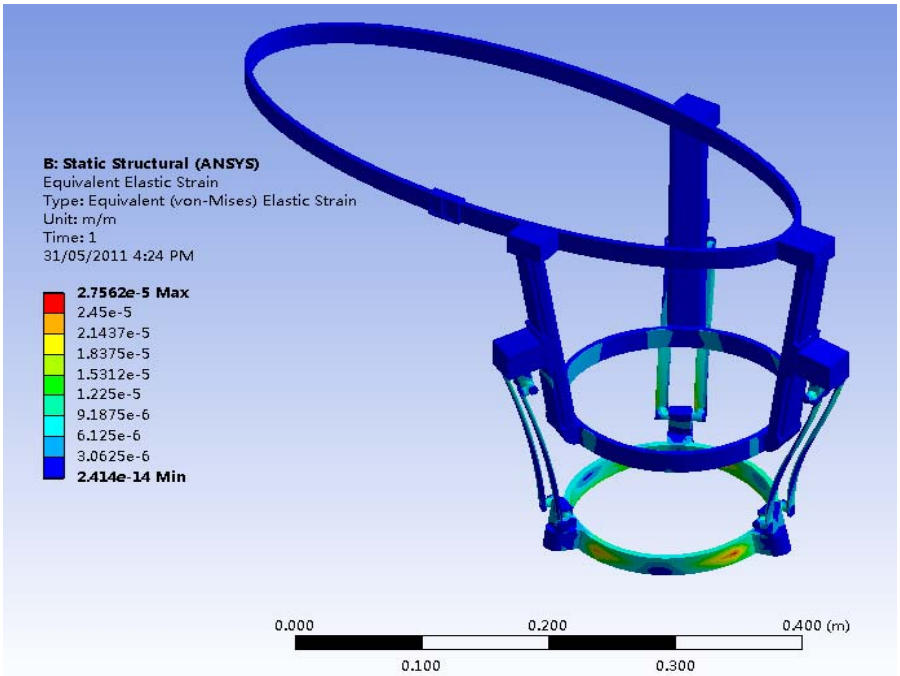


**Figure AI.5: Equivalent Strain based on Applied Force**

# Appendix I.II: Moment Application

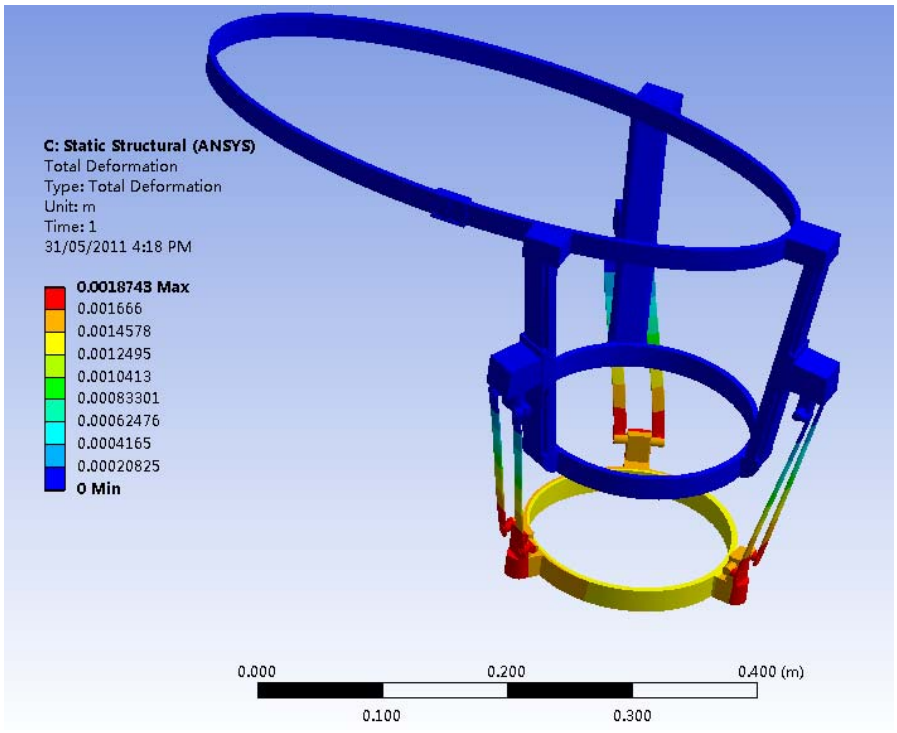


**Figure AI.6: Total Deformation based on Applied Moment**

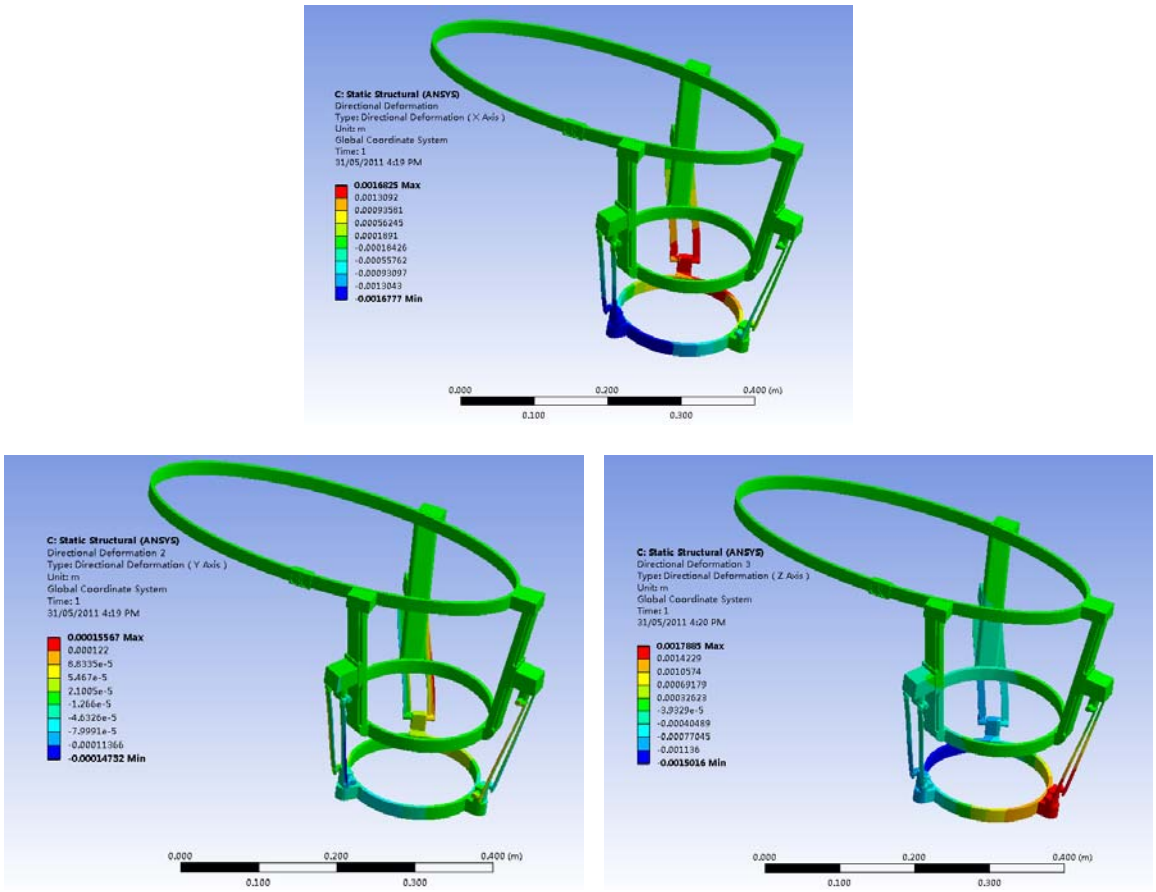


**Figure AI.7: Deformation in X, Y, Z-axis based on Applied Moment**

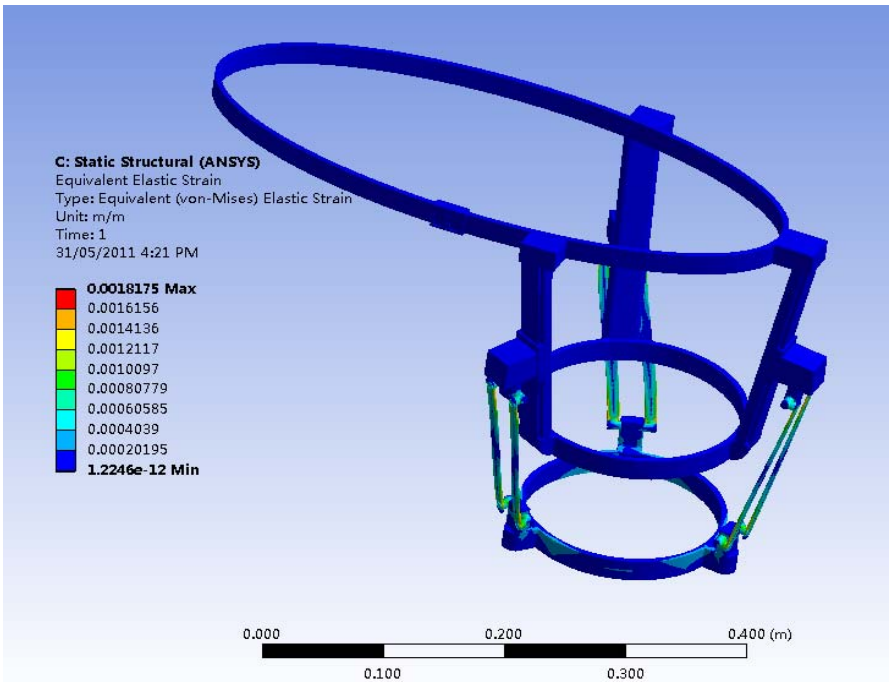


**Figure AI.8: Equivalent Stress based on Applied Moment**

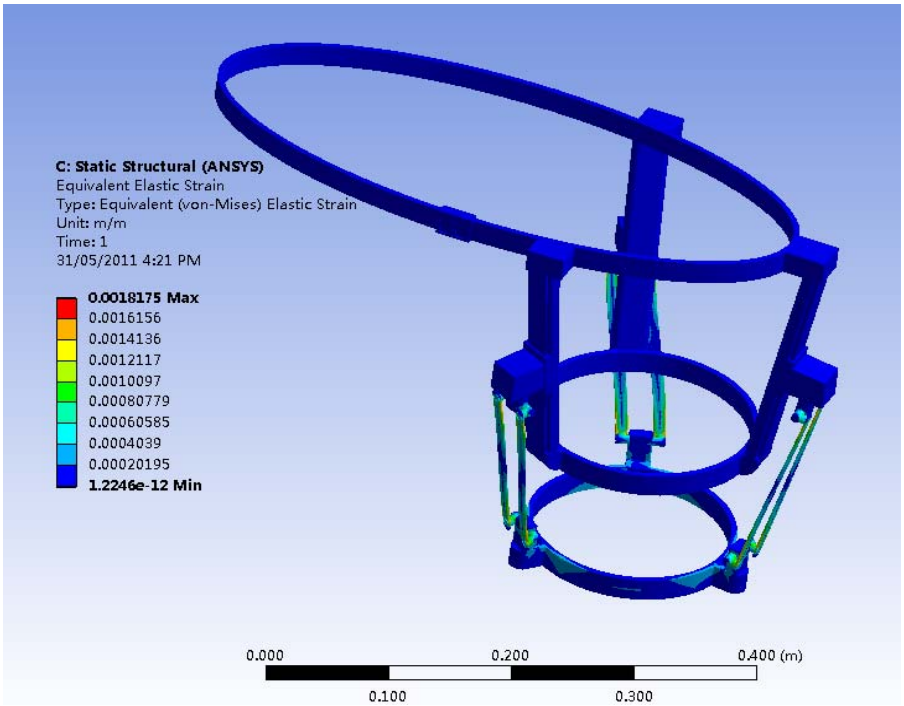


**Figure AI.9: Equivalent Strain based on Applied Moment**

# Appendix II: FEA Report of the Improved Structure

## Project

| | |
|---|---|
| First Saved | Monday, May 30, 2011 |
| Last Saved | Monday, May 30, 2011 |
| Product Version | 12.0.1 Release |

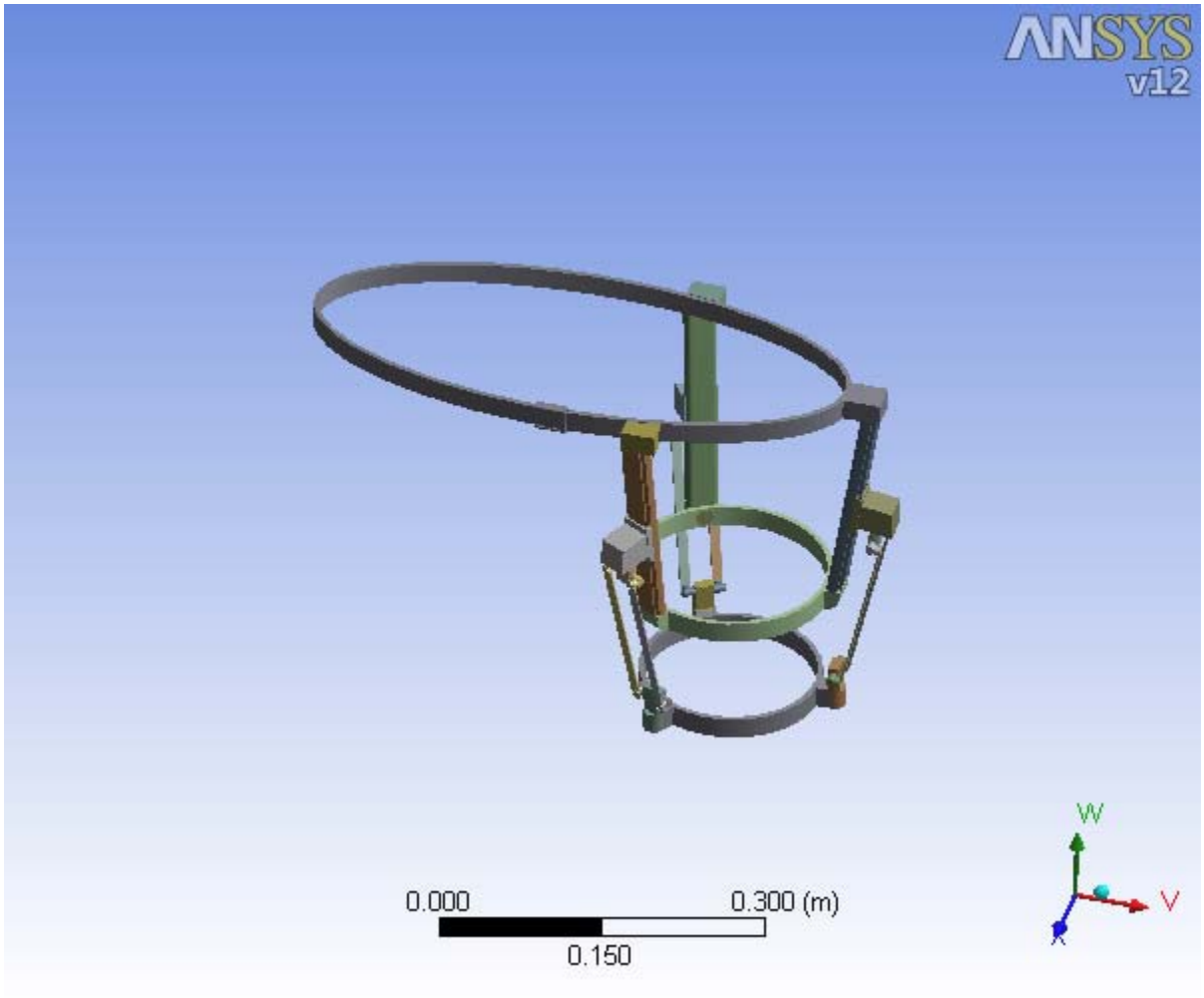

## Contents


- Units
- Model (B4)
  - Geometry
    - Parts
  - Coordinate Systems
  - Connections
    - Contact Regions
  - Mesh
  - Static Structural (B5)
    - Analysis Settings
    - Loads
    - Solution (B6)
      - Solution Information
      - Results
- Material Data
  - Structural Steel


## Units

**TABLE 1**

| | |
|---|---|
| Unit System | Metric (m, kg, N, s, V, A) Degrees rad/s Celsius |
| Angle | Degrees |
| Rotational Velocity | rad/s |
| Temperature | Celsius |

## Model (B4)

### Geometry

**TABLE 2**
**Model (B4) > Geometry**

| | |
|---|---|
| Object Name | *Geometry* |
| State | Fully Defined |
| **Definition** | |
| Source | H:\Users\Administrator\AppData\Local\Temp\WB_WIN-388KFD85MH7_5548_2\unsaved_project_files\dp0\SYS-1\DM\SYS-1.agdb |
| Type | DesignModeler |

| | |
|---|---|
| Length Unit | Meters |
| Element Control | Program Controlled |
| Display Style | Part Color |
| **Bounding Box** | |
| Length X | 0.55783 m |
| Length Y | 0.35516 m |
| Length Z | 0.28404 m |
| **Properties** | |
| Volume | 6.9964e-004 m³ |
| Mass | 5.4922 kg |
| Scale Factor Value | 1. |
| **Statistics** | |
| Bodies | 32 |
| Active Bodies | 32 |
| Nodes | 54126 |
| Elements | 24502 |
| Mesh Metric | None |
| **Preferences** | |
| Import Solid Bodies | Yes |
| Import Surface Bodies | Yes |
| Import Line Bodies | No |
| Parameter Processing | Yes |
| Personal Parameter Key | DS |

| | |
|---|---|
| CAD Attribute Transfer | No |
| Named Selection Processing | No |
| Material Properties Transfer | No |
| CAD Associativity | Yes |
| Import Coordinate Systems | No |
| Reader Save Part File | No |
| Import Using Instances | Yes |
| Do Smart Update | No |
| Attach File Via Temp File | Yes |
| Temporary Directory | H:\Users\Administrator\AppData\Local\Temp |
| Analysis Type | 3-D |
| Mixed Import Resolution | None |
| Enclosure and Symmetry Processing | Yes |

**TABLE 3**
**Model (B4) > Geometry > Parts**

| Object Name | *Leg Joint-2* | *Leg Joint-3* | *Upper Leg Joint-1* | *Upper Leg Joint-2* | *Upper Leg Joint-3* |
|---|---|---|---|---|---|
| State | Meshed | | | | |
| **Graphics Properties** | | | | | |
| Visible | Yes | | | | |
| Transparency | 1 | | | | |

| Definition | | | | | |
|---|---|---|---|---|---|
| Suppressed | No | | | | |
| Stiffness Behavior | Flexible | | | | |
| Coordinate System | Default Coordinate System | | | | |
| Reference Temperature | By Environment | | | | |
| **Material** | | | | | |
| Assignment | Structural Steel | | | | |
| Nonlinear Effects | Yes | | | | |
| Thermal Strain Effects | Yes | | | | |
| **Bounding Box** | | | | | |
| Length X | 4.5407e-002 m | | 2.3013e-002 m | | 2.245e-002 m |
| Length Y | 4.0446e-002 m | | 4.5687e-002 m | | |
| Length Z | 4.9648e-002 m | | 2.3961e-002 m | | 2.e-002 m |
| **Properties** | | | | | |
| Volume | 2.0839e-005 m³ | | 9.9402e-006 m³ | | |
| Mass | 0.16358 kg | | 7.8031e-002 kg | | 7.803e-002 kg |
| Centroid X | -5.8065e-002 m | -5.803e-002 m | -5.9519e-002 m | -5.9553e-002 m | 0.14971 m |
| Centroid Y | 9.6071e-002 m | 9.6678e-002 m | 8.4705e-002 m | 8.4099e-002 m | 8.5743e-002 m |
| Centroid Z | 0.11398 m | -0.12227 m | -0.12484 m | 0.11655 m | -4.0432e-003 m |
| Moment of Inertia Ip1 | 3.461e-005 kg·m² | | 1.2639e-005 kg·m² | | 1.3265e-005 kg·m² |
| Moment of Inertia Ip2 | 3.6374e-005 kg·m² | | 3.5311e-006 kg·m² | 3.531e-006 kg·m² | 3.5306e-006 kg·m² |
| Moment of Inertia | 2.6117e-005 | 2.6116e-005 | 1.3266e-005 kg·m² | | 1.2638e-005 |

| | | | | |
|---|---|---|---|---|
| Ip3 | kg·m² | kg·m² | | kg·m² |
| **Statistics** | | | | |
| Nodes | 1414 | 1428 | 630 | 636 |
| Elements | 668 | 678 | 292 | 297 |
| Mesh Metric | None | | | |

**TABLE 4**
**Model (B4) > Geometry > Parts**

| Object Name | *Scaw-1* | *Scaw-2* | *Scaw-3* | *Scaw-4* | *Scaw-5* |
|---|---|---|---|---|---|
| State | Meshed | | | | |
| **Graphics Properties** | | | | | |
| Visible | Yes | | | | |
| Transparency | 1 | | | | |
| **Definition** | | | | | |
| Suppressed | No | | | | |
| Stiffness Behavior | Flexible | | | | |
| Coordinate System | Default Coordinate System | | | | |
| Reference Temperature | By Environment | | | | |
| **Material** | | | | | |
| Assignment | Structural Steel | | | | |
| Nonlinear Effects | Yes | | | | |
| Thermal Strain Effects | Yes | | | | |
| **Bounding Box** | | | | | |
| Length X | 4.1142e-002 m | 1.4619e-002 m | 4.0952e-002 m | 4.0937e-002 m | 4.0952e-002 m |
| Length Y | 1.0403e-002 m | 1.0018e-002 m | 1.0263e-002 m | 1.0403e-002 m | 1.0263e-002 m |

| | | | | | |
|---|---|---|---|---|---|
| Length Z | 3.1692e-002 m | 4.e-002 m | 3.1824e-002 m | 3.1811e-002 m | 3.1824e-002 m |
| **Properties** | | | | | |
| Volume | 2.6746e-006 m³ | | | | |
| Mass | 2.0996e-002 kg | | | | |
| Centroid X | -5.9082e-002 m | 0.14874 m | -5.8999e-002 m | -3.65e-002 m | -3.6503e-002 m |
| Centroid Y | 6.5218e-002 m | 6.6933e-002 m | 6.5851e-002 m | -8.9537e-002 m | -8.9511e-002 m |
| Centroid Z | 0.11568 m | -4.0714e-003 m | -0.12401 m | 8.1917e-002 m | -9.3076e-002 m |
| Moment of Inertia Ip1 | 3.3821e-007 kg·m² | 3.4223e-006 kg·m² | 3.382e-007 kg·m² | 3.3822e-007 kg·m² | |
| Moment of Inertia Ip2 | 3.5907e-006 kg·m² | 3.5916e-006 kg·m² | 3.5905e-006 kg·m² | | |
| Moment of Inertia Ip3 | 3.4213e-006 kg·m² | 3.3832e-007 kg·m² | 3.4211e-006 kg·m² | | |
| **Statistics** | | | | | |
| Nodes | 619 | 581 | 656 | 659 | |
| Elements | 301 | 285 | 323 | 324 | |
| Mesh Metric | None | | | | |

**TABLE 5**
**Model (B4) > Geometry > Parts**

| Object Name | *Scaw-6* | *Upper Leg Joint-4* | *Upper Leg Joint-5* | *Upper Leg Joint-6* | *Lower Leg Belt-3* |
|---|---|---|---|---|---|
| State | Meshed | | | | |
| **Graphics Properties** | | | | | |
| Visible | Yes | | | | |
| Transparency | 1 | | | | |
| **Definition** | | | | | |

| | | | | |
|---|---|---|---|---|
| Suppressed | No | | | |
| Stiffness Behavior | Flexible | | | |
| Coordinate System | Default Coordinate System | | | |
| Reference Temperature | By Environment | | | |
| **Material** | | | | |
| Assignment | Structural Steel | | | |
| Nonlinear Effects | Yes | | | |
| Thermal Strain Effects | Yes | | | |
| **Bounding Box** | | | | |
| Length X | 1.4619e-002 m | 2.e-002 m | | 0.18441 m |
| Length Y | 1.0018e-002 m | 4.4e-002 m | | 2.e-002 m |
| Length Z | 4.e-002 m | 2.e-002 m | | 0.18218 m |
| **Properties** | | | | |
| Volume | 2.6746e-006 m³ | 9.9402e-006 m³ | | 5.9939e-005 m³ |
| Mass | 2.0996e-002 kg | 7.8031e-002 kg | | 0.47052 kg |
| Centroid X | 0.11501 m | 0.11339 m | -3.5723e-002 m | 1.3947e-002 m |
| Centroid Y | -8.9466e-002 m | -0.10776 m | | -0.11561 m |
| Centroid Z | -5.5469e-003 m | -5.5751e-003 m | 8.0515e-002 m | -9.1669e-002 m | -5.5854e-003 m |
| Moment of Inertia Ip1 | 3.4223e-006 kg·m² | 1.3266e-005 kg·m² | 1.2639e-005 kg·m² | 1.6595e-003 kg·m² |
| Moment of Inertia Ip2 | 3.5916e-006 kg·m² | 3.5306e-006 kg·m² | 3.5307e-006 kg·m² | 3.2862e-003 kg·m² |

| | | | | |
|---|---|---|---|---|
| Moment of Inertia Ip3 | 3.3832e-007 kg·m² | 1.2639e-005 kg·m² | 1.3266e-005 kg·m² | 1.6583e-003 kg·m² |
| **Statistics** | | | | |
| Nodes | 581 | 655 | 656 | 1110 |
| Elements | 285 | 306 | 308 | 132 |
| Mesh Metric | None | | | |

**TABLE 6**
**Model (B4) > Geometry > Parts**

| Object Name | *Sensor-1* | *Sensor-2* | *Sensor-3* | *Upper Leg Belt-2* | *leg-1* |
|---|---|---|---|---|---|
| State | Meshed | | | | |
| **Graphics Properties** | | | | | |
| Visible | Yes | | | | |
| Transparency | 1 | | | | |
| **Definition** | | | | | |
| Suppressed | No | | | | |
| Stiffness Behavior | Flexible | | | | |
| Coordinate System | Default Coordinate System | | | | |
| Reference Temperature | By Environment | | | | |
| **Material** | | | | | |
| Assignment | Structural Steel | | | | |
| Nonlinear Effects | Yes | | | | |
| Thermal Strain Effects | Yes | | | | |
| **Bounding Box** | | | | | |
| Length X | 1.8856e-002 m | 1.e-002 m | 1.8856e-002 m | 0.20381 m | 3.2552e-002 m |

| | | | | | |
|---|---|---|---|---|---|
| Length Y | 1.6e-002 m | | | 2.e-002 m | 0.1702 m |
| Length Z | 1.666e-002 m | 1.6e-002 m | 1.666e-002 m | 0.20346 m | 3.8606e-002 m |
| **Properties** | | | | | |
| Volume | 2.0106e-006 m³ | | | 7.3247e-005 m³ | 3.2173e-006 m³ |
| Mass | 1.5783e-002 kg | | | 0.57499 kg | 2.5256e-002 kg |
| Centroid X | -3.7349e-002 m | 0.10515 m | -3.7349e-002 m | 1.0107e-002 m | -3.7859e-002 m |
| Centroid Y | -5.039e-004 m | -5.05e-004 m | -5.039e-004 m | -9.8067e-005 m | -1.3574e-002 m |
| Centroid Z | -8.6359e-002 m | -4.0865e-003 m | 7.8186e-002 m | -3.9278e-003 m | -0.12249 m |
| Moment of Inertia Ip1 | 3.7686e-007 kg·m² | 4.9467e-007 kg·m² | 3.7686e-007 kg·m² | 2.5913e-003 kg·m² | 5.6572e-005 kg·m² |
| Moment of Inertia Ip2 | 3.7671e-007 kg·m² | 3.7743e-007 kg·m² | 3.7661e-007 kg·m² | 5.1482e-003 kg·m² | 2.1995e-007 kg·m² |
| Moment of Inertia Ip3 | 4.9351e-007 kg·m² | 3.7757e-007 kg·m² | 4.9341e-007 kg·m² | 2.5953e-003 kg·m² | 5.6771e-005 kg·m² |
| **Statistics** | | | | | |
| Nodes | 579 | 1394 | 519 | 1825 | 4856 |
| Elements | 99 | 260 | 87 | 822 | 2619 |
| Mesh Metric | None | | | | |

**TABLE 7**
**Model (B4) > Geometry > Parts**

| Object Name | *leg-2* | *leg-3* | *leg-4* | *leg-7* | *leg-8* |
|---|---|---|---|---|---|
| State | Meshed | | | | |
| **Graphics Properties** | | | | | |
| Visible | Yes | | | | |

| | | | | | |
|---|---|---|---|---|---|
| Transparency | 1 | | | | |
| **Definition** | | | | | |
| Suppressed | No | | | | |
| Stiffness Behavior | Flexible | | | | |
| Coordinate System | Default Coordinate System | | | | |
| Reference Temperature | By Environment | | | | |
| **Material** | | | | | |
| Assignment | Structural Steel | | | | |
| Nonlinear Effects | Yes | | | | |
| Thermal Strain Effects | Yes | | | | |
| **Bounding Box** | | | | | |
| Length X | 3.2552e-002 m | 3.2808e-002 m | 3.8656e-002 m | | |
| Length Y | 0.1702 m | 0.16955 m | 0.1713 m | | |
| Length Z | 3.8606e-002 m | 4.1478e-002 m | 1.1338e-002 m | | |
| **Properties** | | | | | |
| Volume | 3.2173e-006 m³ | | | | |
| Mass | 2.5256e-002 kg | | | | |
| Centroid X | -6.4621e-002 m | -6.4724e-002 m | -3.7962e-002 m | 0.13905 m | |
| Centroid Y | -1.3578e-002 m | -1.4016e-002 m | -1.4017e-002 m | -1.2815e-002 m | -1.281e-002 m |
| Centroid Z | -0.10704 m | 9.7226e-002 m | 0.11268 m | 1.0642e-002 m | -2.0261e-002 m |
| Moment of Inertia Ip1 | 5.6501e-005 kg·m² | 5.6575e-005 kg·m² | 5.647e-005 kg·m² | 5.6783e-005 kg·m² | 5.6991e-005 kg·m² |
| Moment of Inertia | 2.2074e-007 | 2.2006e-007 | 2.2127e-007 | 2.1833e-007 | 2.1835e-007 |

| | | | | | |
|---|---|---|---|---|---|
| Ip2 | kg·m² | kg·m² | kg·m² | kg·m² | kg·m² |
| Moment of Inertia Ip3 | 5.6698e-005 kg·m² | 5.6774e-005 kg·m² | 5.6666e-005 kg·m² | 5.6581e-005 kg·m² | 5.6789e-005 kg·m² |
| **Statistics** | | | | | |
| Nodes | 4807 | 4854 | 4915 | 3673 | 3613 |
| Elements | 2583 | 2617 | 2668 | 1978 | 1939 |
| Mesh Metric | None | | | | |

**TABLE 8**
**Model (B4) > Geometry > Parts**

| Object Name | *Upper Leg-4* | *Upper Leg-5* | *Upper Leg-6* | *Boss-Extrude3[1]* | *Boss-Extrude3[2]* |
|---|---|---|---|---|---|
| State | Meshed | | | | |
| **Graphics Properties** | | | | | |
| Visible | Yes | | | | |
| Transparency | 1 | | | | |
| **Definition** | | | | | |
| Suppressed | No | | | | |
| Stiffness Behavior | Flexible | | | | |
| Coordinate System | Default Coordinate System | | | | |
| Reference Temperature | By Environment | | | | |
| **Material** | | | | | |
| Assignment | Structural Steel | | | | |
| Nonlinear Effects | Yes | | | | |
| Thermal Strain Effects | Yes | | | | |
| **Bounding Box** | | | | | |
| Length X | 4.2835e-002 | 4.3536e-002 | 4.3537e-002 | 3.2e-002 m | |

| | | | | | |
|---|---|---|---|---|---|
| | m | m | m | | |
| Length Y | 0.19805 m | | | 2.e-002 m | |
| Length Z | 3.e-002 m | 4.8761e-002 m | 4.876e-002 m | 2.5054e-002 m | |
| **Properties** | | | | | |
| Volume | 7.9778e-005 m³ | | | 1.4327e-005 m³ | |
| Mass | 0.62625 kg | | | 0.11247 kg | |
| Centroid X | 0.12594 m | -4.7741e-002 m | -4.7745e-002 m | -4.9502e-002 m | -4.95e-002 m |
| Centroid Y | 0.10852 m | | | 0.21755 m | |
| Centroid Z | -4.0843e-003 m | -0.10436 m | 9.6189e-002 m | -0.11861 m | 0.11044 m |
| Moment of Inertia Ip1 | 2.1257e-003 kg·m² | 2.0961e-003 kg·m² | | 8.4688e-006 kg·m² | 8.4687e-006 kg·m² |
| Moment of Inertia Ip2 | 5.0669e-005 kg·m² | | | 1.4427e-005 kg·m² | 1.4428e-005 kg·m² |
| Moment of Inertia Ip3 | 2.0961e-003 kg·m² | 2.1257e-003 kg·m² | | 1.3466e-005 kg·m² | |
| **Statistics** | | | | | |
| Nodes | 1266 | 1360 | | 733 | |
| Elements | 209 | 231 | | 120 | |
| Mesh Metric | None | | | | |

**TABLE 9**
**Model (B4) > Geometry > Parts**

| Object Name | *Chamfer2* | *Leg Joint-1* |
|---|---|---|
| State | Meshed | |
| **Graphics Properties** | | |
| Visible | Yes | |
| Transparency | 1 | |

| Definition | | |
|---|---|---|
| Suppressed | No | |
| Stiffness Behavior | Flexible | |
| Coordinate System | Default Coordinate System | |
| Reference Temperature | By Environment | |
| **Material** | | |
| Assignment | Structural Steel | |
| Nonlinear Effects | Yes | |
| Thermal Strain Effects | Yes | |
| **Bounding Box** | | |
| Length X | 0.54262 m | 4.0585e-002 m |
| Length Y | 2.4e-002 m | 4.0446e-002 m |
| Length Z | 0.22248 m | 3.e-002 m |
| **Properties** | | |
| Volume | 1.3493e-004 m³ | 2.0839e-005 m³ |
| Mass | 1.0592 kg | 0.16358 kg |
| Centroid X | -9.6164e-002 m | 0.14674 m |
| Centroid Y | 0.21771 m | 9.7716e-002 m |
| Centroid Z | -2.6517e-003 m | -4.0418e-003 m |
| Moment of Inertia Ip1 | 6.3336e-003 kg·m² | 2.6117e-005 kg·m² |
| Moment of Inertia Ip2 | 3.8719e-002 kg·m² | 3.6375e-005 kg·m² |
| Moment of Inertia Ip3 | 3.2457e-002 kg·m² | 3.4611e-005 kg·m² |
| **Statistics** | | |
| Nodes | 4522 | 1547 |
| Elements | 2055 | 741 |

| | |
|---|---|
| Mesh Metric | None |

## Coordinate Systems

**TABLE 10**
**Model (B4) > Coordinate Systems > Coordinate System**

| | |
|---|---|
| Object Name | *Global Coordinate System* |
| State | Fully Defined |
| **Definition** | |
| Type | Cartesian |
| Ansys System Number | 0. |
| **Origin** | |
| Origin X | 0. m |
| Origin Y | 0. m |
| Origin Z | 0. m |
| **Directional Vectors** | |
| X Axis Data | [ 1. 0. 0. ] |
| Y Axis Data | [ 0. 1. 0. ] |
| Z Axis Data | [ 0. 0. 1. ] |

## Connections

**TABLE 11**
**Model (B4) > Connections**

| | |
|---|---|
| Object Name | *Connections* |
| State | Fully Defined |
| **Auto Detection** | |
| Generate Contact On Update | Yes |
| Tolerance Type | Slider |
| Tolerance Slider | 0. |

| | |
|---|---|
| Tolerance Value | 1.7993e-003 m |
| Face/Face | Yes |
| Face/Edge | No |
| Edge/Edge | No |
| Priority | Include All |
| Group By | Bodies |
| Search Across | Bodies |
| Revolute Joints | Yes |
| Fixed Joints | Yes |
| **Transparency** | |
| Enabled | Yes |

**TABLE 12**
**Model (B4) > Connections > Contact Regions**

| Object Name | *Contact Region* | *Contact Region 2* | *Contact Region 3* | *Contact Region 4* | *Contact Region 5* |
|---|---|---|---|---|---|
| State | Fully Defined | | | | |
| **Scope** | | | | | |
| Scoping Method | Geometry Selection | | | | |
| Contact | 2 Faces | 9 Faces | 2 Faces | 9 Faces | 1 Face |
| Target | 2 Faces | 9 Faces | 2 Faces | 9 Faces | 1 Face |
| Contact Bodies | Leg Joint-2 | | Leg Joint-3 | | Upper Leg Joint-1 |
| Target Bodies | Upper Leg Joint-2 | Upper Leg-6 | Upper Leg Joint-1 | Upper Leg-5 | Scaw-3 |
| **Definition** | | | | | |
| Type | Bonded | | | | |
| Scope Mode | Automatic | | | | |

| | |
|---|---|
| Behavior | Symmetric |
| Suppressed | No |
| **Advanced** | |
| Formulation | Pure Penalty |
| Normal Stiffness | Program Controlled |
| Update Stiffness | Never |
| Pinball Region | Program Controlled |

**TABLE 13**
**Model (B4) > Connections > Contact Regions**

| Object Name | *Contact Region 6* | *Contact Region 7* | *Contact Region 8* | *Contact Region 9* | *Contact Region 10* |
|---|---|---|---|---|---|
| State | Fully Defined | | | | |
| **Scope** | | | | | |
| Scoping Method | Geometry Selection | | | | |
| Contact | 1 Face | | 2 Faces | 1 Face | |
| Target | 1 Face | | 2 Faces | 1 Face | |
| Contact Bodies | Upper Leg Joint-2 | Upper Leg Joint-3 | | Scaw-1 | |
| Target Bodies | Scaw-1 | Scaw-2 | Leg Joint-1 | leg-3 | leg-4 |
| **Definition** | | | | | |
| Type | Bonded | | | | |
| Scope Mode | Automatic | | | | |
| Behavior | Symmetric | | | | |
| Suppressed | No | | | | |
| **Advanced** | | | | | |

| | |
|---|---|
| Formulation | Pure Penalty |
| Normal Stiffness | Program Controlled |
| Update Stiffness | Never |
| Pinball Region | Program Controlled |

**TABLE 14**
**Model (B4) > Connections > Contact Regions**

| Object Name | *Contact Region 11* | *Contact Region 12* | *Contact Region 13* | *Contact Region 14* | *Contact Region 15* |
|---|---|---|---|---|---|
| State | Fully Defined | | | | |
| **Scope** | | | | | |
| Scoping Method | Geometry Selection | | | | |
| Contact | 1 Face | | | | |
| Target | 1 Face | | | | |
| Contact Bodies | Scaw-2 | | Scaw-3 | | Scaw-4 |
| Target Bodies | leg-7 | leg-8 | leg-1 | leg-2 | Upper Leg Joint-5 |
| **Definition** | | | | | |
| Type | Bonded | | | | |
| Scope Mode | Automatic | | | | |
| Behavior | Symmetric | | | | |
| Suppressed | No | | | | |
| **Advanced** | | | | | |
| Formulation | Pure Penalty | | | | |
| Normal Stiffness | Program Controlled | | | | |

| | |
|---|---|
| Update Stiffness | Never |
| Pinball Region | Program Controlled |

**TABLE 15**
**Model (B4) > Connections > Contact Regions**

| Object Name | *Contact Region 16* | *Contact Region 17* | *Contact Region 18* | *Contact Region 19* | *Contact Region 20* |
|---|---|---|---|---|---|
| State | Fully Defined | | | | |
| **Scope** | | | | | |
| Scoping Method | Geometry Selection | | | | |
| Contact | 1 Face | | | | |
| Target | 1 Face | | | | |
| Contact Bodies | Scaw-4 | | Scaw-5 | | |
| Target Bodies | leg-3 | leg-4 | Upper Leg Joint-6 | leg-1 | leg-2 |
| **Definition** | | | | | |
| Type | Bonded | | | | |
| Scope Mode | Automatic | | | | |
| Behavior | Symmetric | | | | |
| Suppressed | No | | | | |
| **Advanced** | | | | | |
| Formulation | Pure Penalty | | | | |
| Normal Stiffness | Program Controlled | | | | |
| Update Stiffness | Never | | | | |
| Pinball Region | Program Controlled | | | | |

**TABLE 16**
**Model (B4) > Connections > Contact Regions**

| Object Name | *Contact Region 21* | *Contact Region 22* | *Contact Region 23* | *Contact Region 24* | *Contact Region 25* |
|---|---|---|---|---|---|
| State | Fully Defined | | | | |
| **Scope** | | | | | |
| Scoping Method | Geometry Selection | | | | |
| Contact | 1 Face | | | | |
| Target | 1 Face | | | | |
| Contact Bodies | Scaw-6 | | | Upper Leg Joint-4 | Upper Leg Joint-5 |
| Target Bodies | Upper Leg Joint-4 | leg-7 | leg-8 | Lower Leg Belt-3 | |
| **Definition** | | | | | |
| Type | Bonded | | | | |
| Scope Mode | Automatic | | | | |
| Behavior | Symmetric | | | | |
| Suppressed | No | | | | |
| **Advanced** | | | | | |
| Formulation | Pure Penalty | | | | |
| Normal Stiffness | Program Controlled | | | | |
| Update Stiffness | Never | | | | |
| Pinball Region | Program Controlled | | | | |

**TABLE 17**
**Model (B4) > Connections > Contact Regions**

| Object Name | *Contact Region 26* | *Contact Region 27* | *Contact Region 28* | *Contact Region 29* | *Contact Region 30* |
|---|---|---|---|---|---|

| | | | | | |
|---|---|---|---|---|---|
| State | Fully Defined | | | | |
| **Scope** | | | | | |
| Scoping Method | Geometry Selection | | | | |
| Contact | 1 Face | 2 Faces | | | 1 Face |
| Target | 1 Face | 2 Faces | | | 1 Face |
| Contact Bodies | Upper Leg Joint-6 | Sensor-1 | Sensor-2 | Sensor-3 | Upper Leg Belt-2 |
| Target Bodies | Lower Leg Belt-3 | Upper Leg Belt-2 | | | Upper Leg-4 |
| **Definition** | | | | | |
| Type | Bonded | | | | |
| Scope Mode | Automatic | | | | |
| Behavior | Symmetric | | | | |
| Suppressed | No | | | | |
| **Advanced** | | | | | |
| Formulation | Pure Penalty | | | | |
| Normal Stiffness | Program Controlled | | | | |
| Update Stiffness | Never | | | | |
| Pinball Region | Program Controlled | | | | |

**TABLE 18**
**Model (B4) > Connections > Contact Regions**

| Object Name | *Contact Region 31* | *Contact Region 32* | *Contact Region 33* | *Contact Region 34* | *Contact Region 35* |
|---|---|---|---|---|---|
| State | Fully Defined | | | | |
| **Scope** | | | | | |
| Scoping | Geometry Selection | | | | |

| | | | | | |
|---|---|---|---|---|---|
| Method | | | | | |
| Contact | 1 Face | | | 9 Faces | 1 Face |
| Target | 1 Face | | | 9 Faces | 1 Face |
| Contact Bodies | Upper Leg Belt-2 | | Upper Leg-4 | | Upper Leg-5 |
| Target Bodies | Upper Leg-5 | Upper Leg-6 | Chamfer2 | Leg Joint-1 | Boss-Extrude3[1] |
| **Definition** | | | | | |
| Type | Bonded | | | | |
| Scope Mode | Automatic | | | | |
| Behavior | Symmetric | | | | |
| Suppressed | No | | | | |
| **Advanced** | | | | | |
| Formulation | Pure Penalty | | | | |
| Normal Stiffness | Program Controlled | | | | |
| Update Stiffness | Never | | | | |
| Pinball Region | Program Controlled | | | | |

**TABLE 19**
**Model (B4) > Connections > Contact Regions**

| Object Name | *Contact Region 36* | *Contact Region 37* | *Contact Region 38* | *Contact Region 39* | *Contact Region 40* |
|---|---|---|---|---|---|
| State | Fully Defined | | | | |
| **Scope** | | | | | |
| Scoping Method | Geometry Selection | | | | |
| Contact | 1 Face | | | | |
| Target | 1 Face | | | | |

| | | | | |
|---|---|---|---|---|
| Contact Bodies | Upper Leg-5 | Upper Leg-6 | Boss-Extrude3[1] | Boss-Extrude3[2] |
| Target Bodies | Chamfer2 | Boss-Extrude3[2] | Chamfer2 | |
| **Definition** | | | | |
| Type | Bonded | | | |
| Scope Mode | Automatic | | | |
| Behavior | Symmetric | | | |
| Suppressed | No | | | |
| **Advanced** | | | | |
| Formulation | Pure Penalty | | | |
| Normal Stiffness | Program Controlled | | | |
| Update Stiffness | Never | | | |
| Pinball Region | Program Controlled | | | |

## Mesh

**TABLE 20**
**Model (B4) > Mesh**

| | |
|---|---|
| Object Name | *Mesh* |
| State | Solved |
| **Defaults** | |
| Physics Preference | Mechanical |
| Relevance | 0 |
| **Sizing** | |
| Use Advanced Size Function | Off |
| Relevance Center | Coarse |
| Element Size | Default |

| | |
|---|---|
| Initial Size Seed | Active Assembly |
| Smoothing | Medium |
| Transition | Fast |
| Span Angle Center | Coarse |
| Minimum Edge Length | 7.0711e-004 m |
| **Inflation** | |
| Use Automatic Tet Inflation | None |
| Inflation Option | Smooth Transition |
| Transition Ratio | 0.272 |
| Maximum Layers | 5 |
| Growth Rate | 1.2 |
| Inflation Algorithm | Pre |
| View Advanced Options | No |
| **Advanced** | |
| Shape Checking | Standard Mechanical |
| Element Midside Nodes | Program Controlled |
| Straight Sided Elements | No |
| Number of Retries | Default (4) |
| Rigid Body Behavior | Dimensionally Reduced |
| Mesh Morphing | Disabled |
| **Pinch** | |
| Pinch Tolerance | Please Define |
| Generate on Refresh | No |
| **Statistics** | |
| Nodes | 54126 |

| | |
|---|---|
| Elements | 24502 |
| Mesh Metric | None |

## Static Structural (B5)

**TABLE 21**
**Model (B4) > Analysis**

| | |
|---|---|
| Object Name | *Static Structural (B5)* |
| State | Solved |
| **Definition** | |
| Physics Type | Structural |
| Analysis Type | Static Structural |
| Solver Target | ANSYS Mechanical |
| **Options** | |
| Environment Temperature | 22. °C |
| Generate Input Only | No |

**TABLE 22**
**Model (B4) > Static Structural (B5) > Analysis Settings**

| | |
|---|---|
| Object Name | *Analysis Settings* |
| State | Fully Defined |
| **Step Controls** | |
| Number Of Steps | 1. |
| Current Step Number | 1. |
| Step End Time | 1. s |
| Auto Time Stepping | Program Controlled |
| **Solver Controls** | |
| Solver Type | Program Controlled |

| | |
|---|---|
| Weak Springs | Program Controlled |
| Large Deflection | Off |
| Inertia Relief | Off |
| **Nonlinear Controls** | |
| Force Convergence | Program Controlled |
| Moment Convergence | Program Controlled |
| Displacement Convergence | Program Controlled |
| Rotation Convergence | Program Controlled |
| Line Search | Program Controlled |
| **Output Controls** | |
| Calculate Stress | Yes |
| Calculate Strain | Yes |
| Calculate Results At | All Time Points |
| **Analysis Data Management** | |
| Solver Files Directory | H:\Users\Administrator\Desktop\min\Graduate Study\Thesis\2011-05\2011-05-Ansys\New Design FEA_files\dp0\SYS-1\MECH\ |
| Future Analysis | None |
| Scratch Solver Files Directory | |
| Save ANSYS db | No |
| Delete Unneeded Files | Yes |
| Nonlinear Solution | No |
| Solver Units | Active System |

| | |
|---|---|
| Solver Unit System | mks |

**TABLE 23**
**Model (B4) > Static Structural (B5) > Loads**

| Object Name | *Fixed Support* | *Force* |
|---|---|---|
| State | Fully Defined | |
| **Scope** | | |
| Scoping Method | Geometry Selection | |
| Geometry | 1 Face | |
| **Definition** | | |
| Type | Fixed Support | Force |
| Suppressed | No | |
| Define By | | Vector |
| Magnitude | | 100. N (ramped) |
| Direction | | Defined |

**FIGURE 1**
**Model (B4) > Static Structural (B5) > Force**

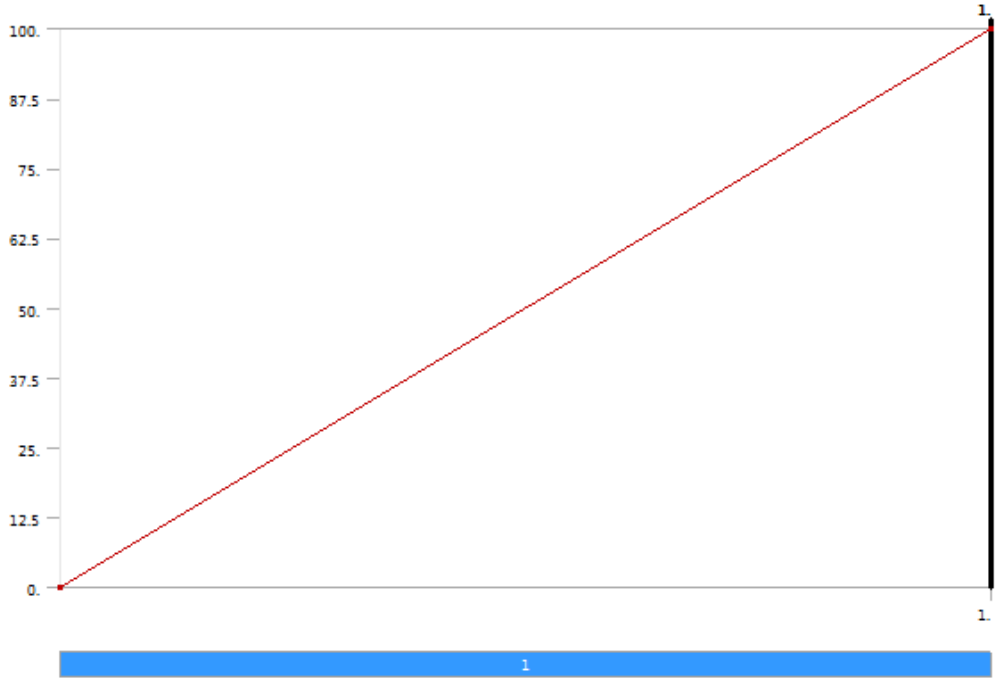

## Solution (B6)

**TABLE 24**
**Model (B4) > Static Structural (B5) > Solution**

| | |
|---|---|
| Object Name | *Solution (B6)* |
| State | Solved |
| **Adaptive Mesh Refinement** | |
| Max Refinement Loops | 1. |
| Refinement Depth | 2. |

**TABLE 25**
**Model (B4) > Static Structural (B5) > Solution (B6) > Solution Information**

| | |
|---|---|
| Object Name | *Solution Information* |
| State | Solved |
| **Solution Information** | |
| Solution Output | Solver Output |
| Newton-Raphson Residuals | 0 |
| Update Interval | 2.5 s |
| Display Points | All |

**TABLE 26**
**Model (B4) > Static Structural (B5) > Solution (B6) > Results**

| Object Name | *Total Deformation* | *Directional Deformation* | *Directional Deformation 2* | *Directional Deformation 3* | *Equivalent Elastic Strain* |
|---|---|---|---|---|---|
| State | Solved | | | | |
| **Scope** | | | | | |
| Scoping Method | Geometry Selection | | | | |
| Geometry | All Bodies | | | | |
| **Definition** | | | | | |
| Type | Total Deformation | Directional Deformation | | | Equivalent (von-Mises) Elastic |

| | | | | | |
|---|---|---|---|---|---|
| | | | | | Strain |
| By | Time | | | | |
| Display Time | Last | | | | |
| Calculate Time History | Yes | | | | |
| Identifier | | | | | |
| Orientation | | X Axis | Y Axis | Z Axis | |
| Coordinate System | | Global Coordinate System | | | |
| Use Average | | | | | Yes |
| **Results** | | | | | |
| Minimum | 0. m | -2.2037e-005 m | -1.2181e-005 m | -5.9442e-006 m | 2.414e-014 m/m |
| Maximum | 2.2417e-005 m | 1.0934e-006 m | 2.9046e-006 m | 1.2524e-005 m | 2.7562e-005 m/m |
| Minimum Occurs On | Chamfer2 | leg-7 | Lower Leg Belt-3 | leg-4 | Chamfer2 |
| Maximum Occurs On | leg-8 | leg-3 | leg-7 | leg-1 | Lower Leg Belt-3 |
| **Information** | | | | | |
| Time | 1. s | | | | |
| Load Step | 1 | | | | |
| Substep | 1 | | | | |
| Iteration Number | 1 | | | | |

**TABLE 27**
**Model (B4) > Static Structural (B5) > Solution (B6) > Results**

| Object Name | *Equivalent Stress* |
|---|---|
| State | Solved |

| Scope | |
|---|---|
| Scoping Method | Geometry Selection |
| Geometry | All Bodies |
| **Definition** | |
| Type | Equivalent (von-Mises) Stress |
| By | Time |
| Display Time | Last |
| Calculate Time History | Yes |
| Use Average | Yes |
| Identifier | |
| **Results** | |
| Minimum | 4.828e-003 Pa |
| Maximum | 5.5125e+006 Pa |
| Minimum Occurs On | Chamfer2 |
| Maximum Occurs On | Lower Leg Belt-3 |
| **Information** | |
| Time | 1. s |
| Load Step | 1 |
| Substep | 1 |
| Iteration Number | 1 |

## Material Data

### Structural Steel

**TABLE 28**
**Structural Steel > Constants**

| | |
|---|---|
| Density | 7850 kg m^-3 |
| Coefficient of Thermal Expansion | 1.2e-005 C^-1 |

| | |
|---|---|
| Specific Heat | 434 J kg^-1 C^-1 |
| Thermal Conductivity | 60.5 W m^-1 C^-1 |
| Resistivity | 1.7e-007 ohm m |

**TABLE 29**
**Structural Steel > Compressive Ultimate Strength**

| Compressive Ultimate Strength Pa |
|---|
| 0 |

**TABLE 30**
**Structural Steel > Compressive Yield Strength**

| Compressive Yield Strength Pa |
|---|
| 2.5e+008 |

**TABLE 31**
**Structural Steel > Tensile Yield Strength**

| Tensile Yield Strength Pa |
|---|
| 2.5e+008 |

**TABLE 32**
**Structural Steel > Tensile Ultimate Strength**

| Tensile Ultimate Strength Pa |
|---|
| 4.6e+008 |

**TABLE 33**
**Structural Steel > Alternating Stress**

| Alternating Stress Pa | Cycles | Mean Stress Pa |
|---|---|---|
| 3.999e+009 | 10 | 0 |
| 2.827e+009 | 20 | 0 |
| 1.896e+009 | 50 | 0 |
| 1.413e+009 | 100 | 0 |
| 1.069e+009 | 200 | 0 |
| 4.41e+008 | 2000 | 0 |

| | | |
|---|---|---|
| 2.62e+008 | 10000 | 0 |
| 2.14e+008 | 20000 | 0 |
| 1.38e+008 | 1.e+005 | 0 |
| 1.14e+008 | 2.e+005 | 0 |
| 8.62e+007 | 1.e+006 | 0 |

**TABLE 34**
**Structural Steel > Strain-Life Parameters**

| Strength Coefficient Pa | Strength Exponent | Ductility Coefficient | Ductility Exponent | Cyclic Strength Coefficient Pa | Cyclic Strain Hardening Exponent |
|---|---|---|---|---|---|
| 9.2e+008 | -0.106 | 0.213 | -0.47 | 1.e+009 | 0.2 |

**TABLE 35**
**Structural Steel > Relative Permeability**

| Relative Permeability |
|---|
| 10000 |

**TABLE 36**
**Structural Steel > Isotropic Elasticity**

| Temperature C | Young's Modulus Pa | Poisson's Ratio |
|---|---|---|
| | 2.e+011 | 0.3 |